156
17

AN AUTOMATIC METHOD FOR INSPECTING PLYWOOD SHEAR SAMPLES

by

R. Richard Avent, III

Thesis submitted to the Faculty of the
Virginia Polytechnic Institute and State University
in partial fulfillment of the requirements for the degree of
Master of Science
in
Electrical Engineering

APPROVED:

Richard W. Conners, Chairman

A. Lynn Abbott

D. Earl Kline

June, 1990

Blacksburg, Virginia

AN AUTOMATIC METHOD FOR INSPECTING PLYWOOD SHEAR SAMPLES

by

R. Richard Avent, III

Committee Chairman: Richard W. Conners

Electrical Engineering

(ABSTRACT)

Plywood is composed of several thin layers of wood bonded together by glue. The adhesive integrity of the glue formulation employed must surpass the structural integrity of the wood species within a given panel of plywood. The American Plywood Association (APA) regularly tests the plywood produced at various plywood manufacturing plants to ensure that this particular performance requirement is consistently met. One of the procedures used by the APA to test this requirement consists of 1) milling a plywood panel to be tested into small rectangular blocks called samples, 2) conditioning these samples with various treatments to simulate natural aging, 3) shearing each sample into two halves, and 4) estimating the percent wood failure (as opposed to glue failure) produced by the shear by visually inspecting these sample halves. A region of solid wood or a region of wood fibers embedded in glue on the shear of a sample half is a region of wood failure while a region of glue is a region of glue failure. If the wood failure of samples from a significant number of panels is too low, the right to use APA trademarks is withdrawn from the plant where the sampling occurred. Since measurements obtained by human visual inspection can contain inaccuracies due to fatigue,

boredom, state of mind, etc., an automatic vision system to determine percent wood failure is proposed. The method presented is a refinement of the method developed by McMillin and is divided into three tasks. The first task is to locate the area of shear on a given sample half. The second task is to distinguish the areas of wood from the areas of glue on the shear of a sample half. Solid wood is distinguished from glue based on the difference in gray level intensity that exists between solid wood and glue. Wood fiber is distinguished from glue based on the difference in texture, i.e., edge patterns, that exists between fiber and glue. The third task is to compare the areas of shear on the two sample halves comprising a sample to determine the percent wood failure of the sample.

ACKNOWLEDGEMENTS

I would like to thank my advisor, Dr. Richard Conners, for the immeasurable patience and support he has given me throughout the development of this thesis. I would also like to thank Dr. Lynn Abbott and Dr. Earl Kline for their helpful advice and for being on my committee. I am grateful to the American Plywood Association and to Georgia-Pacific for the information they provided concerning the manufacturing and inspection of plywood. I wish to thank the graduate students of the Spatial Data Analysis Laboratory and the faculty and staff of the Electrical Engineering Department for making my three year stay at Virginia Tech both rewarding and enjoyable. Of these I especially wish to thank Sue Ellen Cline and soon-to-be-Dr. Chong Ng for their technical assistance, Loretta Estes for her administrative assistance, and Mrs. Jeanette Conners for her proofreading assistance. Most of all, I want to thank my friends and family (especially my parents) for their unlimited understanding and support during this project.

TABLE OF CONTENTS

NOMENCLATURE

A	A column matrix used to store the results of evaluating d_i using the elements of B_r as the independent variables.
b_{BS}	The constant value used to define the straight line $x = m_{BS}y + b_{BS}$ that best fits a specimen's bottom side boundary.
B_c	The column matrix of column coordinates of adjacent boundary points of a specimen ordered in a clockwise manner.
b_{LS}	The constant value used to define the straight line $y = m_{LS}x + b_{LS}$ that best fits a specimen's left side boundary.
b'_{LS}	The constant value used to define the line $y = m'_{LS}x + b'_{LS}$ that best fits the left side boundary of a specimen's inspection area.
B_r	The column matrix of row coordinates of adjacent boundary points of a specimen ordered in a clockwise manner.
b_{RS}	The constant value used to define the straight line $y = m_{RS}x + b_{RS}$ that best fits a specimen's right side boundary.
b_{TS}	The constant value used to define the straight line $x = m_{TS}y + b_{TS}$ that best fits a specimen's top side boundary.
B_rG_r	A labeled image that indicates areas that are background, areas that are solid wood, areas that are fiber, and areas that are glue.
BS_c	A column matrix containing the column coordinates of the clockwise ordered boundary points of a specimen's bottom side.

BS_r A column matrix containing the row coordinates of the clockwise ordered boundary points of a specimen's bottom side.

C A color image with components P_r, P_g, and P_b.

CR A labeled image that identifies the various 8-connected regions that are part of the inspection area but are not thought to be solid wood.

D A column matrix used to store the results of evaluating d_{t^2} using the elements of A as the independent variables.

D_{iff} A column matrix containing the first derivative values of the elements of H'.

d_t A function that approximates an average of $dx(t)/dt$ for the $(x(t), y(t))$ parameterized version of a curve in the x-y plane.

d_{t^2} A function that approximates the derivative of the function d_t.

E_H An image that contains both labeling information as to which pixels are solid wood, which are background, and which are border pixels, as well as gradient information obtained from an edge detector sensitive to horizontal edges.

$\underline{e}_k$ The vector defining the kth edge pixel extracted from the image S_a.

E_V An image that contains both labeling information as to which pixels are solid wood, which are background, and which are border pixels, as well as gradient information obtained from an edge detector sensitive to vertical edges.

f The estimated percent wood failure of a plywood shear sample.

F_{ib} A labeled image that indicates areas that are background, areas that are solid wood, areas that are fiber, areas that are glue, and areas that represent border pixels that could not have an edge detector applied to them.

G A column matrix that contains a discrete version of a Gaussian function.

$G_r F_{ib}$ A labeled image that indicates areas that are background, areas that are solid wood, areas that are glue, areas that are grouped fiber, i.e., a region containing fiber and narrow regions of glue between the fibers, and areas that represent border pixels that could not have an edge detector applied to them.

h The number of pixels per inch in the horizontal (y-axis) direction.

H A column matrix that is a gray level histogram of a black and white image.

H' A column matrix that is a low pass filtered version of a histogram H.

H_{rb} The two dimensional histogram of the red/blue color components of a color image.

I_a The labeled image that defines the region that corresponds to a specimen's inspection area.

l The number of pixels per inch along a line with a given orientation of $l = h - \theta(2/\pi)(h - v)$.

L_{BS} Denotes the graph of $x = m_{BS}y+b_{BS}$ that defines a specimen's bottom side boundary.

L_{LS} Denotes the graph of $y = m_{LS}x + b_{LS}$ that defines a specimen's left side boundary.

L'_{LS} Denotes the graph of $y = m'_{LS}x+b'_{LS}$ that defines the left side boundary of a specimen's inspection area.

L_{RS} Denotes the graph of $y = m_{RS}x + b_{RS}$ that defines a specimen's right side boundary.

L_{TS} Denotes the graph of $x = m_{TS}y + b_{TS}$ that defines a specimen's top side boundary.

LI A labeled image that represents the final result of processing a specimen's inspection area in which areas of background, areas of wood, and areas of glue are indicated.

LI_1 A labeled image LI of one of a sample's specimen's inspection areas.

LI_2 A labeled image LI of a sample's other specimen's inspection area.

LS_c A column matrix containing the column coordinates of the clockwise ordered boundary points of a specimen's left side.

LS_r A column matrix containing the row coordinates of the clockwise ordered boundary points of a specimen's left side.

m_{BS} The slope of the straight line $x = m_{BS}y+b_{BS}$ that best fits a specimen's bottom side boundary.

m_{LS} The slope of the straight line $y = m_{LS}x+b_{LS}$ that best fits a specimen's left side boundary.

m'_{LS} The slope of the straight line $y = m'_{LS}x + b'_{LS}$ that best fits the left side boundary of a specimen's inspection area.

m_{RS} The slope of the straight line $y = m_{RS}x+b_{RS}$ that best fits a specimen's right side boundary.

m_{TS} The slope of the straight line $x = m_{TS}y+b_{TS}$ that best fits a specimen's top side boundary.

Min The smallest gray level value that can occur in the black and white image P.

Max The largest gray level value that can occur in the black and white image P.

N The number of rows in the column matrices B_r, B_c, A, and D.

N_T The total number of pixel pairs evaluated when a specimen's two inspection areas are mapped onto one another.

N_W The total number of pixel pairs determined to be wood failure when a sample's two inspection areas are mapped onto one another.

P A black and white image.

r A rounding function that rounds a real number to an integer.

R_1 The region in LI_1 bounded by the line equations $L^{(1)}_{TS}$, $L^{(1)}_{RS}$, $L^{(1)}_{BS}$, and $L^{'(1)}_{LS}$.

R_2 The region in LI_2 bounded by the line equations $L_{TS}^{(2)}$, $L_{RS}^{(2)}$, $L_{BS}^{(2)}$, and $L_{LS}^{'(2)}$.

RC The x-y rectangular coordinates of P.

RC_1 The x-y rectangular coordinates of R_1.

RC_2 The x-y rectangular coordinates of R_2.

RS_c A column matrix containing the column coordinates of the clockwise ordered boundary points of the specimen's right side.

RS_r A column matrix containing the row coordinates of the clockwise ordered boundary points of the specimen's right side.

S_a The labeled image that defines the region that corresponds to a specimen.

T The threshold of a black and white image.

T_{op} An integer column matrix that indicates which gray levels of P represent large peaks in the low pass filtered histogram H'.

TS_c A column matrix containing the column coordinates of the clockwise ordered boundary points of a specimen's top side.

TS_r A column matrix containing the row coordinates of the clockwise ordered boundary points of a specimen's top side.

v The number of pixels per inch in the vertical (x-axis) direction.

V_{LL} The lower left vertex of a specimen corresponding to the intersection of L_{BS} and L_{LS}.

V'_{LL} The lower left vertex of a specimen's inspection area corresponding to the intersection of L_{BS} and L'_{LS}.

V_{LR} The lower right vertex of a specimen corresponding to the intersection of L_{RS} and L_{BS}.

V_{UL} The upper left vertex of a specimen corresponding to the intersection of L_{LS} and L_{TS}.

V'_{UL} The upper left vertex of a specimen's inspection area corresponding to the intersection of L_{TS} and L'_{LS}.

V_{UR} The upper right vertex of a specimen's inspection area corresponding to the intersection of L_{TS} and L_{RS}.

W_s A labeled image that identifies those regions of a specimen image P that are part of the specimen's inspection area and are solid wood.

x'_{LL} The x-coordinate of $V'_{LL} = (x'_{LL}, y'_{LL})$.

x_{LR} The x-coordinate of $V_{LR} = (x_{LR}, y_{LR})$.

x'_{UL} The x-coordinate of $V'_{UL} = (x'_{UL}, y'_{UL})$.

x_{UR} The x-coordinate of $V_{UR} = (x_{UR}, y_{UR})$.

y'_{LL} The y-coordinate of $V'_{LL} = (x'_{LL}, y'_{LL})$.

y_{LR} The y-coordinate of $V_{LR} = (x_{LR}, y_{LR})$.

y'_{UL} The y-coordinate of $V'_{UL} = (x'_{UL}, y'_{UL})$.

y_{UR} The y-coordinate of $V_{UR} = (x_{UR}, y_{UR})$.

Δy The difference in y-coordinate values of V'_{UL} and V_{UR} where $\Delta y = l \cos\theta$.

ϕ The positive angle subtended between the graph L_{TS} and the y-axis of the coordinate system used to define the line equations where $\phi = |\arctan m_{TS}|$.

θ The positive angle subtended between the graph L_{TS} and the y-axis of the coordinate system used to define the line equations where $\theta = \arctan m_{TS}$.

1. INTRODUCTION

Over 20 billion square feet of plywood is produced in the United States each year [APA, 1983]. Plywood is made from dozens of wood species and is manufactured into hundreds of structural wood panel products. To help assure quality control, the American Plywood Association (APA) was established in 1933. Since plywood is composed of several thin layers of wood bonded together by glue, a major concern of the APA in terms of quality control is the adhesive integrity of the glue formulation employed. Specifically, the adhesive integrity of the glue formulation must surpass the structural integrity of the wood species within a given panel of plywood.

The APA regularly tests the plywood produced at various plants to ensure that this particular performance requirement is consistently met [APA, 1984]. One of the procedures used by the APA to test this requirement consists of 1) milling a plywood panel to be tested into small rectangular blocks called samples, 2) conditioning these samples with various treatments to simulate natural aging, 3) shearing each sample into two halves, and 4) estimating the percent wood failure (as opposed to glue failure) produced by the shear by visually inspecting these sample halves. A region of wood on the shear of a sample half is a region of wood failure while a region of glue on the shear of a sample half is a region of glue failure. If the wood failure of samples from a significant number of panels is too low, the right to use APA trademarks is withdrawn from the plant that produced the panels.

The percent wood failure of the shear on a pair of sample halves is visually estimated to the nearest 5% increment by a human inspector. As a

quality control measure, some samples are evaluated by more than one inspector. A set of samples evaluated by multiple inspectors consists of 25 or more samples. The percent wood failures assigned to the samples in this set by an inspector are considered accurate if their average is within 5% of the mean of the averages computed from the percent wood failures assigned to this set by each inspector. In terms of speed, experienced evaluators have been observed to inspect as many as 15 samples in one minute. Unfortunately, different interpretations between experienced evaluators indicate that measurements obtained by human visual inspection can contain inaccuracies due to fatigue, boredom, state of mind, etc. [McMillin, 1984]. An automatic method for determining percent wood failure would overcome these inaccuracies. If the automatic method to inspect plywood shear were implemented as an automatic vision system, the methodology employed to perform the inspection task in the automatic method could be modeled after the methodology employed by the human inspector. The purpose of this thesis is to present the design of an automatic method for inspecting plywood shear based on the vision approach thus described.

To be cost-effective, an automatic vision system to inspect plywood shear must meet two objectives: 1) the accuracy of the system must surpass that of a human inspector and 2) the speed of the system must surpass that of a human inspector. Experimentation showed that the accuracy of an algorithm employed in the automatic vision method is proportional to the spatial resolution of the images of plywood shear operated upon by the algorithm. Thus, to achieve a high rate of accuracy, the spatial resolution of the scanning system employed in the automatic vision method must be high. To achieve a high rate of speed, relatively simple methods must be employed to perform the evaluations. In the automatic vision system presented in this thesis, each

processing step is accomplished using relatively simple methods; however, the determination of the overall processing speed is deferred until a later study.

There are three reasons for this deferral. First, the feasibility of an automatic vision system must be established before a real-time solution is attempted. The goal of this thesis is to establish the feasibility of an automatic vision system for determining percent wood failure. Second, to aid system testing and debugging the algorithms employed are currently implemented as separate computer programs. Some of the processing time and the majority of the I/O time will be eliminated when the algorithms are implemented as one program. Finally, the processing speed of the computer currently used to support the system software is slower than the computer that would be used in an actual industrial setting. The computer currently used can process one million instructions per second. This processing speed is slower than the processing speed of current PC systems. Since researchers predict that a computer capable of processing one billion instructions per second will be developed before the turn of the century, it is felt that the use of computers developed during the next few years to support the software presented in this thesis will yield an automatic vision system possessing an inspection rate surpassing that of an experienced human evaluator.

2. BACKGROUND

2.1 APA Plywood Testing Procedure

The sampling rate of a plywood manufacturing plant is the number of times per month that plywood panels from the plant are tested by the APA [APA, 1984]. The sampling rate can range from 10 to over 100 times per month, depending on the number of panels produced, the plywood grade, and the previous performance level of the plant with regard to the tests that are performed by the APA. During a sampling, two panels from each glued-up press load are tagged by an APA Supervisor or Certified Inspector. Five 3 1/4-inch by 1-inch samples are cut from each panel tagged. Two 1/8-inch wide grooves are sawn into each sample, one on each side of the sample. The location of these saw grooves is shown in Figure 2–1a. All samples are sent to an APA laboratory for testing.

At the APA laboratory, each sample is subjected to treatments to simulate natural aging. The treatments consist of either a vacuum-pressure test, a boiling test, or both. In a typical vacuum-pressure test procedure, a sample is placed within a pressure vessel and submerged in cold tap water for 60 minutes. A vacuum of 25 inches of mercury is drawn and maintained for the first 30-minute period followed by the application of 65-70 pounds per square inch of pressure for the duration of the second 30-minute period. In a typical boiling test procedure, a sample is boiled for 4 hours, dried at 145°F for 20 hours, boiled for 4 more hours, and cooled in cold tap water.

While wet from the application of either of the above treatments, each sample is sheared into two halves by tension loading, as shown in Figure 2–1b.

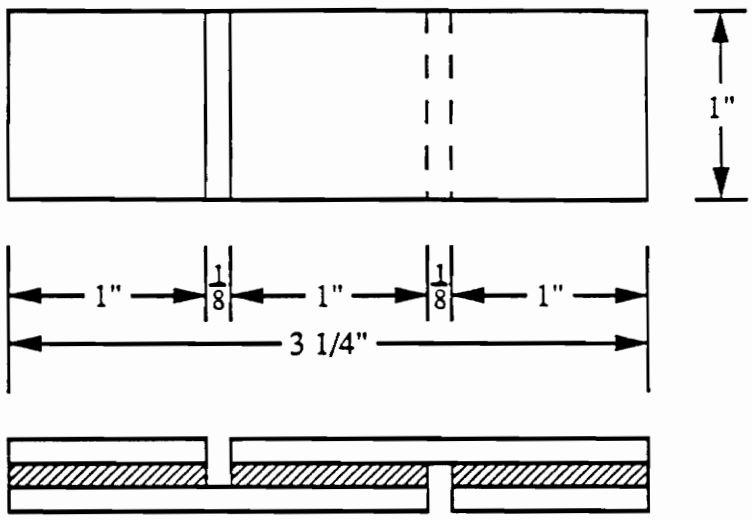

(a)

Figure 2–1 (a) Dimensions of a sample.

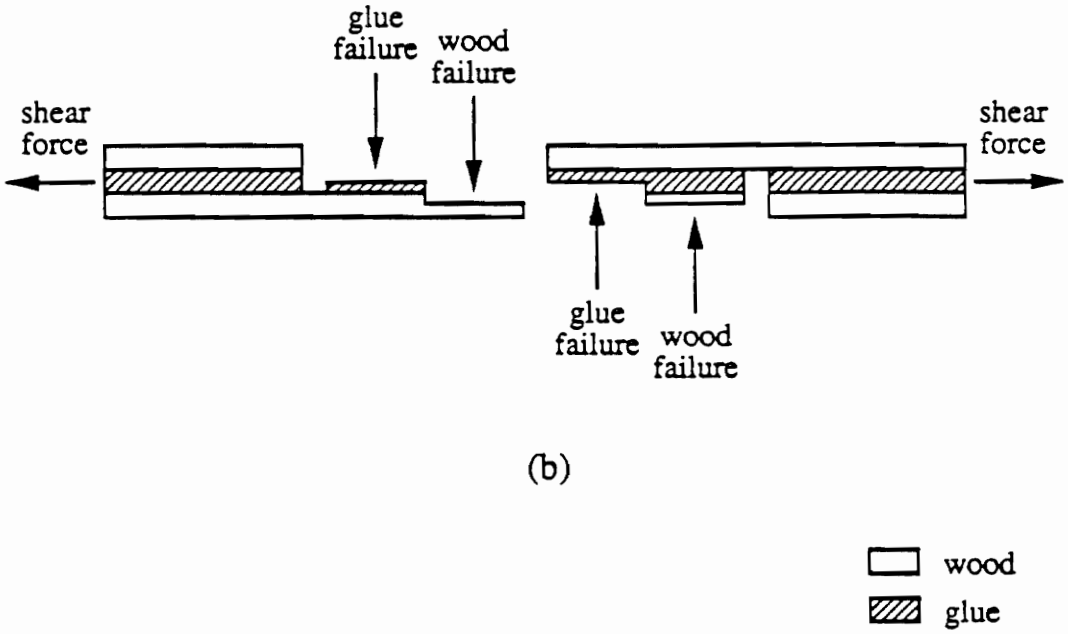

Figure 2–1 (b) Method of shearing a sample.

The ends of a sample are gripped in the jaws of the shear testing machine in such a way that only the middle portion of a sample (the portion between the two grooves) fails. After a sample has been forced into shear failure, the dimensions of the resulting shear surface area on each sample half is one inch by one inch. After both sample halves have dried, the shear surface areas of both sample halves are visually inspected to determine the percent wood failure of the sample.

The nomenclature used to describe a sample throughout the rest of this thesis is illustrated in Figure 2–2. Each sample half produced from a sample that has been forced into shear failure is called a specimen. The one inch by one inch shear surface area on a specimen is called the specimen inspection area. As will be noted, a 1/8-inch wide groove separates the inspection area from the rest of the surface area on a specimen.

A region on a specimen inspection area is either wood or glue [APA, 1970]. Regions of wood correspond to areas where the wood failed during the application of shear force while regions of glue correspond to areas where the glue failed (see Figure 2–1b). Regions of wood fiber, which are regions of closely spaced strands of wood embedded in glue, are considered regions of wood failure although glue between individual strands may be visible. The percent wood failure of a sample is obtained by comparing small regions on the inspection area of one specimen to corresponding regions on the inspection area of the other specimen. If a given region on the inspection area of one specimen and its corresponding region on the inspection area of the other specimen are both evaluated to be wood failure, the pair of regions constitute wood failure for the sample. If both regions are evaluated to be glue failure, the pair consititute glue failure for the sample. If one region is evaluated to

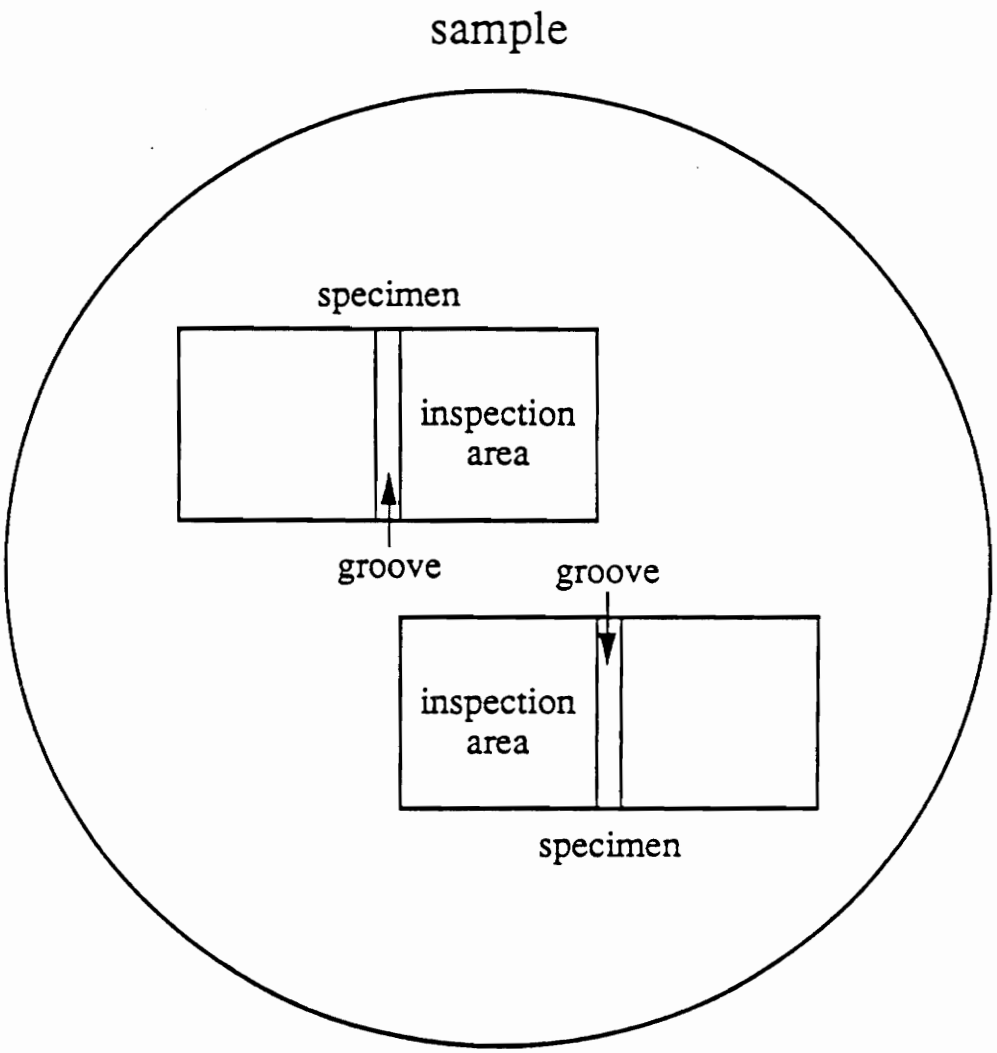

Figure 2–2 Nomenclature used to describe a sample.

be wood failure while the other region is evaluated to be glue failure, the pair constitute glue failure for the sample since a failure of the glue to adhere to the wood is implied. The percentage of the one inch by one inch shear area evaluated to be wood failure (rounded to the nearest 5% increment) is the percent wood failure assigned to the sample. The percent wood failure of a panel is the average percent wood failure of all samples milled from the panel.

The test reporting and performance requirements are approximately the same for all plywood grades [APA, 1984]. For the exterior type grade, the test reports list the percent wood failure of each panel tested as well as the number of panels rating below 80%, 60%, and 30%. In general, the performance requirements apply only to the last 20 panels tested. For the exterior type grade, the last 20 panels tested must meet the following requirements: 1) the average wood failure of all 20 panels must be 85% or higher, 2) 15 panels of the 20 panels must show 80% or higher wood failure, 3) 18 panels of the 20 panels must show 60% or higher wood failure, and 4) 19 panels of the 20 panels must show 30% or higher wood failure. In addition to these requirements, the last 100 panels tested must have no more than 8 panels showing less than 60% wood failure.

The consequences of failing to meet performance requirements is the same for almost all grades. In the event of such an occurence, another 20-panel sampling is taken from the current production and tested as before. If this set of panels fails to meet performance requirements, a state of plant delinquency exists and yet another 20-panel sampling is tested. If this last set of panels fails to meet performance requirements, the right to use APA trademarks is withdrawn.

2.2 Automating the Visual Inspection Task

A vision system that completely automates this visual inspection task can conceptually be divided into two stages, the scanning stage and the processing stage. In the scanning stage, each of the two specimens comprising a sample are scanned to create a digital image, one digital image for each specimen. The general form of one of these digital images is shown in Figure 2–3. In the processing stage, the percent wood failure of a sample is determined from the information contained in the images of both specimens that comprise the sample. Black and white and/or color images can be used in this analysis.

In general, a black and white digital image is an $n \times m$ matrix P containing n rows ranging from 0 to $n-1$ and m columns ranging from 0 to $m-1$. Each element $p(x,y)$ of P is an integer ranging from 0 to 2^k-1 where k is an integer greater than 0. The resolution of P is said to be $n \times m \times k$. Typically $k = 8$ so that the elements of P range from 0 to 255. Each element $p(x,y)$ of the matrix P represents the gray level intensity of the point in the scene that corresponds to the (x,y) location in P. If $p(x,y) = 0$, the corresponding point in the scene is completely black. If $p(x,y) = 255$, the corresponding point in the scene is completely white. Values between 0 and 255 represent gray level increments between completely black and completely white. Each element $p(x,y)$ of P is called a pixel.

A color image C is actually a set of three images: a red image P_r, a green image P_g, and a blue image P_b. Each of these three images is an $n \times m$ matrix where each element is an integer value ranging from 0 to 2^k-1 where k is an integer greater than 0. The matrices P_r, P_g, and P_b are called the color components of C. The resolution of the color image C is said to be $n \times m \times 3k$.

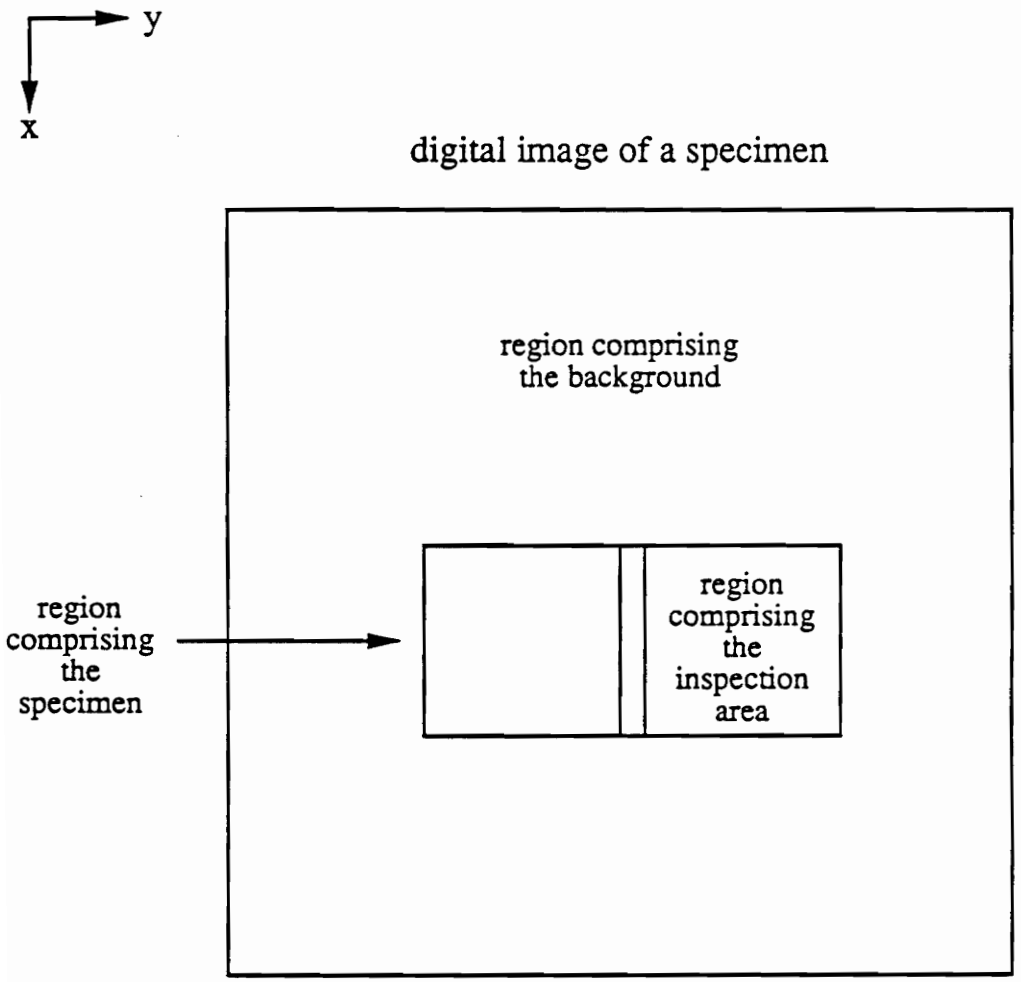

Figure 2–3 General form of a digital image of a specimen.

Typically $k = 8$ so that an element of any of the color component images ranges from 0 to 255. The elements $p_r(x,y)$, $p_g(x,y)$, and $p_b(x,y)$ represent the red level intensity, green level intensity, and blue level intensity, respectively, of the point in the scene that corresponds to the (x,y) location in C. A value of 0 for an element of a color component of C means that the corresponding point in the scene does not possess any of that component color. A value of 255 implies that the corresponding point in the scene is saturated in that component color. The vector $[p_r(x,y) \quad p_g(x,y) \quad p_b(x,y)]^t$ is called a pixel of the color image C.

To aid the explanation of geometrical operations, each pixel of P and C is considered a point in a two-dimensional rectangular coordinate plane. The positive x- and y-axes of the plane correspond to the rows and columns, respectively, of P and C such that the intensity level at location (x,y) in a given image has coordinates (x,y) in the image plane (see Figure 2–3).

The processing stage of the vision system must perform three operations. The first operation that must be performed is to determine which pixels in an image of a specimen represent the inspection area of the specimen and which represent the background. The second operation that must be performed is to determine which pixels in the inspection area of the specimen represent wood failure and which pixels represent glue failure. The algorithms employed must be able to perform this last operation regardless of the wood species or the glue formulation used in making the plywood from which the sample was taken. The algorithms used must also be able to handle instances of wood fiber, labeling pixels wood even though they may actually represent points of glue lying between wood fibers.

In the final operation, the results of applying the first two operations to the images of the specimens comprising a sample must be combined to determine the percent wood failure of that sample. This is achieved by mapping each pixel in the inspection area of one image onto its corresponding pixel in the inspection area of the other image, i.e., the pixel from which it was pulled apart during the shearing operation (see Figure 2–4). Each pixel pair derived from this mapping is evaluated as follows: 1) if both pixels represent wood failure, the pair constitute wood failure, 2) if both pixels represent glue failure, the pair constitute glue failure, and 3) if one pixel represents wood failure while the other pixel represents glue failure, the pair are considered to constitute glue failure since a failure of the glue to adhere to the wood is implied. The percentage of pixel pairs evaluated to be wood failure is the percent wood failure assigned to the sample.

2.3 Previous Work

A computer aided method for inspecting plywood shear samples was first proposed by McMillin [McMillin, 1984]. This method is neither completely automatic, since it requires manual intervention, nor does it aim to solve the complete problem. Its aim is limited to aiding an operator to determine the areas of the sample that represent wood failure and those that represent glue failure. Because of this limited objective a number of simplifications are employed, simplifications that are not possible in the more general problem setting. The method consists of five processing steps.

First, the specimen to be analyzed is scanned to create the needed digital image. Black and white images are used with an unspecified resolution. Only the inspection area is scanned so there is no need to have to separate pixels

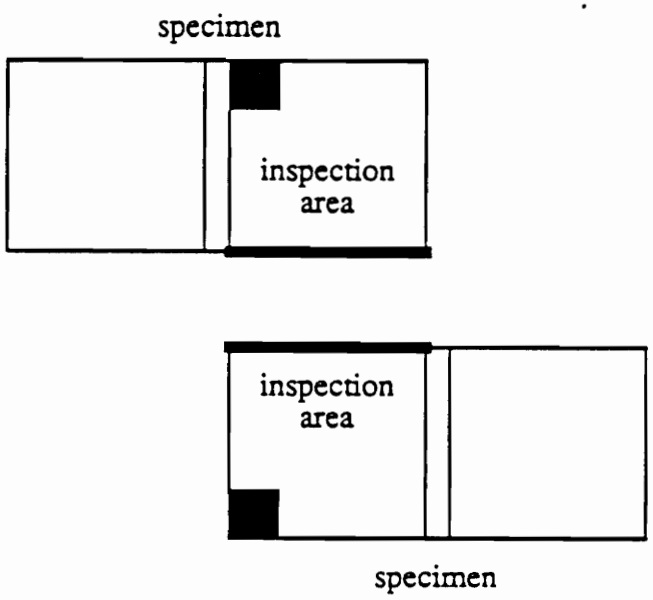

Figure 2–4 Corresponding areas in mapping operation.

of the inspection area from pixels of the background. Next, a gray level histogram H is computed from the image of the inspection area. The gray level histogram H of a black and white image is a column matrix containing k elements ranging from 0 to $k-1$, where k is the number of distinct gray levels that can be quantized by the particular scanning system utilized. Each element $h(i)$ of H is the number of pixels in the image that have gray level i.

The third step in the processing is to have a human operator determine a threshold, T, by inspecting a plot of H. The basis by which the operator is to make the selection comes from the fact that, in general, the glue used to bind plywood together is darker than wood. Hence, a pixel coming from an area of glue should have, in general, a smaller gray level value than a pixel coming from an area of wood. Since a pixel in the inspection area must come from either an area of glue or an area of wood, the graph of the gray level histogram tends to be bimodal. The optimum threshold to use in such cases to separate pixels of glue from pixels of wood is one that lies at the bottom of the valley between the two histogram peaks.

Figure 2–5 illustrates this procedure. The gray level values on the left half of the graph in Figure 2–5 are the gray level values of the pixels comprising the regions of glue in the image of the specimen inspection area. The gray level values on the right half of the graph are the gray level values of the pixels comprising the regions of wood. The gray level value corresponding to the valley between the two peaks in the graph is the gray level value that separates these two gray level ranges.

The fourth step is to automatically threshold an image of a specimen inspection area using the threshold value determined in Step 3. In the threshold operation, the gray levels of all pixels in the image of the specimen inspection

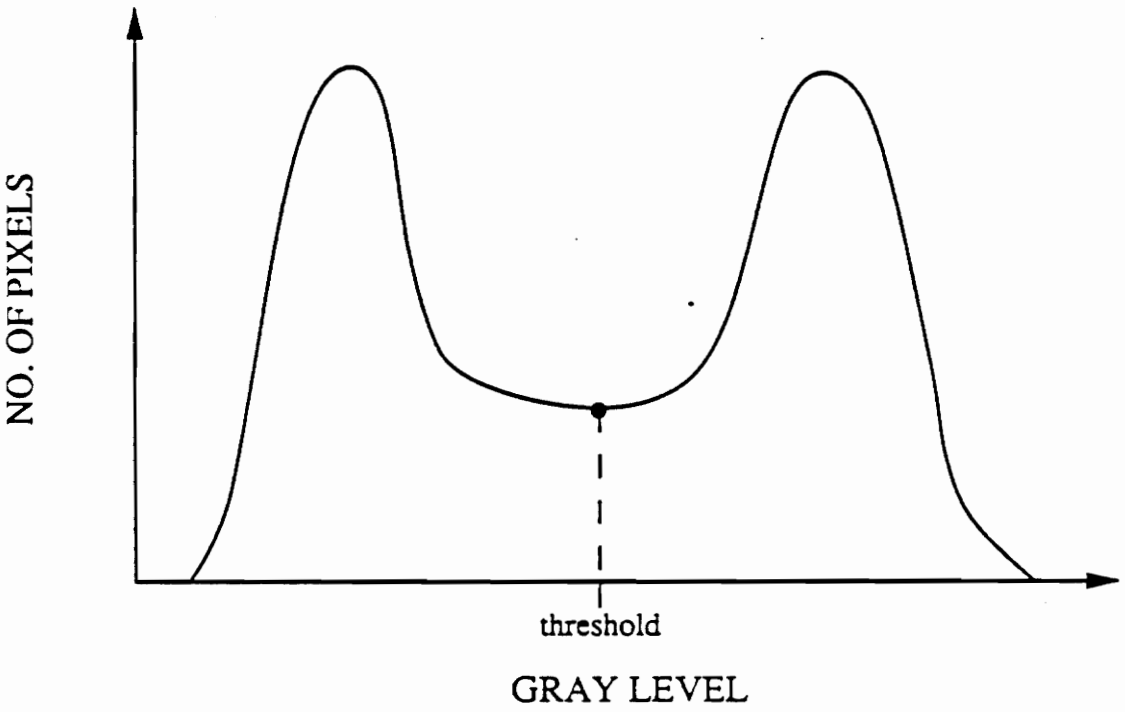

Figure 2–5 McMillin's method of threshold determination.

area that have gray level values greater than or equal to the threshold value are assigned the wood label. The gray levels of all pixels in the image of the specimen inspection area that have gray level values less than the threshold value are assigned the glue label. The final step is to automatically determine the percentage of pixels that were assigned the wood label in a thresholded image. This is the percent wood failure assigned to the associated specimen.

Although McMillin reports that the percent wood failure cumulative running averages between the human and computer evaluations of 320 samples showed no significant differences, the method described above is limited in four important ways. First, the procedure is not completely automatic, i.e., Step 3 is performed by a human. The use of a human in determining the appropriate threshold value from a gray level histogram defeats the purpose of automating the inspection process. Second, the percent wood failure of a sample is not determined. The percent wood failures of the individual specimens comprising a sample are determined, but the thresholded images of the inspection areas of the associated specimens are not compared in the manner described in Section 2.2.

Third, a region of wood fiber in the image of a specimen inspection area is thresholded as a region of glue failure. Experimentation has shown that fiber cannot be distinguished from glue in the gray level histogram of such an image. As discussed in Section 2.1, a region of fiber in the inspection area of a specimen is a region of wood failure. Finally, a scanning system in which only the inspection area of a specimen is scanned in order to create an image may not be feasible in an industrial setting. The images scanned in such a setting may consist of the entire specimen set against a background. No methods are given that will locate the specimen inspection area in such an image.

Despite these limitations, the results of McMillin's experiment indicate that a thresholding scheme based on the gray level histogram of a specimen inspection area is the basic approach to take in the design of a purely automated sytem.

2.4 Basic Approach

Our basic approach in automating the visual inspection task is to emulate the methodology employed by a human inspector. As explained in Section 2.2, the procedure used to automate this task is divided into two stages, the scanning stage and the processing stage. The scanning stage corresponds to the visual activity performed by a human inspector to see the pair of specimens comprising a sample. The processing stage corresponds to the mental activity utilized by a human inspector to determine the percent wood failure of the sample being viewed.

As discussed in Section 2.2, the processing stage is divided into three operations or steps: 1) location of the inspection areas of the two specimens comprising a sample, 2) location of the regions of wood and the regions of glue on these inspection areas, and 3) comparison of each pixel in the region comprising the inspection area of one specimen to the corresponding pixel in the region comprising the inspection area of the other specimen to determine the percent wood failure of the sample.

In the first and second processing steps, each of the images of the two specimens comprising a sample is processed separately. The input of the first processing step is an image of a specimen in the form given in Figure 2–3. The output is an image identical to the input image except that the region

comprising the inspection area has been extracted (set apart from the rest of the image in some way). The inspection area extraction is accomplished by first locating the region comprising the specimen. The pixels comprising the boundary of the region comprising the specimen are determined, and the boundary pixels that correspond to the sides (as opposed to the corners) of the specimen region are labeled. The line equations that approximate the four sides of the region comprising the specimen are calculated from the coordinates of the boundary pixels that have been labeled as corresponding to the sides of the specimen region. The region comprising the inspection area is determined geometrically from the line equations that approximate the four sides of the specimen region. These line equations are also used in the mapping function of the third processing step. The first processing step is discussed in more detail in Chapter 3.

The input of the second processing step is the output of the previous processing step, i.e., an image of a specimen in which the region comprising the inspection area has been determined. The output is an image identical to the input image except that the areas of wood in the region comprising the inspection area have been extracted. As discussed in Section 2.3, experimentation showed that wood fiber is usually indistinguishable from glue in the gray level histogram of the region comprising an inspection area; however, it was found that this histogram could be used to extract solid wood (wood that is not fiber). The method developed to accomplish this task determines an appropriate threshold value based on the number of peaks and the shape of the peaks in the gray level histogram of the region comprising the inspection area. This method is discussed in Chapter 4.

Further study revealed that fiber and glue tend to be indistinguishable within all one- and two-dimensional red, green, and blue level histograms. A

feature other than intensity or color would have to be utilized to distinguish the areas of fiber from the areas of glue. One such distinguishing feature is texture. The texture of glue tends to be smooth whereas that of fiber tends to be rough due to the separation of the individual wood strands within fiber. Furthermore, the orientation of each fiber strand within a region of glue is the same since each strand was shorn from the same layer of wood. Since plywood is composed of alternating grains of wood, the orientation of fiber is either vertical or horizontal with respect to the image in Figure 2–3. Experimentation showed that the orientation of the fiber within a region of glue could be determined from gray level histograms of the region if vertical and horizontal edge detectors are applied before the histograms are obtained. An appropriate threshold is determined by comparing the histogram of the region after the vertical edge detector is applied to the histogram of the region after the horizontal edge detector is applied. The region is then thresholded using the threshold value determined. This procedure is performed separately on all regions in the inspection area that were not extracted as solid wood during the previous thresholding operation. After a region in the inspection area has been thresholded and the fiber extracted in the manner described above, areas of glue between closely spaced strands of fiber extracted from this region are extracted as fiber due to APA specifications on what constitutes wood failure (see Section 2.1). The overall procedure for extracting fiber is discussed in more detail in Chapter 5.

In the third processing step, the results of the previous processing steps obtained from each of the images of the two specimens comprising a sample are combined to determine the percent wood failure of the sample. Each pixel in the region comprising the inspection area of one specimen is mapped to its corresponding pixel in the region comprising the inspection area of the other

specimen. Each pixel pair derived from this mapping is evaluated as explained in Section 2.2. The percentage of pixel pairs evaluated as wood failure is the percent wood failure assigned to the sample. This final processing step is discussed in Chapter 6.

2.5 Conventions

Let P_1 and P_2 denote images. A pixel in P_1 and a pixel in P_2 are said to correspond to one another if both pixels have the same coordinates in their respective images, i.e., the pixel $p_1(x, y)$ of P_1 and the pixel $p_2(x, y)$ of P_2 are said to correspond. A labeled image is a black and white image where the pixels comprising a region in this labeled image have the same gray level value such that any two pixels belonging to any two distinct regions in this labeled image have distinct gray level values.

3. INSPECTION AREA EXTRACTION

As discussed in Section 2.2, the processing stage of the automated vision system is divided into three steps. The first processing step is to locate the inspection areas of the two specimens comprising a sample. The algorithms employed to extract the region comprising the inspection area of one specimen do not require any information concerning the other specimen. Thus in this processing step, each of the images of the two specimens comprising a sample is processed separately, i.e., the operations discussed in this chapter are performed on one image at a time. After the image of one specimen has been processed, the identical operations are performed on the image of the other specimen.

Let C denote the color image of a specimen in the form given in Figure 2–3. The inputs of this processing step are the red and blue level component images of C, denoted by P_r and P_b, respectively. The output is a labeled image where a pixel in this labeled image has gray level value 255 if the corresponding pixel in both P_r and P_b is thought to be part of the region that corresponds to the inspection area of the specimen. Otherwise, a pixel in the labeled image will have gray level value 0. Let I_a denote this labeled image. Based on the discussion given in Section 2.4, this processing step is divided into the following five substeps: 1) specimen extraction, 2) specimen boundary extraction, 3) specimen side extraction, 4) line fitting of the specimen sides, and 5) inspection area determination.

3.1 Specimen Extraction

The inputs of this substep are P_r and P_b as described above. The output

is a labeled image where a pixel in this labeled image has gray level value 255 if the corresponding pixel in both P_r and P_b is thought to be part of the region that corresponds to the specimen. Otherwise, a pixel in the labeled image will have gray level value 0. Let S_a denote this labeled image.

In order to get maximum sensitivity from the 256 possible gray levels of the black and white images to be used in most of the analysis, the scanning parameters were set so that the darkest glue has a gray level of 0 while the lightest wood has a gray level of 255. While setting the scanning parameters in this manner provides the maximun sensitivity for differentiating glue from wood, it complicates the segmentation of the specimen from the background. To reduce the complexity of this segmentation operation, the red and blue color components of a color image of a specimen are used. The motivation for using the red and blue color components is due to the fact that the color of both wood and glue contains a substantial amount of red but almost no blue [Ng, 1990]. Hence, employing a blue background and using red and blue color components provides a simple method for accomplishing the required specimen/background differentiation.

A two-dimensional histogram is an extension of the one-dimensional histogram defined in Section 2.3. A two-dimensional histogram is a two-dimensional matrix containing 256 rows ranging from 0 to 255 and 256 columns ranging from 0 to 255 of integer values greater than or equal to zero. Let H_{rb} denote the red/blue two-dimensional histogram of P_r and P_b. Each element $h_{rb}(x, y)$ of the matrix H_{rb} represents the number of pixels in P_r having a red level value of x whose corresponding pixels in P_b have a blue level value of y.

A graph of the red/blue two-dimensional histogram of the black and white image shown in Figure 3–1 is shown in Figure 3–2. The gray level intensity at location (x, y) in the graph shown in Figure 3–2 is proportional to the number of pixels contained in element $h_{rb}(x, y)$ of H_{rb} derived from the color image of the specimen shown in Figure 3–1. A gray level intensity of pure black at location (x, y) in the graph of Figure 3–2 indicates that no pixels having an intensity level of x in P_r and an intensity level of y in P_b exist for the specimen of Figure 3–1 while a gray level intensity of pure white indicates the red and blue intensity combination with the highest frequency of occurrence.

The shapes and locations of the pixel clusters shown in Figure 3–2 tend to remain unchanged regardless of the specimen represented by C. Due to this observation, H_{rb} derived from one randomly chosen specimen is partitioned into two regions as shown in Figure 3–3. One of the partitioned regions contains the background pixel cluster while the other contains the specimen pixel cluster. The partitioning shown in Figure 3–3 was performed by a human through the use of graphic overlays. The region containing the background pixel cluster is partitioned to allow slight variation in background color. The elements of H_{rb} that comprise the region containing the background pixel cluster are set to 255 while the elements that comprise the region containing the specimen pixel cluster are set to 0. If $h_{rb}(x, y) = 0$, $s_a(x, y)$ is set equal to 255. If $h_{rb}(x, y) = 255$, $s_a(x, y)$ is set equal to 0. S_a for the specimen of Figure 3–1 is shown in Figure 3–4.

3.2 Specimen Boundary Extraction

The input of this substep is the labeled image S_a created by the specimen extractor as described in Section 3.1. The outputs are two column matrices,

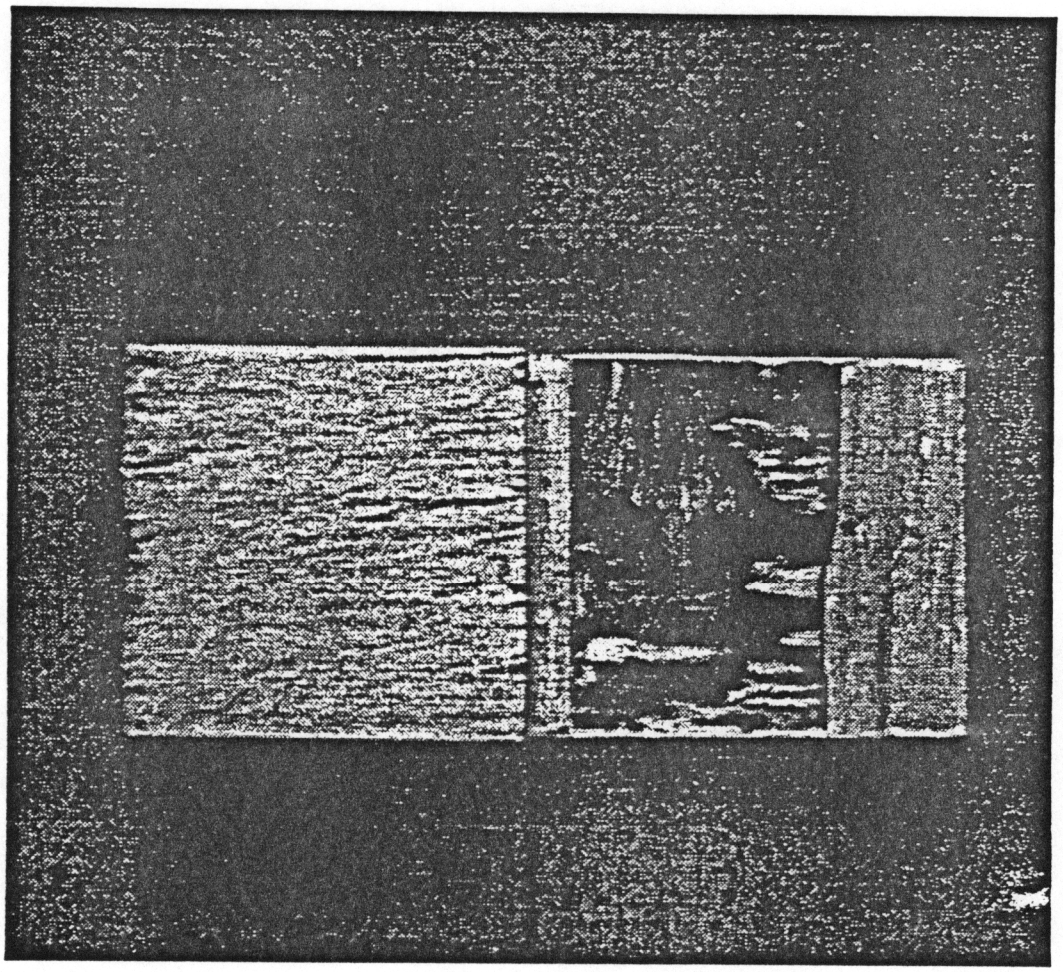

Figure 3–1 Black and white image of a specimen.

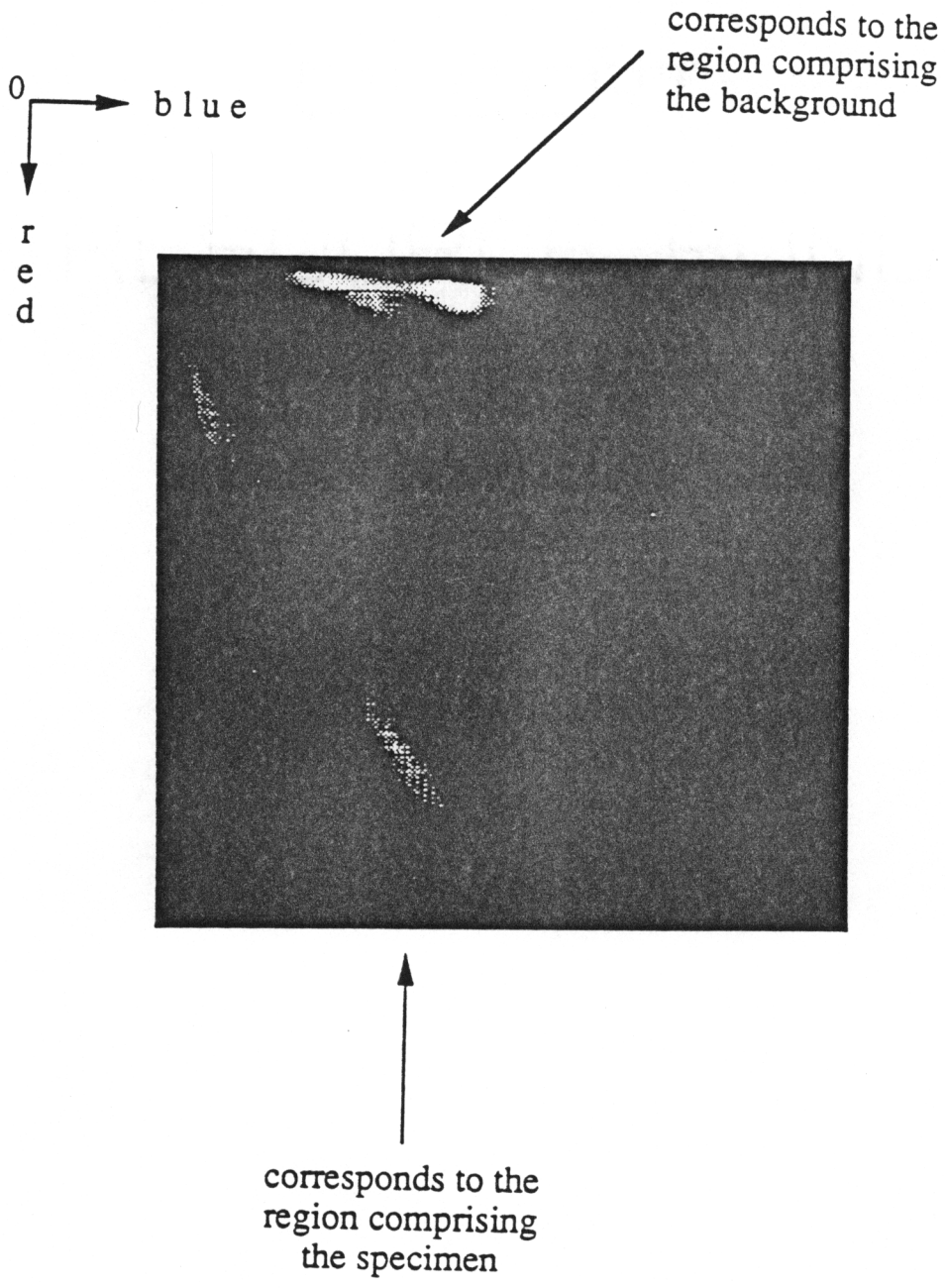

Figure 3–2 The red/blue 2-D histogram of the specimen of Figure 3–1.

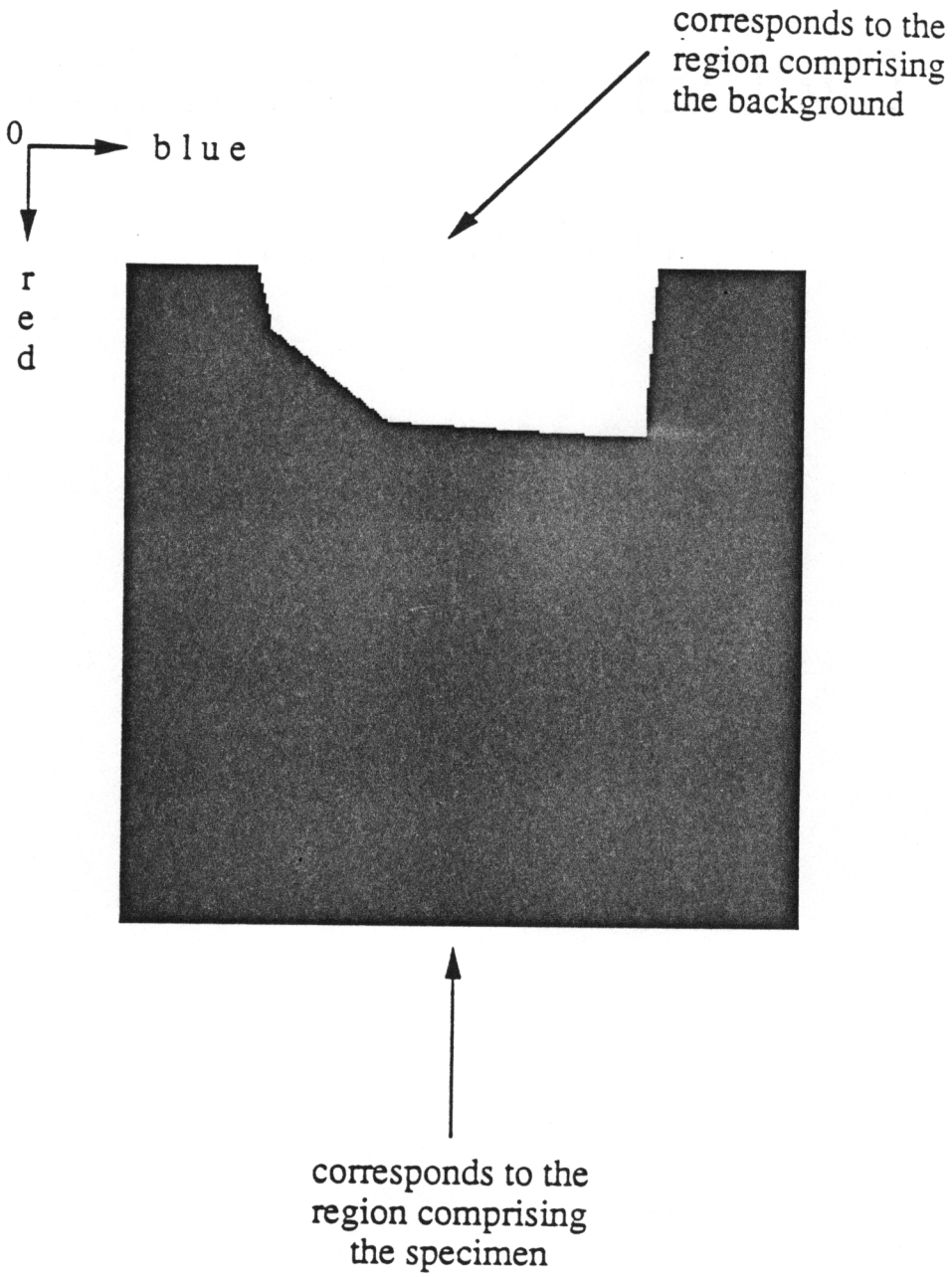

Figure 3–3 Partitioning of the graph of Figure 3–2.

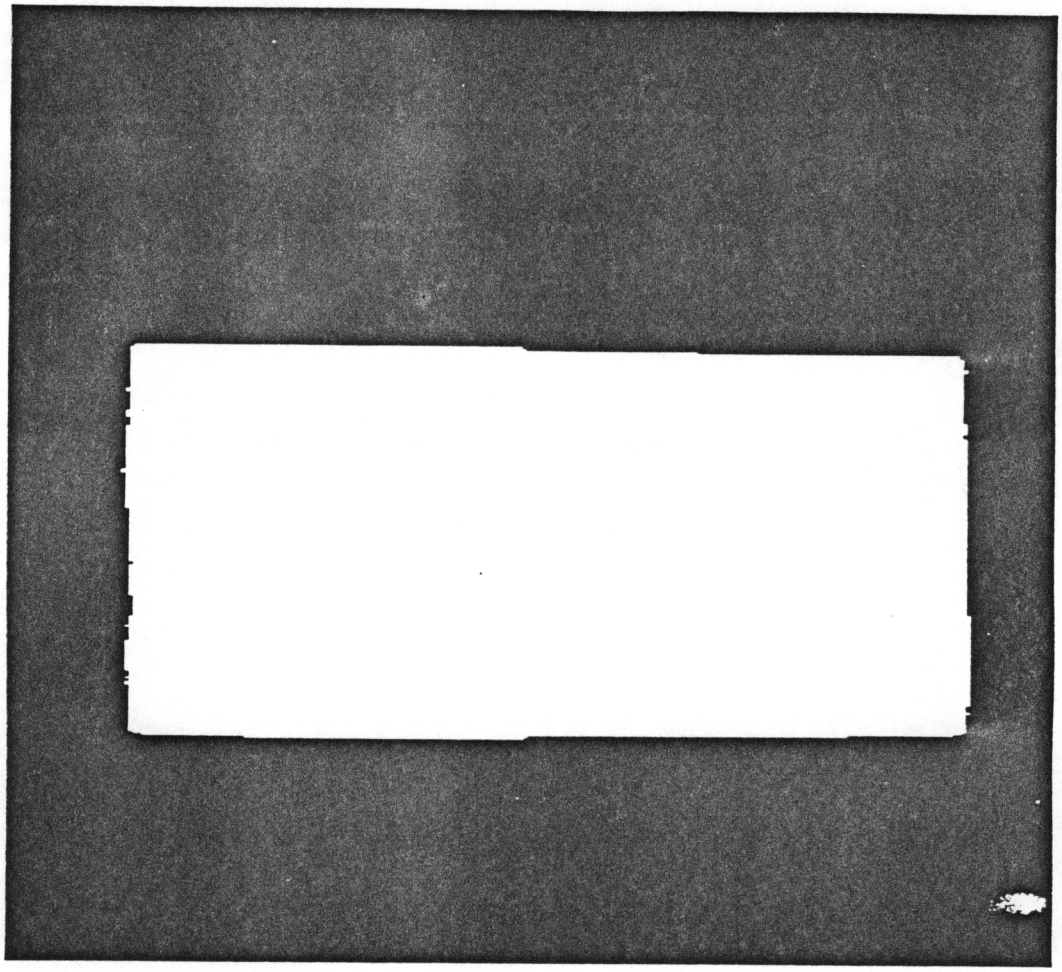

Figure 3–4 S_a for the specimen of Figure 3–1.

B_r and B_c, where the elements of B_r are the row numbers and the elements of B_c are the column numbers of the pixels comprising the specimen boundary in S_a. Two definitions are in order at this point. The pixels that are 8-connected to the pixel $s_a(x,y)$ in S_a are defined to be $s_a(x-1,y-1)$, $s_a(x-1,y)$, $s_a(x-1,y+1)$, $s_a(x,y-1)$, $s_a(x,y+1)$, $s_a(x+1,y-1)$, $s_a(x+1,y)$, and $s_a(x+1,y+1)$. A specimen boundary pixel is defined to be a pixel belonging to the set of pixels that comprise the specimen and 8-connected to one or more pixels belonging to the set of pixels that comprise the background in S_a. The elements $b_r(k)$ and $b_c(k)$ are the row number and column number, respectively, of the kth boundary pixel obtained by the specimen boundary extractor. Pixels represented by adjacent matrix elements are adjacent boundary pixels such that an ascending traversal of the matrix elements corresponds to a clockwise traversal of the specimen boundary.

The specimen boundary is extracted using a boundary following algorithm similar to the one given by Shirai [Shirai, 1987]. To explain this technique, let the vector $\underline{e}_k$ represent the kth edge element extracted by this procedure. To find $\underline{e}_1$, a row-by-row, pixel-by-pixel scan of S_a is performed until a specimen pixel is encountered. Note that the 8-connected region of this pixel must contain at least one pixel of the background. The row-column address of this first edge pixel are the components of $\underline{e}_1$. The element $b_r(1)$ of B_r is set equal to the row component of $\underline{e}_1$ and the element $b_c(1)$ of B_c is set equal to the column component of $\underline{e}_1$. The edge point $\underline{e}_2$ is found by scanning the 8-connected neighbors of $\underline{e}_1$ in a clockwise direction using the search procedure shown in Figure 3–5a. The element $b_r(2)$ of B_r is set equal to the row component of $\underline{e}_2$ and the element $b_c(2)$ of B_c is set equal to the column component of $\underline{e}_2$.

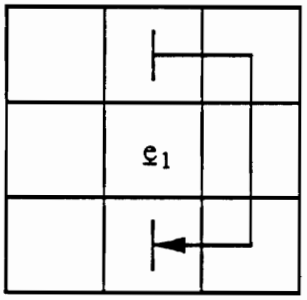

Figure 3–5 (a) Search procedure for $\underline{\varepsilon}_2$.

Once $\underline{e}_1$ and $\underline{e}_2$ have been found, the rest of the edge elements are found using the search geometries shown in Figure 3–5b. As can be seen in Figure 3–5b, the search procedure for locating edge point $\underline{e}_{k+1}$ is based on the known location of edge points $\underline{e}_k$ and $\underline{e}_{k-1}$. After $\underline{e}_{k+1} = (x_{k+1}, y_{k+1})$ is found, $b_r(k+1)$ is set equal to the row component, x_{k+1}, and $b_c(k+1)$ is set equal to the column component, y_{k+1}.

As edge points are being found it is possible that a "spike" can occur. An example of such a spike is shown in Figure 3–6. If $\underline{e}_k$ is the end pixel of a boundary spike, no specimen pixel will be found in the scan of the pixels that are 8-connected to $\underline{e}_k$ in the search for $\underline{e}_{k+1}$. In this case, the coordinates of $\underline{e}_k$ are eliminated from B_r and B_c, and a new scan is performed on the pixels that are 8-connected to $\underline{e}_{k-1}$. In this new scan, however, $\underline{e}_k$ is excluded from the scan. If no specimen pixel is encountered in this new scan, the coordinates of $\underline{e}_{k-1}$ are eliminated from B_r and B_c, and a new scan excluding $\underline{e}_{k-1}$ is performed on the pixels that are 8-connected to $\underline{e}_{k-2}$. This process is repeated until a specimen pixel is encountered in a scan. The first specimen pixel encountered is extracted as a specimen boundary pixel, and the algorithm resumes its normal manner of operation. Figure 3–7 shows the specimen boundary extracted (shown in white) for the specimen of Figure 3–1.

3.3 Specimen Side Extraction

The inputs of this substep are the matrices B_r and B_c created by the specimen boundary extractor as described in Section 3.2. The outputs are the matrices TS_r, TS_c, RS_r, RS_c, BS_r, BS_c, LS_r, LS_c where TS_r is a column matrix containing the row coordinates of the clockwise ordered boundary pixels of

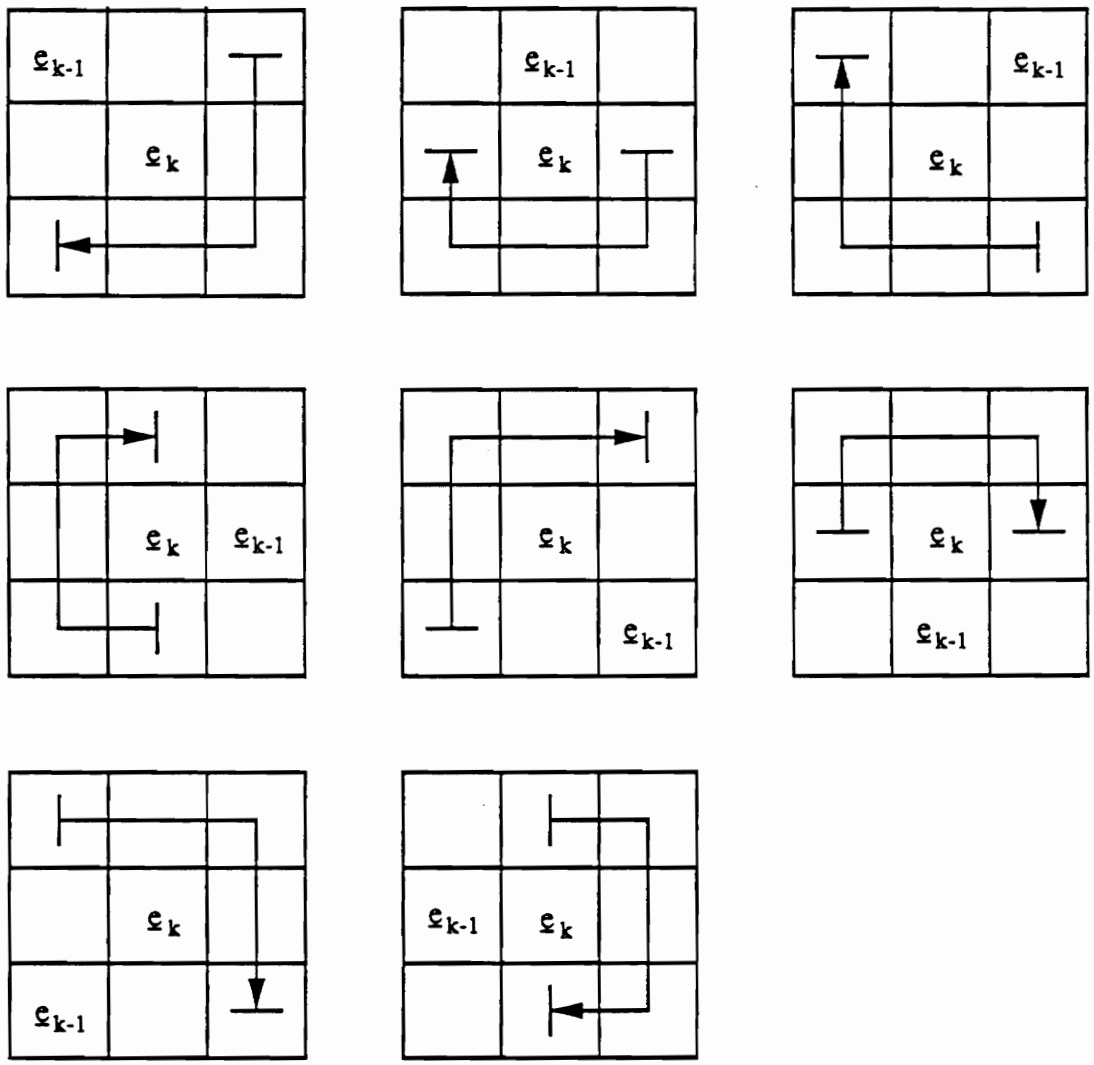

Figure 3–5 (b) Search procedure for $\underline{e}_{k+1}$.

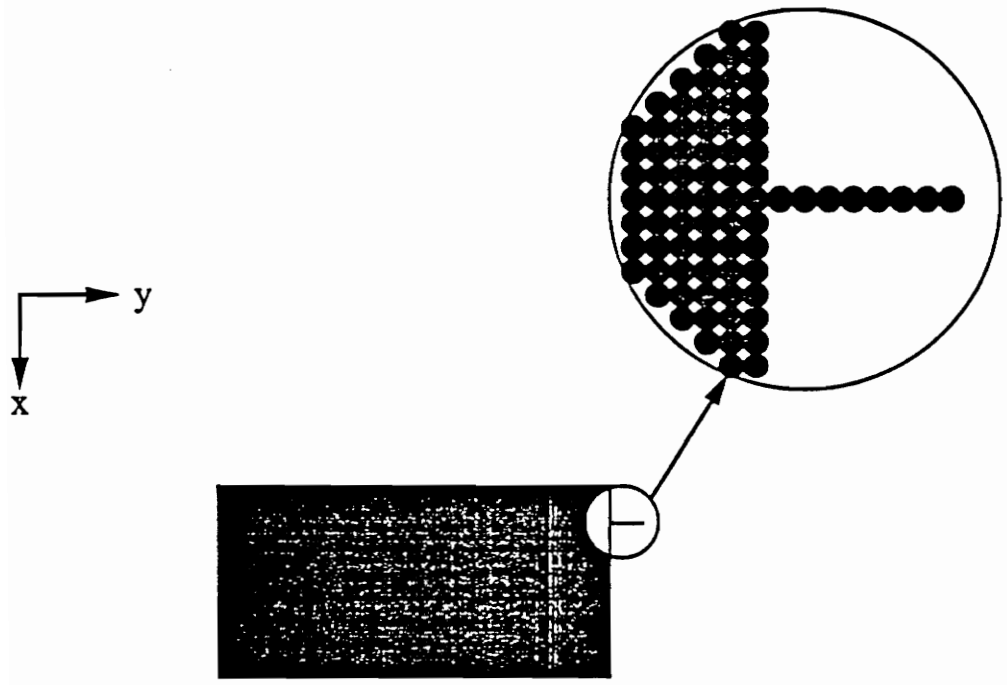

Figure 3–6 An example of an edge spike.

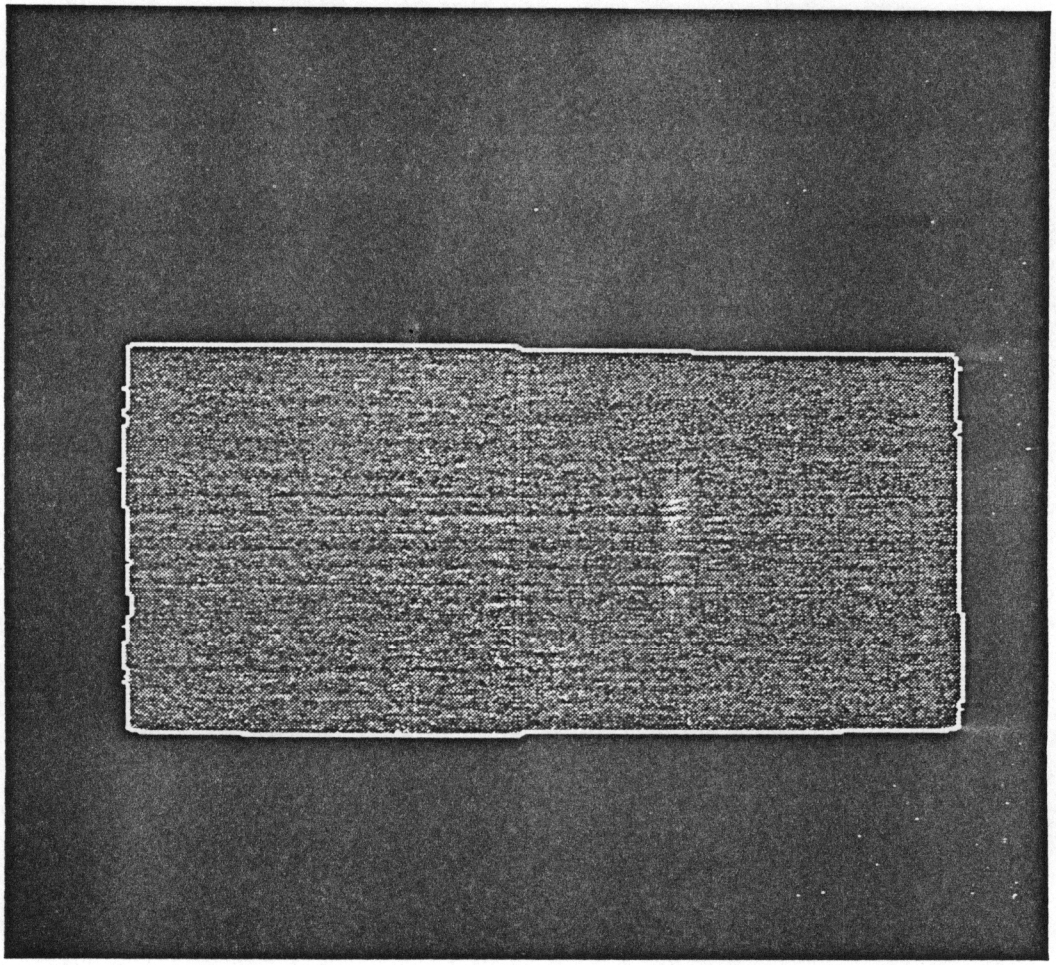

Figure 3–7 Boundary extracted for the specimen of Figure 3–1.

the top side of a specimen, TS_c is a column matrix containing the column coordinates of the clockwise ordered boundary pixels of the top side of a specimen, RS_r is a column matrix containing the row coordinates of the clockwise ordered boundary pixels of the right side of a specimen, RS_c is a column matrix containing the column coordinates of the clockwise ordered boundary pixels of the right side of a specimen, BS_r is a column matrix containing the row coordinates of the clockwise ordered boundary pixels of the bottom side of a specimen, BS_c is a column matrix containing the column coordinates of the clockwise ordered boundary pixels of the bottom side of a specimen, LS_r is a column matrix containing the row coordinates of the clockwise ordered boundary pixels of the left side of a specimen, LS_c is a column matrix containing the column coordinates of the clockwise ordered boundary pixels of the left side of a specimen. The pixels in S_a that comprise the corners of the specimen boundary are not included in the output matrices.

The side extraction substep comprises four tasks. The first task is to evaluate the function, f, given by

$$a(k) = d_t(b_r(k)) = \frac{\sum_{n=k}^{k+\Delta} [b_r(n) - b_r(n-\Delta)]}{\Delta + 1}, \qquad (3-1)$$

for each element $b_r(k)$ in B_r where Δ is a preselected positive integer. The results of f are stored in the column matrix A. Because of the nature of f, A and B_r have the same number of rows, say N rows. In performing the evaluation of f and for other calculations to be described later, it is convenient to consider B_r and A as "circular" matrices, i.e., if $k = 1$ then $a(k-1) = a(N)$ where $a(N)$ is the last element of A. Likewise if $k = N$ then $a(k+1) = a(1)$.

The motivation for using the function d_t comes form differential geometry [Kreyszig, 1972]. It is well known that any arbitrary curve lying in the x-y

plane can be parameterized as a function of one variable. The curve is then given by the vector valued function $\underline{x}(t) = (x(t), y(t))$. The function d_t represents an approximation of $dx(t)/dt$ averaged over $\Delta + 1$ points. This average is used to reduce the noise on the estimated value of the derivative. Since the sides of a specimen are relatively straight, the row numbers of specimen boundary pixels in S_a lying along the same side vary linearly. The values of A for pixels lying on such a straight boundary should all be approximately equal. Since the row numbers of specimen boundary pixels in S_a lying along a corner change in an abrupt, nonlinear fashion, the values of A for these pixels tend to differ significantly in magnitude. Figure 3–8a shows the values of A for the specimen of Figure 3–1. The use of B_c in place of B_r in equation (3–1) produces similar results.

Since the values of A are relatively constant for side boundary pixels but change abruptly for corner boundary pixels, numerical differentiation of each element $a(k)$ of A is performed to distinguish these two types of specimen boundary pixels. This second task of the side extraction substep is developed from basic calculus [James, 1977]. The Taylor series for the function $y = f(x)$ at x_{i+h} expanded about x_i is

$$f(x_{i+h}) = y_{i+h} = y_i + y_i' h + \frac{y_i'' h^2}{2!} + \frac{y_i''' h^3}{3!} + \cdots, \qquad (3-2)$$

where h is a nonnegative integer. The function at x_{i-h} is similarly given by

$$f(x_{i-h}) = y_{i-h} = y_i - y_i' h + \frac{y_i'' h^2}{2!} - \frac{y_i''' h^3}{3!} + \cdots. \qquad (3-3)$$

Subtracting equation (3–3) from equation (3–2) and neglecting all but the first four terms of the resulting difference yields

$$y_{i+h} - y_{i-h} = 2\left(y_i' h + \frac{y_i''' h^3}{3!} + \frac{y_i^{(5)} h^5}{5!} + \frac{y_i^{(7)} h^7}{7!}\right). \qquad (3-4)$$

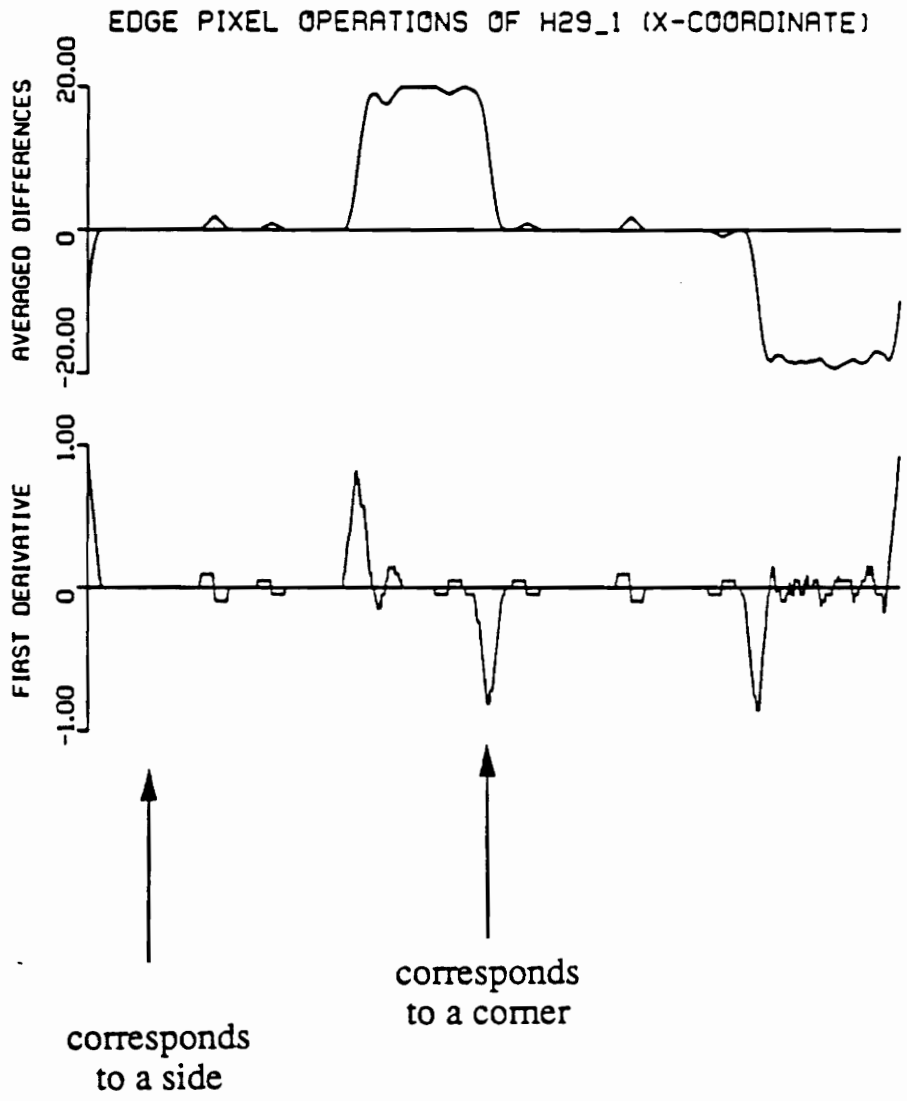

Figure 3–8 (a) Averaged differences and (b) first derivative of B_r.

Setting h successively to 1, 2, 3, and 4 in equation (3–4) produces a set of four linear equations given by the matrix equation

$$2\begin{bmatrix} 1 & 1/3! & 1/5! & 1/7! \\ 2 & 2^3/3! & 2^5/5! & 2^7/7! \\ 3 & 3^3/3! & 3^5/5! & 3^7/7! \\ 4 & 4^3/3! & 4^5/5! & 4^7/7! \end{bmatrix}\begin{bmatrix} y_i' \\ y_i''' \\ y_i^{(5)} \\ y_i^{(7)} \end{bmatrix} = \begin{bmatrix} y_{i+1} - y_{i-1} \\ y_{i+2} - y_{i-2} \\ y_{i+3} - y_{i-3} \\ y_{i+4} - y_{i-4} \end{bmatrix}. \qquad (3-5)$$

Solving for y_i' in equation (3–5) yields

$$y_i' = 0.8(y_{i+1} - y_{i-1}) - 0.2(y_{i+2} - y_{i-2}) + 0.038095238(y_{i+3} - y_{i-3}) - 0.003571428(y_{i+4} - y_{i-4}). \qquad (3-6)$$

Let the mapping defined by equation (3–6) be denoted d_{t^2}. Evaluating d_{t^2} on the elements of A is an approximation of the derivative of d_t. Conceptually d_{t^2} approximates $d(\overline{dx(t)/dt})/dt$ where $\overline{dx(t)/dt}$ is a smoothed version of $dx(t)/dt$ discussed above. In equation (3–6) $y_i = a(i)$, $y_{i-1} = a(i-1)$, $y_{i+1} = a(i+1)$, etc., with A being treated as a "circular" matrix. The result of each evaluation is stored in the matrix D, i.e., $d(i) = d_{t^2}(a(i)) = y_i'$.

Obviously, when the values of A are constant (side boundary pixels), the corresponding values of D are approximately zero. When the values of A change abruptly (corner boundary pixels), the corresponding values of D have high magnitude and resemble a sharp spike. Figure 3–8b shows the values of D corresponding to the values of A shown in Figure 3–8a. The Taylor series expansions used in the derivation of equation (3–6) could have included more terms; however, studies suggest that additional accuracy is not required to extract the specimen sides.

The averaging width parameter Δ used in equation (3–1) is adjusted experimentally and is a function of the image resolution. If the resolution is

high, Δ should be high; if the resolution is low, Δ should be low, also. If Δ is set too low, the values of A will be noisy so that the corresponding values of D might contain large spikes for boundary pixels other than corner boundary pixels. This could cause the detection of false corners during later processing in this substep. If Δ is set too high, the values of A for corner boundary pixels will change gradually rather than abruptly. The resulting spikes contained in the corresponding values of D will be short and elongated so that some corners may be overlooked. In the processing of the specimens used in the experiment set, a Δ value of 20 yielded the best results.

Using the values of D, the third task of the side extraction substep is to determine which specimen boundary pixels lie on the corners of the specimen in S_a. This is accomplished by setting to zero the elements of B_r that correspond to the corner boundary pixels, i.e., $b_r(k)$ is set to zero if $b_r(k)$ is the row number of a corner boundary pixel. As explained above, the elements of D that contain spikes correspond to corner boundary pixels. Since a spike is a local maximum in magnitude, the task is implemented as follows. The row number in B_r of the specimen boundary pixel having the maximum value in D is set to zero. Let $b_r(k)$ denote the row number of the specimen boundary pixel having the maximum value in D. Since, at our scanning resolution, the length of a specimen boundary at a corner is approximately 15 pixels, the elements $b_r(k-7)$ through $b_r(k-1)$ and $b_r(k+1)$ through $b_r(k+7)$ are set to zero in addition to $b_r(k)$ being set to zero. The value of $d(k)$ and the values of D corresponding to all adjacent pixels within half an inch on either side of the specimen boundary pixel corresponding to $d(k)$ are set to zero so that a new maximum in D can be found. Since the specimen contains four corners, the process is repeated three times.

In the last task, the row numbers and column numbers of the specimen boundary pixels having a nonzero row number in B_r are copied into the appropriate pair of output matrices. Figure 3–9 shows the three possible locations of the boundary pixel represented by $b_r(1)$. It is assumed that the boundary pixel represented by $b_r(1)$ is positioned as shown in either Figure 3–9a or Figure 3–9c (this assumption will be tested and, if necessary, the appropriate corrections will be made). B_r is traversed starting at $b_r(1)$ until an element is found to be zero. Under the aforementioned assumption, the boundary pixel represented by the first element of B_r found to be zero is located on the top right corner of the specimen in S_a. From this point, B_r is traversed until an element is found to be nonzero. From this point, B_r is again traversed until an element is found to be zero; however, in this traversal the row number and column number in B_r and B_c, respectively, of the boundary pixel associated with each element traversed in B_r are copied into RS_r and RS_c, respectively. After an element of B_r is found to be zero in this last traversal, B_r is traversed until an element of B_r is found to be nonzero. After an element of B_r is found to be nonzero, B_r is traversed until an element of B_r is found to be zero. During this traversal, the row number and column number in B_r and B_c, respectively, of the boundary pixel associated with each element traversed in B_r are copied into BS_r and BS_c, respectively. The procedure is repeated until all four pairs of output matrices are filled.

If the number of elements in TS_r is greater than the number of elements in RS_r, the assumption that the boundary pixel in S_a associated with $b_r(1)$ is positioned as shown in either Figure 3–9a or Figure 3–9c is true since the top side of the specimen is longer than the right side of the specimen. If the number of elements in TS_r is less than the number of elements in RS_r, the assumption that the boundary pixel in S_a associated with $b_r(1)$ is positioned

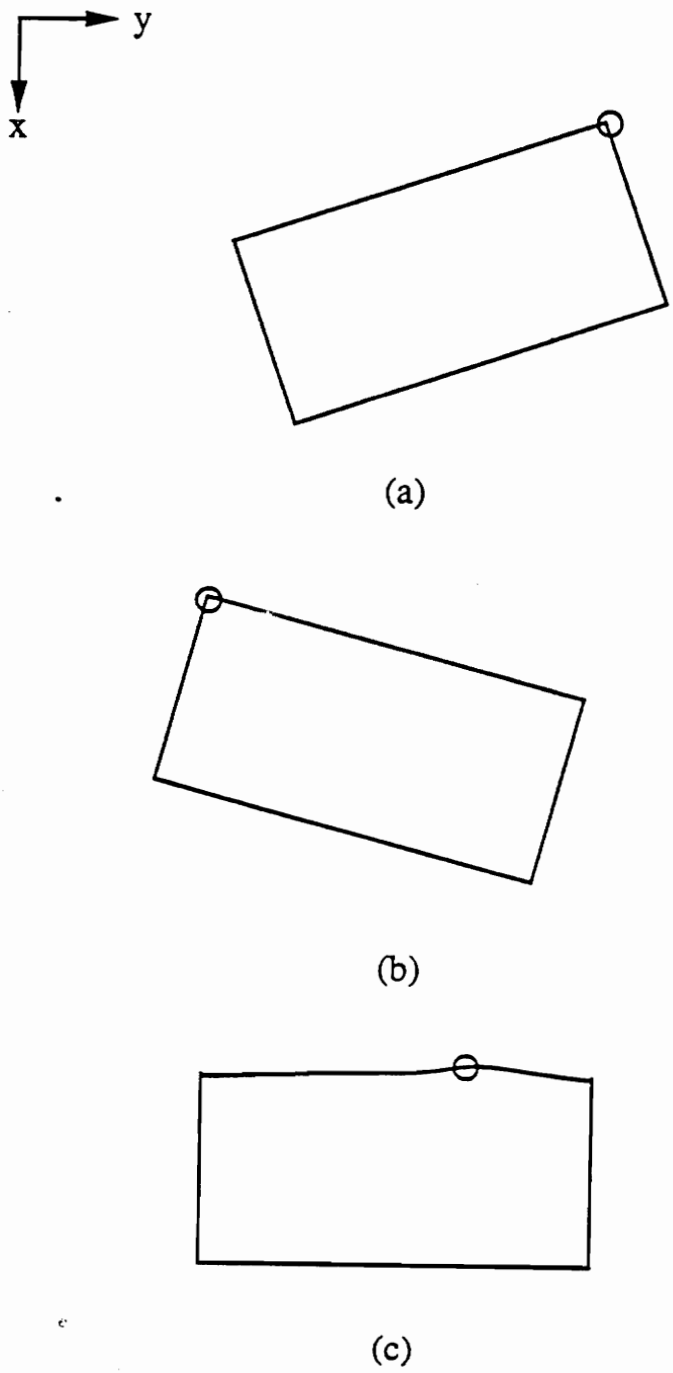

Figure 3–9 Possible locations of $b_r(1)$.

as shown in either Figure 3–9a or Figure 3–9c is false and the boundary pixel represented by $b_r(1)$ is positioned as shown in Figure 3–9b. In this case, the row and column numbers stored in RS_r and RS_c, respectively, are the row and column numbers of the boundary pixels located on the top side of the specimen, the row and column numbers stored in BS_r and BS_c, respectively, are the row and column numbers of the boundary pixels located on the right side of the specimen, etc., and the appropriate transferrals of values are made among the four pairs of output matrices. Figure 3–10 shows the side boundary pixels (in white) extracted for the specimen of Figure 3–1.

3.4 Line Fitting of the Specimen Sides

The inputs of this substep are the four pairs of output matrices created by the previous substep as described in Section 3.3. The outputs are the variables m_{TS}, b_{TS}, m_{RS}, b_{RS}, m_{BS}, b_{BS}, m_{LS}, and b_{LS} such that $x = m_{TS}y + b_{TS}$ is the straight line that best fits a specimen's top side boundary segment, $y = m_{RS}x + b_{RS}$ is the straight line that best fits a specimen's right side boundary segment, $x = m_{BS}y + b_{BS}$ is the straight line that best fits a specimen's bottom side boundary segment, and $y = m_{LS}x + b_{LS}$ is the straight line that best fits a specimen's left side boundary segment. These line equations are given with respect to the coordinate system shown in Figure 2–3. The forms of these equations ($y = mx + b$ or $x = my + b$) were chosen so as to ensure that none of the slopes computed would be infinite.

The line fitting method used is the least-squares approximation method (Scheid, 1968). Let $O = \{(x_1, y_1), (x_2, y_2), \ldots, (x_n, y_n)\}$ be a set of n observed data points and $y = mx + b$ be the line that "best" approximates O. The computed

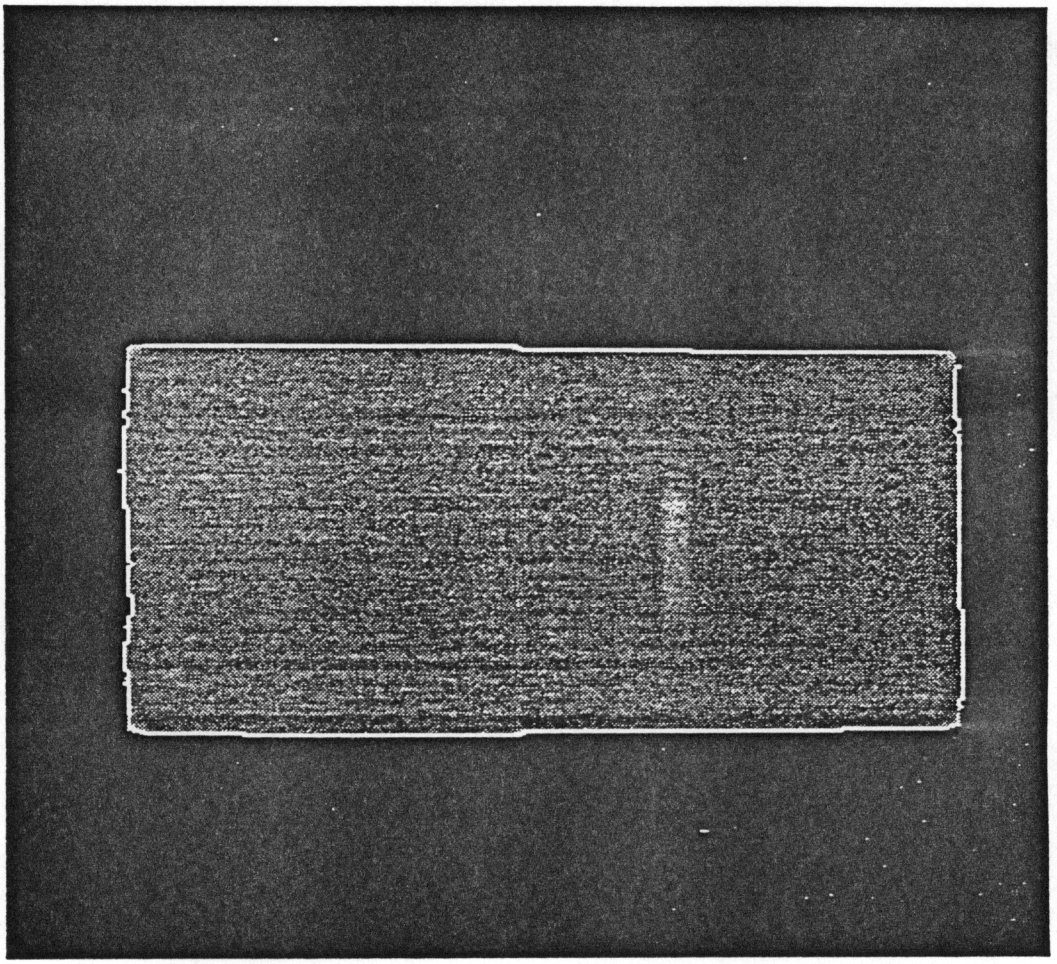

Figure 3–10 Side boundary pixels for the specimen of Figure 3–1.

value of y for any observed x_i is thus given by $mx_i + b$. The residual, or error, is the difference between the observed y_i and the computed y for a given x_i:

$$r_i = y_i - (mx_i + b). \tag{3-7}$$

The line that best approximates O is the line that minimizes the sum of the squares of all the residuals:

$$\begin{aligned}\sum_{i=1}^{n} r_i^2 &= \sum_{i=1}^{n} [y_i - (mx_i + b)]^2 \\ &= \sum_{i=1}^{n} (y_i^2 - 2mx_iy_i - 2by_i + m^2y_i^2 + 2mbx_i + b^2). \end{aligned} \tag{3-8}$$

The values of m and b that minimize equation (3–8) are found by 1) taking the partial derivatives of the equation with respect to m and b, and 2) setting the resulting equations equal to zero and solving for m and b. Taking the partial derivatives of equation (3–8) yields:

$$\frac{\partial}{\partial m} \sum_{i=1}^{n} (y_i^2 - 2mx_iy_i - 2by_i + m^2x_i^2 + 2mbx_i + b^2) = \sum_{i=1}^{n} (-2x_iy_i + 2mx_i^2 + 2bx_i); \tag{3-9}$$

$$\frac{\partial}{\partial b} \sum_{i=1}^{n} (y_i^2 - 2mx_iy_i - 2by_i + m^2x_i^2 + 2mbx_i + b^2) = \sum_{i=1}^{n} (-2y_i + 2mx_i + 2b). \tag{3-10}$$

Setting equations (3–9) and (3–10) equal to zero gives us:

$$m \sum_{i=1}^{n} x_i^2 + b \sum_{i=1}^{n} x_i = \sum_{i=1}^{n} x_iy_i; \tag{3-11}$$

$$m \sum_{i=1}^{n} x_i + bn = \sum_{i=1}^{n} y_i. \tag{3-12}$$

The solutions to the simultaneous equations (3–11) and (3–12) are:

$$m = \frac{\sum_{i=1}^{n} x_iy_i - \frac{1}{n} \sum_{i=1}^{n} x_i \sum_{i=1}^{n} y_i}{\sum_{i=1}^{n} x_i^2 - \frac{1}{n} \left(\sum_{i=1}^{n} x_i \right)^2}; \tag{3-13}$$

$$b = \frac{1}{n} \sum_{i=1}^{n} y_i - \frac{m}{n} \sum_{i=1}^{n} x_i. \tag{3-14}$$

If the equation $x = my + b$ is used to approximate O, equations (3–13) and (3–14) are the same except that x_i is replaced by y_i and y_i is replaced by x_i.

In either case, x_i is the row number and y_i is the column number in the ith elements of the appropriate pair of input matrices (TS_r and TS_c or RS_r and RS_c or etc.). Figure 3–11 shows the lines computed (in white) for the specimen of Figure 3–1.

3.5 Inspection Area Determination

The inputs of this substep are m_{TS}, b_{TS}, m_{RS}, b_{RS}, m_{BS}, b_{BS}, m_{LS}, b_{LS}, and the image S_a. The output is the final output of this processing step, the image I_a described at the beginning of this chapter. Recall that the region comprising the inspection area does not encompass the entire specimen; it is a one-inch by one-inch square subregion of the region comprising the specimen as shown in Figure 2–3. The right side boundary of the region comprising the inspection area is the right side boundary of the region comprising the specimen while the top and bottom side boundaries of the region comprising the inspection area are subboundaries of the top and bottom side boundaries, respectively, of the region comprising the specimen. Hence, the line equations that approximate the top, right, and bottom side boundaries of the region comprising the specimen approximate the top, right, and bottom side boundaries, respectively, of the region comprising the inspection area. The left side boundary of the region comprising the inspection area is not a subboundary of the left side boundary of the region comprising the specimen although the two boundaries are parallel. Since the dimensions of the region comprising the inspection area are known, the line equation that approximates the left side boundary of the region comprising the inspection area is computed from the line equations that approximate the other three side boundaries of this region. The region comprising the inspection area is the region bounded by the lines described by these four equations.

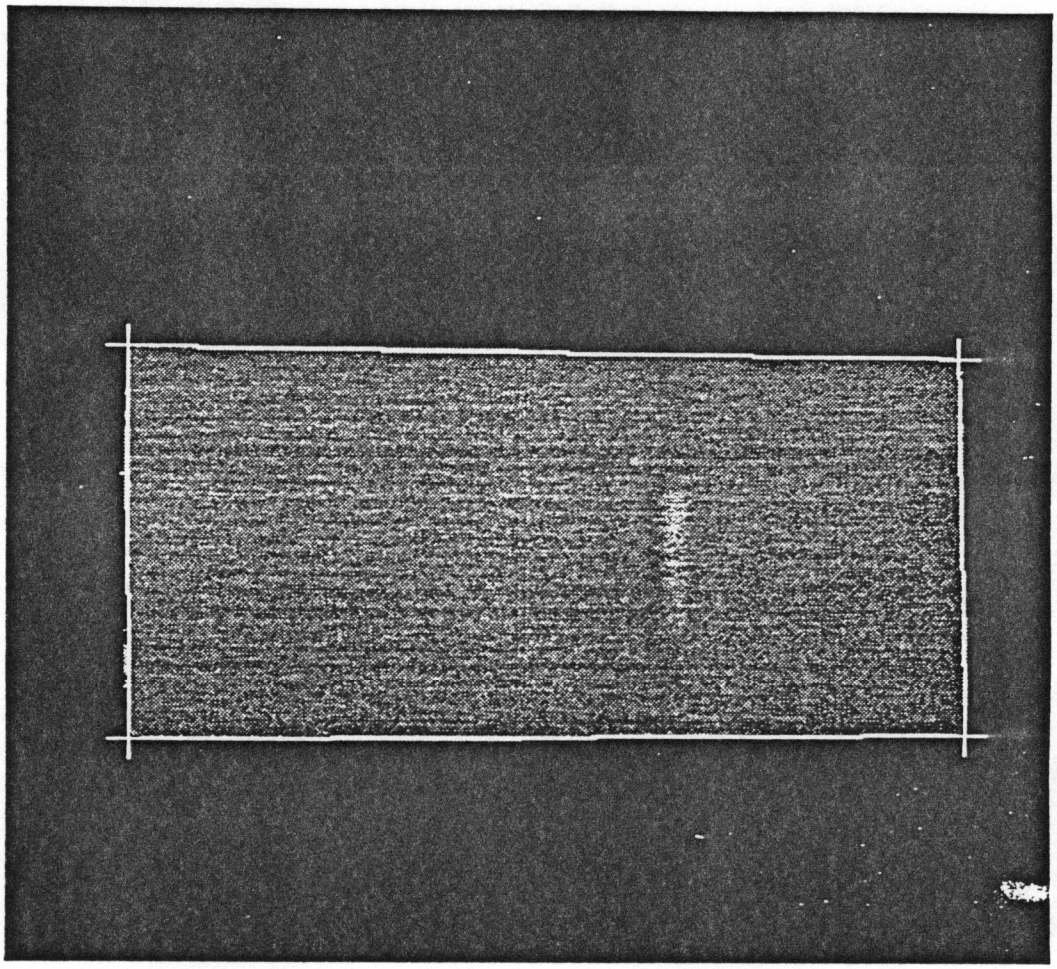

Figure 3–11 Lines computed for the specimen of Figure 3–1.

Let L_{TS}, L_{RS}, and L_{BS} denote the graphs of the line equations that approximate the top, right, and bottom side boundaries, respectively, of both the region comprising the specimen and the region comprising the inspection area (since the line equations are the same for both sets of boundaries). Let L_{LS} and L'_{LS} denote the graphs of the line equations that approximate the left side boundaries of the region comprising the specimen and the region comprising the inspection area, respectively. A graph L of the equation $y = mx+b$ is the set of all points (x, y) that satisfy the equation. Furthermore, let V_{UR}, V_{LR}, V_{LL}, V_{UL}, V'_{LL}, and V'_{UL} denote the specimen vertices formed by the intersection of the graphs of straight lines that define a specimen's boundaries where V_{UR} is the intersection of L_{TS} and L_{RS}, V_{LR} is the intersection of L_{RS} and L_{BS}, V_{LL} is the intersection of L_{BS} and L_{LS}, V_{UL} is the intersection of L_{LS} and L_{TS}, V'_{LL} is the intersection of L_{BS} and L'_{LS}, and V'_{UL} is the intersection of L'_{LS} and L_{TS}. These notations are illustrated in Figure 3–12. Since, as mentioned above, L_{LS} and L'_{LS} are parallel, L'_{LS} has the same line equation form as L_{LS}, i.e., L'_{LS} is the graph of $y = m'_{LS}x + b'_{LS}$ where m'_{LS} and b'_{LS} are the values that must be found. By equating the y's of L_{TS} and L_{RS} and solving for x, the coordinates of V_{UR} found are given by:

$$V_{UR} = (x_{UR}, y_{UR});$$

$$x_{UR} = \frac{m_{TS}b_{RS} + b_{TS}}{1 - m_{TS}m_{RS}}, \tag{3-15}$$

$$y_{UR} = m_{RS}x_{UR} + b_{RS}. \tag{3-16}$$

V_{LR} is given similarly by:

$$V_{LR} = (x_{LR}, y_{LR});$$

$$x_{LR} = \frac{m_{BS}b_{RS} + b_{BS}}{1 - m_{BS}m_{RS}}, \tag{3-17}$$

$$y_{LR} = m_{RS}x_{LR} + b_{RS}. \tag{3-18}$$

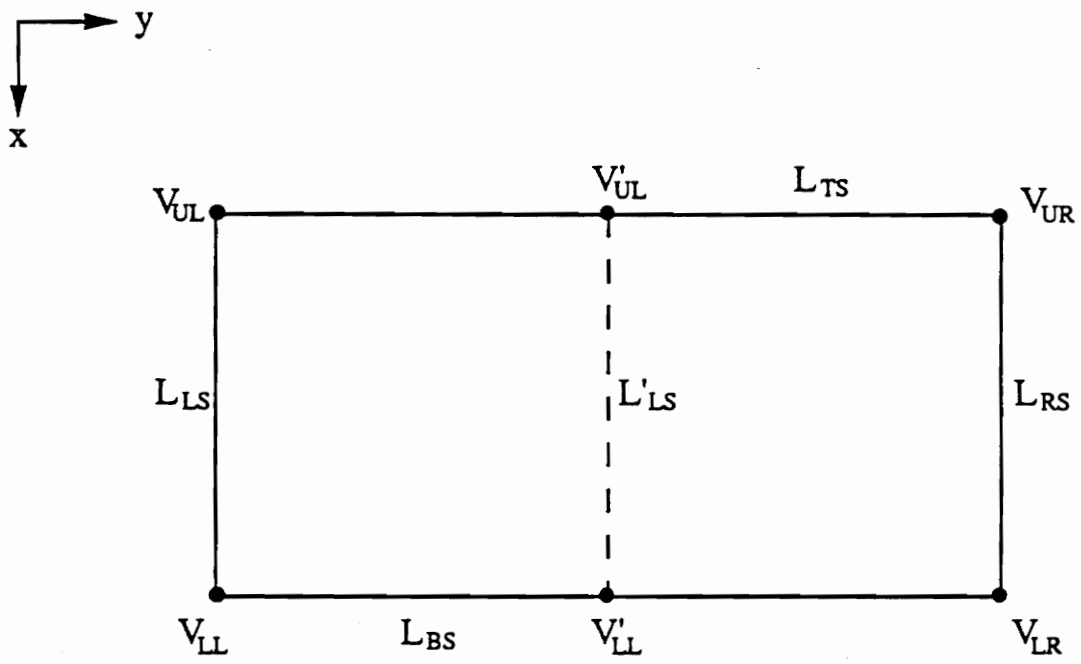

Figure 3–12 Line and vertex notation of a specimen.

V'_{UL} and V'_{LL} lie one inch in the left direction from V_{UR} along L_{TS} and from V_{LR} along L_{BS}, respectively. Since, by definition, V'_{UL} and V'_{LL} lie along L'_{LS}, m'_{LS} and b'_{LS} are computed from the coordinates of these two points.

Figure 3–13 illustrates the procedure for determining the y-coordinates of V'_{UL} and V'_{LL} for the case involving V'_{UL}. From trigonometry, the difference in y-coordinates, Δy, is given by

$$\Delta y = l \cos\theta, \tag{3-19}$$

where $\theta = \arctan m_{TS}$ (since L_{TS} is given by $x = m_{TS}y + b_{TS}$) and l is equal to the number of pixels in an inch. Because cameras do have aspect ratios that are not always 1-to-1, the variable l is a function of spatial orientation. Let h be the number of pixels in a horizontal inch and v be the number of pixels in a vertical inch. These parameters are functions of the scanning resolution and were experimentally found in our case to be 191 and 186, respectively. The determination of l for the case involving V'_{UL} is illustrated in Figure 3–14, where it is found to be:

$$l = h - (\phi)(2/\pi)(h - v), \tag{3-20}$$

where $\phi = |\arctan m_{TS}|$. Since, by definition, V'_{UL} and V'_{LL} lie on L_{TS} and L_{BS}, respectively, V'_{UL} is given by

$$V'_{UL} = (x'_{UL}, y'_{UL});$$

$$y'_{UL} = y_{UR} - \Delta y, \tag{3-21}$$

$$x'_{UL} = m_{TS}y'_{UL} + b_{TS}. \tag{3-22}$$

By replacing m_{TS} in equations (3–19) and (3–20) with m_{BS}, V'_{LL} is given similarly by

$$V'_{LL} = (x'_{LL}, y'_{LL});$$

$$y'_{LL} = y_{LR} - \Delta y, \tag{3-23}$$

$$x'_{LL} = m_{BS}y'_{LL} + b_{BS}. \tag{3-24}$$

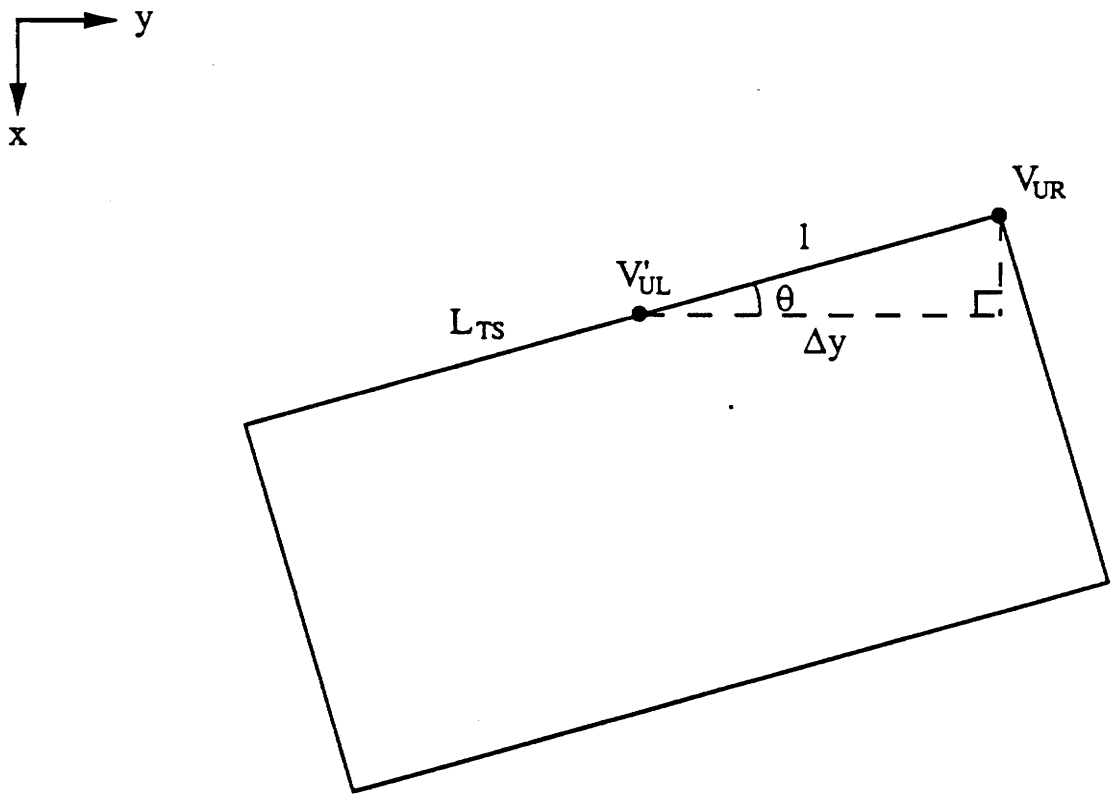

Figure 3–13 Procedure for determining the y-coordinate of V'_{UL}.

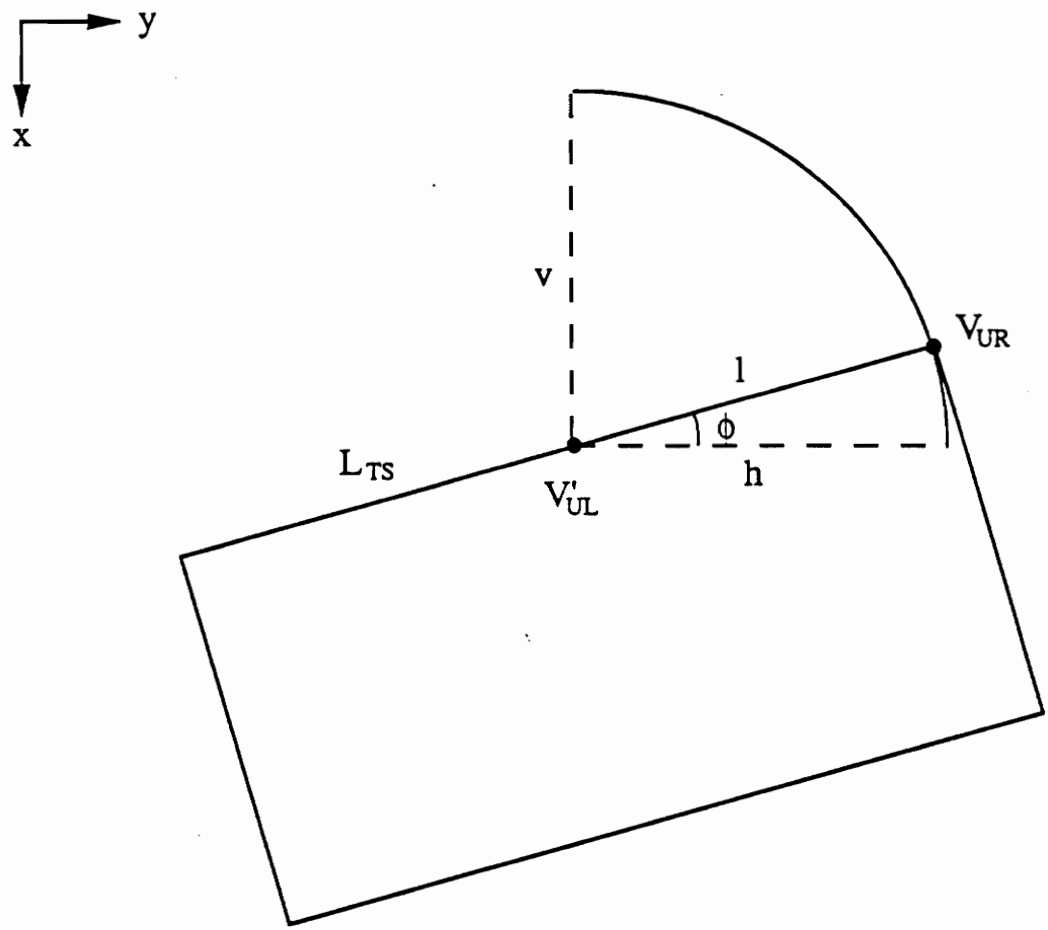

Figure 3–14 Procedure for determining l.

From the coordinates of V'_{UL} and V'_{LL}, m'_{LS} and b'_{LS} are given by

$$m'_{LS} = \frac{y'_{LL} - y'_{UL}}{x'_{LL} - x'_{UL}}, \tag{3-25}$$

$$b'_{LS} = y'_{UL} - m_{LS}x'_{UL}. \tag{3-26}$$

It should be noted that m'_{LS} is not necessarily equal to m_{LS} since L'_{LS} is seldom perfectly parallel to L_{LS}.

Having found m'_{LS} and b'_{LS} that define L'_{LS}, a specimen's inspection area is analytically the region bounded by L_{TS}, L_{RS}, L_{BS}, and L'_{LS}. Hence a pixel with coordinates (x, y) in I_a is labeled as being part of a specimen's inspection area if it is bounded by these lines. Otherwise it is labeled as being part of the background region. A pixel with coordinates (x, y) is bounded by L_{TS}, L_{RS}, L_{BS}, and L'_{LS} if $x \geq m_{TS}y + b_{TS}$, $y \leq m_{RS}x + b_{RS}$, $x \leq m_{BS}y + b_{BS}$, and $y \geq m'_{LS}x + b'_{LS}$. Since the sides of an actual specimen are seldom perfectly straight, the corresponding pixel of a pixel labeled as being part of the inspection area in I_a may be labeled as being part of the background region in S_a. Thus a pixel-by-pixel AND operation is performed between I_a and S_a such that $i_a(x, y)$ is labeled as being part of the inspection area in I_a if $i_a(x, y)$ was previously labeled as being part of the inspection area and if $s_a(x, y)$ is labeled as being part of the specimen region in S_a. The inspection area extracted for the specimen of Figure 3–1 is shown in Figure 3–15.

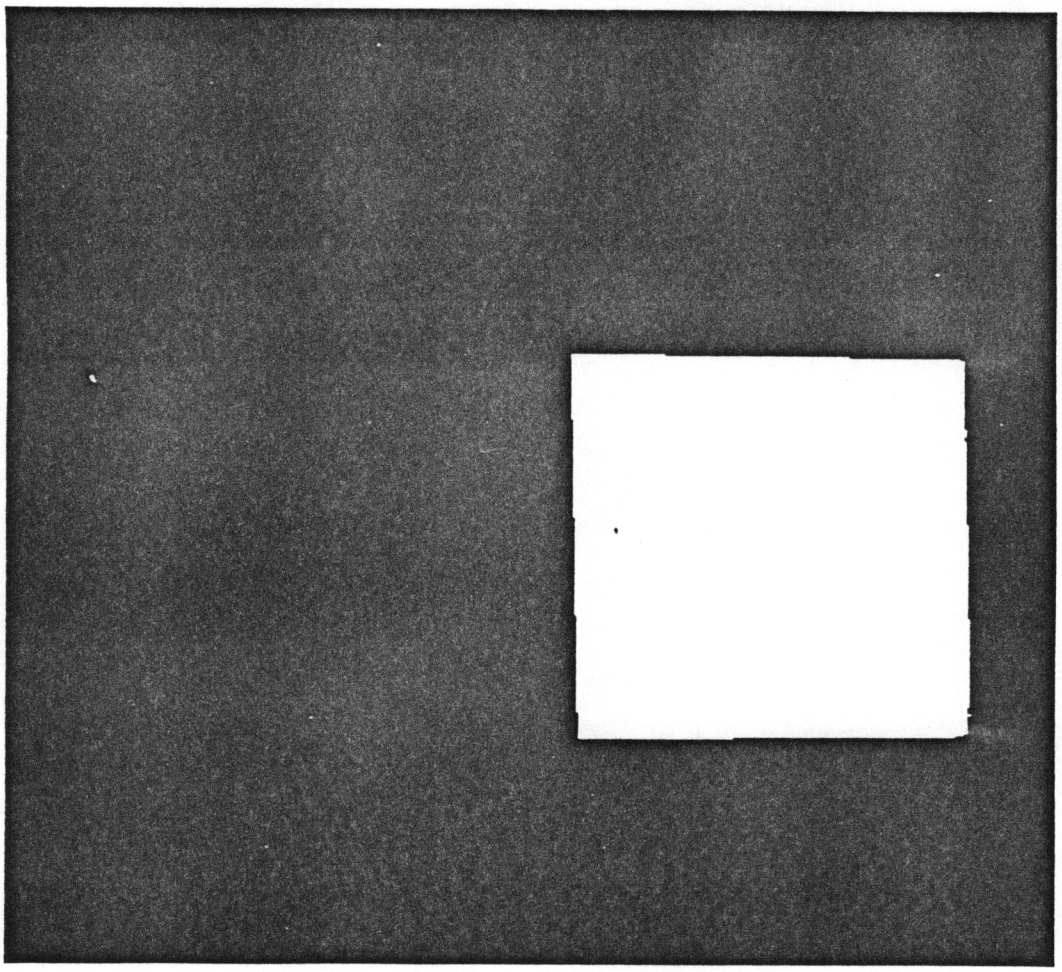

Figure 3–15 Inspection area extracted for the specimen of Figure 3–1.

4. RECOGNITION I: SOLID WOOD EXTRACTION

The second processing step of the automated vision system is to locate the regions that are wood (as opposed to the regions that are glue) on the inspection areas of the two specimens comprising a sample. As discussed in Section 2.4, regions of wood on the inspection area of a specimen are of two types, those comprised of solid wood and those comprised of fiber. The regions of solid wood on a given inspection area are extracted based on the difference in gray level intensity that exists between solid wood and glue. The regions of fiber are extracted based on the difference in texture that exists between fiber and glue since fiber and glue have very similar tonal properties. Thus, this processing step is divided into two separate steps, the solid wood extraction step and the fiber extraction step. The solid wood extraction step is performed before the fiber extraction step is performed. This chapter discusses the solid wood extraction step. The fiber extraction step is discussed in Chapter 5.

As in the case of the first processing step, the algorithms employed to extract the regions of solid wood on the inspection area of one specimen do not require any information concerning the specimen that makes up the other half of the sample. Thus, the inputs of this processing step are 1) the black and white image of a specimen as given in Figure 2–3 and 2) I_a, the output image of the first processing step. Let P denote this black and white image. P is formed from the scanned color image C of a specimen by averaging the color components, i.e., the gray level of a pixel $p(x,y)$ of P is determined by $p(x,y) = [p_r(x,y) + p_g(x,y) + p_b(x,y)]/3$. I_a is a labeled image where a pixel in this labeled image has gray level value 255 if the corresponding pixel in P is

thought to be part of the region that corresponds to the inspection area of the specimen. Otherwise, a pixel in this labeled image has gray level value 0.

The output of this processing step is a labeled image, W_s. A pixel $w_s(x,y)$ of W_s is set equal to 255 if its corresponding pixel $p(x,y)$ of P is thought to be part of the specimen's inspection area and is thought to be solid wood. It is set equal to 127 if $p(x,y)$ of P is thought to be part of the specimen's inspection area and is not thought to be solid wood. It is set equal to 0 if $p(x,y)$ of P is thought not to be part of the specimen's inspection area. Based on the discussion given in Section 2.4, this processing step is divided into the following three substeps: 1) finding the gray level histogram, 2) peak extraction, and 3) threshold selection.

4.1 Finding the Gray Level Histogram

The inputs of this substep are the images P and I_a. The output is a column matrix containing the low pass filtered version of the gray level histogram of the region comprising the inspection area. Let H' denote this output matrix. This substep is divided into two tasks. The first task is to find the gray level histogram of the region comprising the inspection area. Let H denote this histogram. Initially, $h(k) = 0$ for all k. Then, for each pixel $i_a(x,y)$ of I_a that has gray level value 255, i.e., is part of the inspection area, and whose corresponding pixel $p(x,y)$ of P has gray level value k, $h(k)$ is incremented. Figure 4–1 shows a plot of H for the specimen of Figure 3–1.

Since the threshold selection performed in this processing step is based on the number and location of low frequency (large) peaks in H, high frequency components are filtered from H before an analysis of H is performed. This

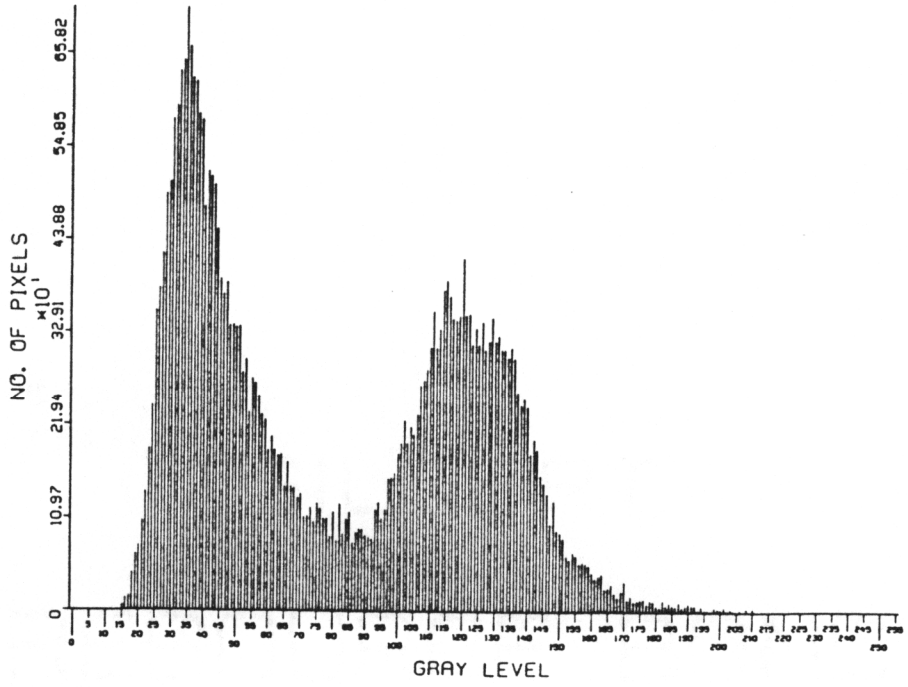

Figure 4–1 Plot of H for the specimen of Figure 3–1.

second task is achieved by convolving H with G, where G is a column matrix containing a discrete Gaussian function [Shirai, 1987]. The result of this convolution is placed in H'. Figure 4–2 shows a plot of H' for the histogram H shown in Figure 4–1.

4.2 Peak Extraction

The input of this substep is the matrix H' created by the previous substep as described in Section 4.1. The output is an integer column matrix containing 256 elements whose indices range from 0 to 255. Let T_{op} denote this output matrix. The element $t_{op}(k) = 1$ if the element $h'(k)$ is a large peak in H'; otherwise, $t_{op}(k) = 0$.

The large peaks of H' are obtained by analyzing the first derivative of H'. The first derivative is found by applying equation (3–6) to the elements of H' by letting $y_0 = h'(0), y_1 = h'(1), \ldots, y_{255} = h'(255)$. It is assumed that $y_{-4} = y_{-3} = y_{-2} = y_{-1} = y_{256} = y_{257} = y_{258} = y_{259} = 0$. The derivatives computed are stored in the column matrix D_{iff} with $d_{iff}(i) = y_i'$ for $i = 0, \ldots, 255$. In general, $h'(k)$ is a peak if $d_{iff}(k-1)$ is positive while $d_{iff}(k)$ is negative. The element $h'(k)$ is a large peak if $d_{iff}(k-1-n)$ through $d_{iff}(k-1)$ are positive while $d_{iff}(k)$ through $d_{iff}(k+n)$ are negative for some large value of n. The parameter n is a nonnegative integer that defines the size of the peak at $h'(k)$. If n is large, the sides of the peak at $h'(k)$ are long, and vice versa.

After the first derivative has been evaluated for each element of H', the peak detection is performed by assigning values to the elements $t_{op}(k)$ of T_{op}. This assignment involves 1) letting $t_{op}(k) = 1$ if $d_{iff}(k-1-n)$ through $d_{iff}(k-1)$ are all positive and $d_{iff}(k)$ through $d_{iff}(k+n)$ are all negative for some n, 2)

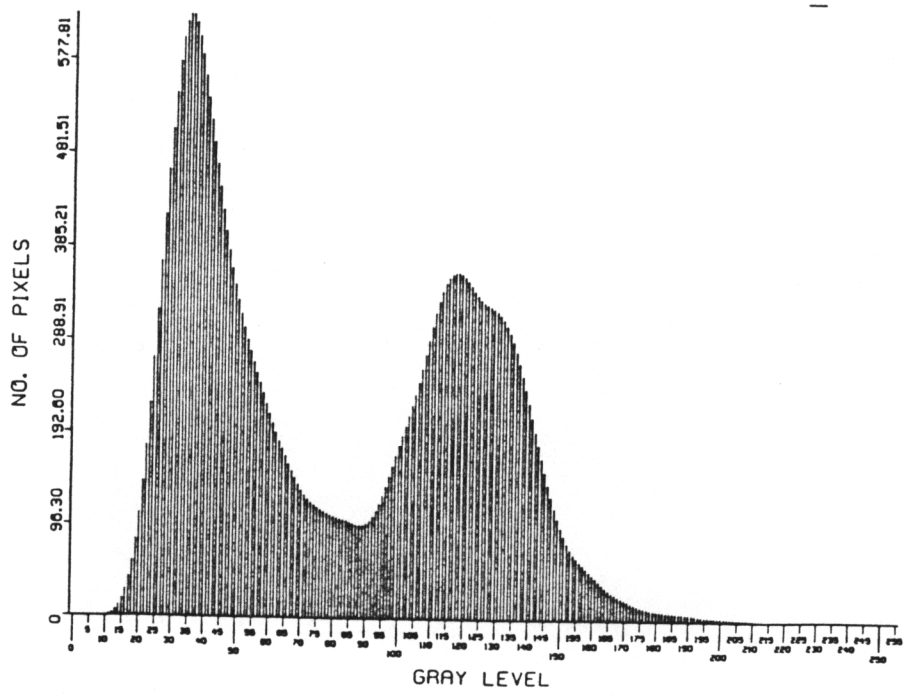

Figure 4–2 Plot of H' for the specimen of Figure 3–1.

letting $t_{op}(k) = -1$ if $d_{iff}(k-1)$ is positive and $d_{iff}(k)$ is negative and either $d_{iff}(k-1-n)$ through $d_{iff}(k-2)$ are all positive or $d_{iff}(k+1)$ through $d_{iff}(k+n)$ are all negative for some n, and 3) letting $t_{op}(k) = 0$ otherwise. The value of n is an input variable. Tests that were conducted indicated that the best value of n for accurate peak extraction is 11. The value of 11 assures that only the largest peaks are detected.

Note that if $t_{op}(k) = -1$ then $h'(k)$ is a "half" peak, i.e., a peak having only one long side. For this analysis, isolated half peaks as shown in Figure 4–3a and Figure 4–3b are unimportant and do not provide any useful information. However, two adjacent half peaks such as that shown in Figure 4–3c are important to detect. Their importance comes from the annual ring structure of wood. The early spring growth is less dense and lighter in color than the growth that occurs later in the year. A histogram of a black and white image of an area of wood containing the early wood and late wood growth patterns will typically have a double peak structure. Hence detecting this structure is very important.

The method developed involves examining places where half peaks have been detected and consolidating each pair of closely spaced half peaks into a single peak in T_{op}. This task is accomplished as follows. A row-by-row scan of T_{op} is performed from $t_{op}(0)$ to $t_{op}(255)$. If $t_{op}(k) = -1$ then the values of $t_{op}(k+1)$ through $t_{op}(k+n')$ are checked to determine if any of these elements equal -1. The check is performed in order starting with row number $k+1$ and ending with row number $k+n'$. Let $t_{op}(k)$ be the first element found to equal -1 and let $t_{op}(i)$ be the second element found to equal -1 where $k+1 \leq i \leq k+n'$. Then $h'(i)$ is compared with $h'(k)$. If $h'(i) \geq h'(k)$ then $t_{op}(i)$ is set equal to 1 and $t_{op}(k)$ is set equal to 0. If $h'(i) < h'(k)$ then $t_{op}(i)$ is set equal to 0 and $t_{op}(k)$ is set equal

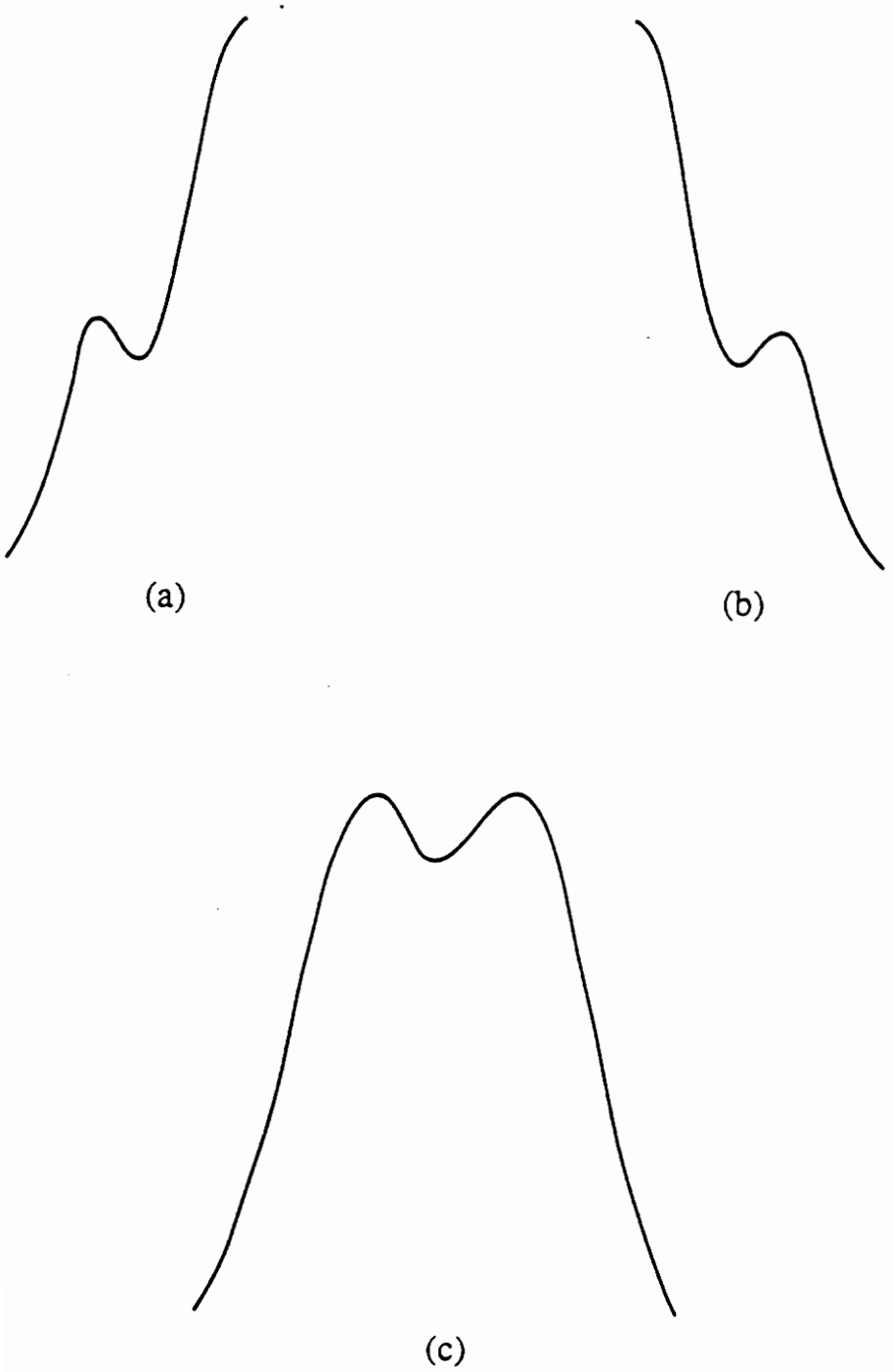

Figure 4–3 Examples of half peaks in H'.

to 1. In either case, a double peak is turned into a single peak that will be examined at a later processing stage. Finally, the element $t_{op}(j)$ is set equal to 0 for all j where $k+1 \leq j \leq i-1$. The scan of T_{op} is then continued starting at $t_{op}(i+1)$. The parameter n' defines the maximum width allowed between two given half peaks in order for the two half peaks to be merged into one peak in the manner described above. The value of n' was experimentally found so that only half peaks within close proximity to each other are merged into a single peak. In the processing of the specimens used in the experiment set, n' was set to 23.

4.3 Threshold Selection

The inputs of this substep are the images P and I_a and the matrices H' and T_{op}. The output is the image W_s described at the beginning of this chapter. A region in the inspection area of a specimen is either solid wood, fiber, or glue. The general form of the low pass filtered gray level histogram corresponding to each of these three region types is shown (superimposed on the same histogram) in Figure 4–4. The relative quantities of solid wood, fiber, and glue on a given inspection area dictate the general shape of the associated H'. Through extensive study and observation, six general shapes of H' were identified. These six shapes were found to correspond to the various combinations of high and low quantities of solid wood, fiber, and glue that could occur on the inspection area of a specimen. These combinations and their associated H' shapes are listed in Table 4–1. Figures 4–5 through 4–10 give the threshold associated with each of these H' shapes.

The thresholds associated with the six H' shapes were determined through observation and experimentation. For the discussion that follows,

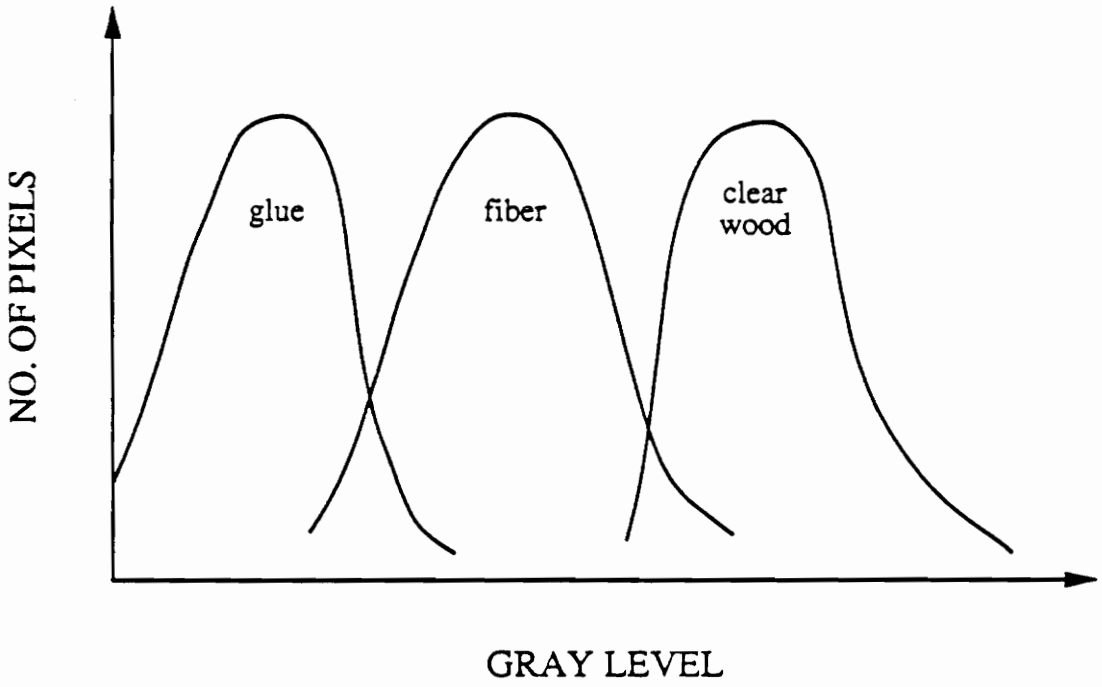

Figure 4–4 General form of H'.

Table 4–1

GLUE	FIBER	SOLID WOOD	HISTOGRAM TYPE(S)
low	low	low	I
low	low	high	II
low	high	low	II or IV
low	high	high	III or VI
high	low	low	IV
high	low	high	V
high	high	low	III or VI
high	high	high	I

let *Min* be the lowest and *Max* be the highest possible gray level values that can occur in the image P. In the system described by this thesis, $Min = 0$ and $Max = 255$. A type I H' shape (Figure 4–5) contains three or more prominent peaks. Since this shape was observed primarily for *low-low-low* (*high-high-high*) specimens, the three largest peaks from left to right in the histogram of Figure 4–5 are thought to correspond to the regions comprising the glue, fiber, and solid wood, respectively, on an inspection area. The threshold should thus be assigned a gray level value occurring between the peak associated with fiber and the peak associated with solid wood. Experiments were performed to determine an analytic method for establishing the best threshold to use. Let i be the gray level where the highest point of the peak associated with fiber occurs in H' and let j be the gray level where the lowest point in the valley between the peak associated with fiber and the peak associated with solid wood occurs. The threshold, T, is selected by determining which $h'(k)$, $i < k < j$, minimizes $|h'(i) - [h'(i) - h'(j)]/3 - h'(k)|$ and then setting T equal to k.

A type II H' shape (Figure 4–6) consists of a single prominent peak in which the left side of this peak is slightly longer than the right side of this peak. Since this shape was observed primarily for *low-low-high* and *low-high-low* specimens, the peak is thought to correspond to either the region comprising the solid wood or to the region comprising the fiber on an inspection area. Since, in the final analysis, a region of fiber is considered to be a region of wood failure, the extraction of fiber in this processing step is inconsequential. As a result, the entire region comprising the inspection area can be extracted as solid wood. The best threshold value is thus *Min*.

A type III H' shape (Figure 4–7) consists of a single prominent peak in which the left side of this peak is significantly longer than the right side of

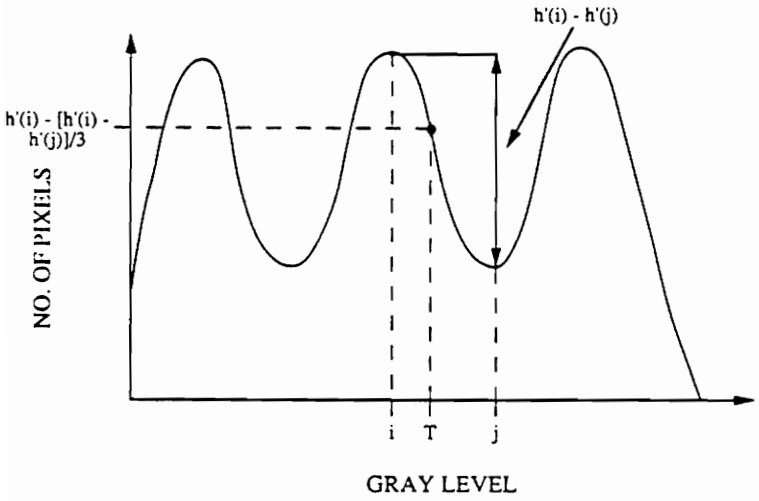

Figure 4–5 Type I H' shape.

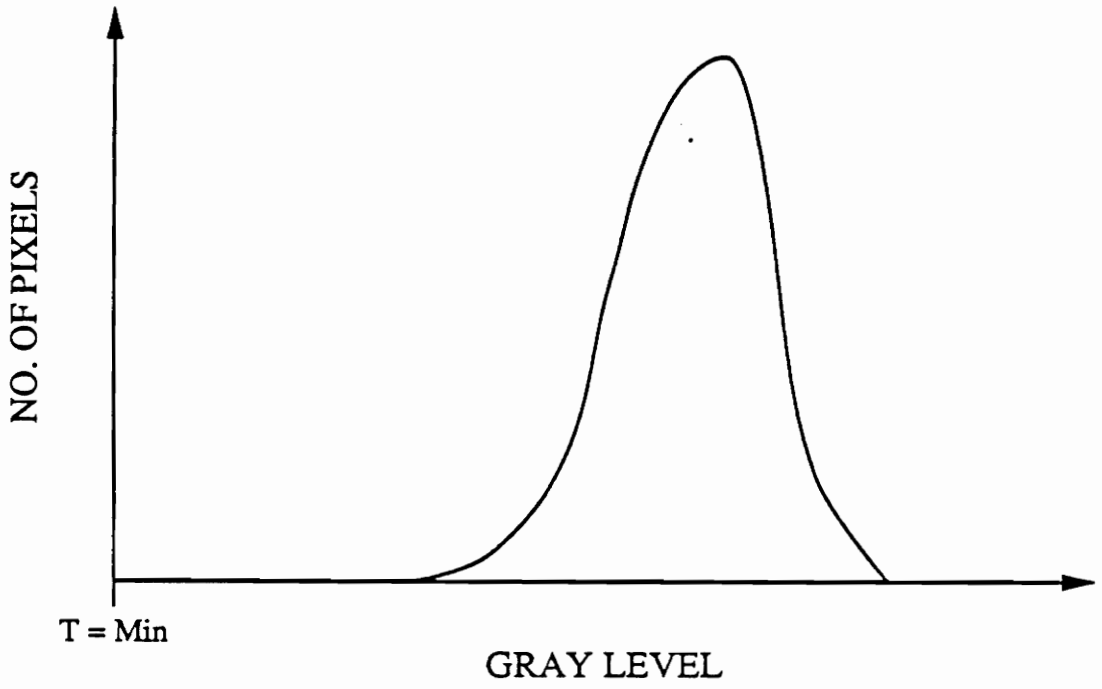

Figure 4–6 Type II H' shape.

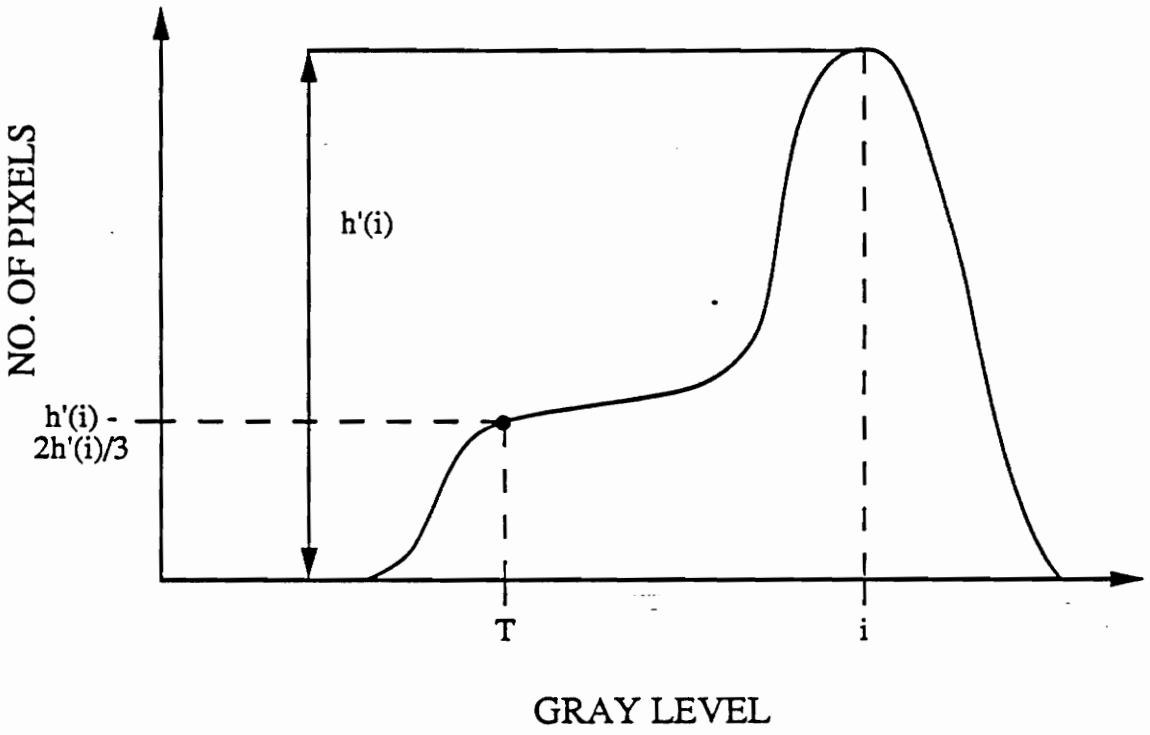

Figure 4–7 Type III H' shape.

this peak, i.e., the left side of this peak contains a bulge. Since this shape was observed primarily for *low-high-high* and *high-high-low* specimens, the bulge and the peak are thought to correspond to either the regions comprising the fiber and solid wood, respectively, or to the regions comprising the glue and fiber, respectively, on an inspection area. The threshold should thus be assigned a gray level value occurring between the bulge and the peak. Experiments were performed to determine an analytic method for establishing the best threshold to use. Let i be the gray level where the highest point of the peak occurs in H'. The threshold, T, is selected by determining which $h'(k)$, $k < i$, minimizes $|h'(i) - 2[h'(i)/3] - h'(k)|$ and then setting T equal to k.

A type IV H' shape (Figure 4–8) consists of a single prominent peak in which the right side of this peak is slightly longer than the left side of this peak. Since this shape was observed primarily for *low-high-low* and *high-low-low* specimens, the peak is thought to correspond to either the region comprising the fiber or to the region comprising the glue on an inspection area. This implies that there is little or no solid wood to extract. The best threshold value is thus $Max + 1$.

A type V H' shape (Figure 4–9) contains two prominent peaks. Since this shape was observed primarily for *high-low-high* specimens, the two peaks from left to right in the histogram of Figure 4–9 are thought to correspond to the region comprising the glue and to the region comprising the solid wood, respectively, on an inspection area. The threshold should thus be assigned a gray level value occuring between these two peaks. Experiments were again performed to determine an expression that seemingly gives the best threshold. Let j be the gray level where the lowest point in the valley between the peak associated with glue and the peak associated with solid wood occurs in H'.

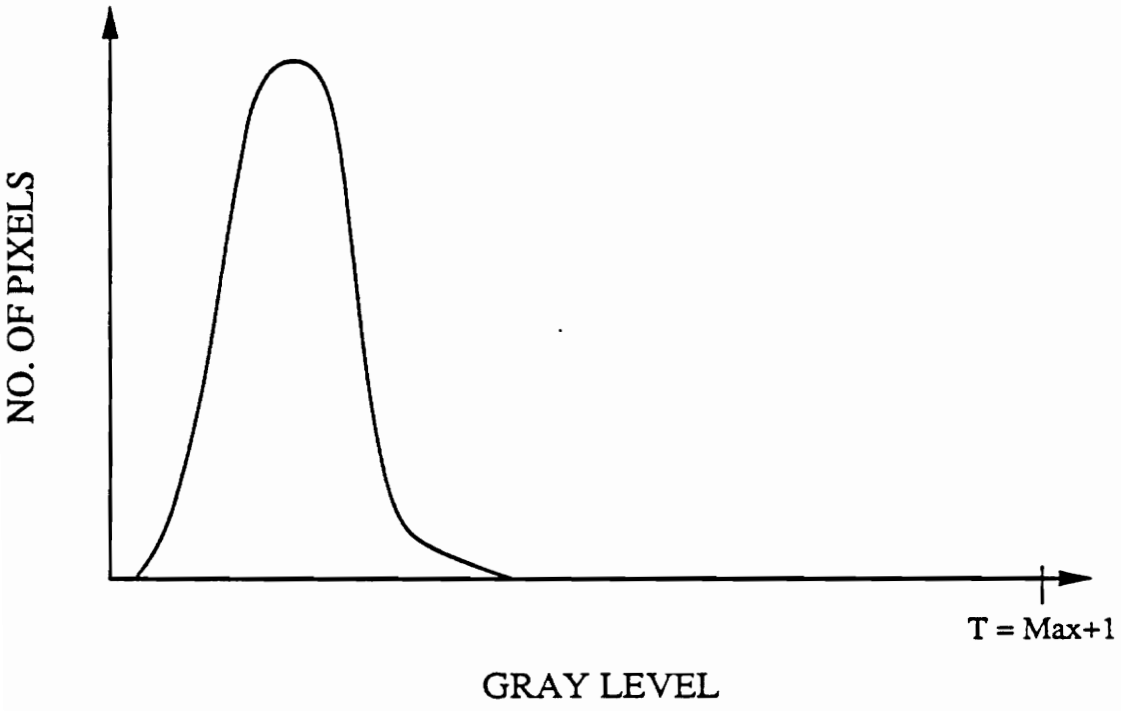

Figure 4–8 Type IV H' shape.

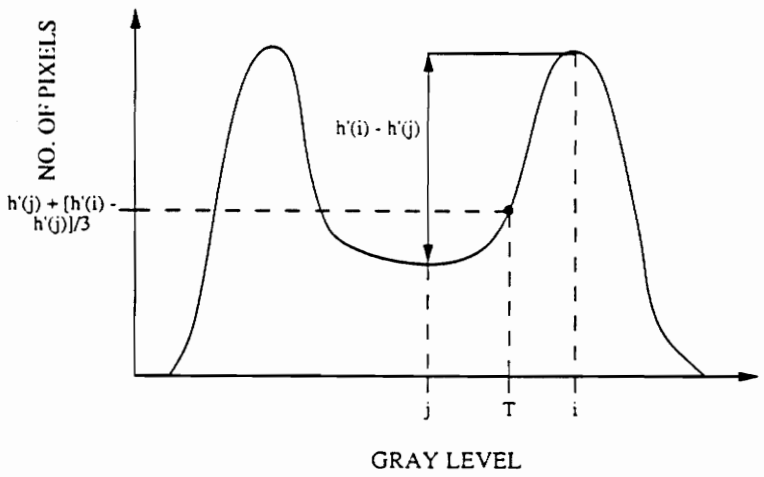

Figure 4–9 Type V H' shape.

Let i be the gray level where the highest point of the peak associated with solid wood occurs in H'. Then the threshold, T, is found by determining the $h'(k)$, $j < k < i$, that minimizes $|h'(j) + [h'(i) - h'(j)]/3 - h'(k)|$ and setting T equal to k.

A type VI H' shape (Figure 4–10) consists of a single prominent peak in which the right side of this peak is significantly longer than the left side of this peak, i.e., the right side of this peak contains a bulge. Since this shape was observed primarily for *low-high-high* and *high-high-low* specimens, the peak and the bulge are thought to correspond to either the regions comprising the fiber and solid wood, respectively, or to the regions comprising the glue and fiber, respectively, on an inspection area. The threshold should thus be assigned a gray level value occurring between the peak and the bulge. Experimentation showed, however, that the best threshold value tends to occur at $Max + 1$. This could be due to the extremely small percentage of *low-high-high* specimens observed having a type VI H' shape.

The threshold selector matches the H' of the inspection area of a specimen to an H' type based on the number of peaks in T_{op}. Suppose T_{op} contains one peak at gray level k in H'. If $Max - k \geq k - Min + n''$ for some n'', the right side of this peak is longer than the left side of this peak. In this case, H' is classified as either type IV or type VI. Since both of these H' types incur the same threshold, further distinction is unnecessary. If $Max - k < k - Min + n''$, the left side of this peak is longer than the right side of this peak. In this case, H' is classified as either type II or type III. If $k - Min \geq n'''$ for some n''', the left side of this peak is significantly longer than the right side of this peak. In this case, H' is classified as type III; otherwise, it is classified as type II. The parameters n'' and n''' are functions of the lighting and scanning resolution

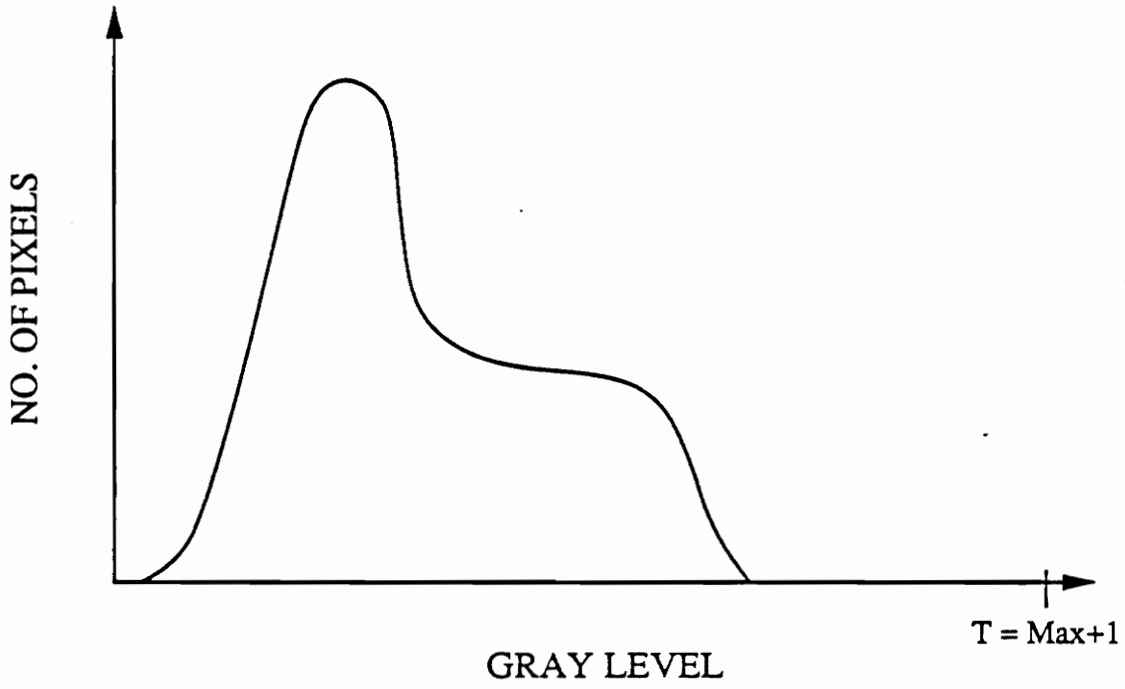

Figure 4–10 Type VI H' shape.

and are experimentally set. In the processing of the specimens used in the experiment set, n'' and n''' were set to 50 and 60, respectively. If T_{op} contains two peaks, H' is classified as type V. If T_{op} contains three or more peaks, H' is classified as type I.

After the H' of the inspection area of a specimen has been matched to the appropriate H' type, the threshold value is determined based on the rules associated with the H' type chosen. Let T denote the threshold value determined in this manner. After T has been determined, a row-by-row, pixel-by-pixel scan of I_a is performed. If $i_a(x,y) = 255$ (inspection area) and $p(x,y) \geq T$, $w_s(x,y)$ is set equal to 255 (inspection area and solid wood). If $i_a(x,y) = 255$ (inspection area) and $p(x,y) < T$, $w_s(x,y)$ is set equal to 127 (inspection area but not solid wood). If $i_a(x,y) = 0$ (background), $w_s(x,y)$ is set equal to 0 (background). W_s for the specimen of Figure 3–1 is shown in Figure 4–11.

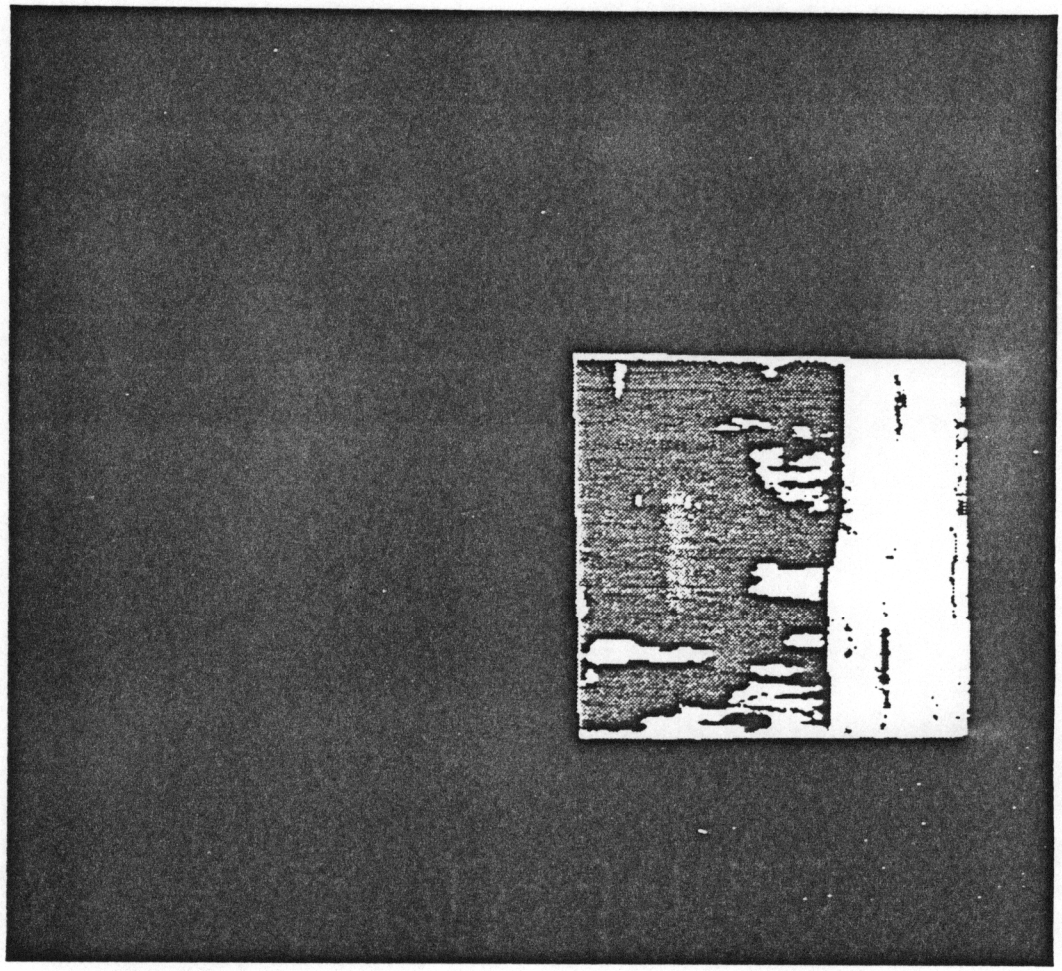

Figure 4–11 W, for the specimen of Figure 3–1.

5. RECOGNITION II: WOOD FIBER EXTRACTION

As explained in Chapter 4, the second processing step of the automated vision system is divided into two separate steps, the solid wood extraction step and the fiber extraction step. The solid wood extraction step is discussed in Chapter 4; this chapter discusses the fiber extraction step. As in the case of the solid wood extraction step, the results of the previous processing step obtained from each of the images of the two specimens comprising a sample are processed separately in this processing step. Thus the inputs of this processing step are P, the black and white image of a specimen as given in Figure 2–3 and W_s, the output image of the previous processing step. W_s is a labeled image where a pixel $w_s(x,y)$ in this labeled image has 1) gray level value 255 if the corresponding pixel in P is thought to be a part of the region comprising the inspection area that is solid wood, 2) gray level value 127 if the corresponding pixel in P is thought to be a part of the region comprising the inspection area that is not solid wood, or 3) gray level value 0 if the corresponding pixel in P is thought not to be part of the region comprising the inspection area (the background of P).

The output of this processing step is a revised version of W_s. In this version of W_s a pixel $w_s(x,y)$ has 1) gray level value 255 if the corresponding pixel in P is thought to be a part of the inspection area that is wood (solid wood or fiber), 2) gray level value 127 if the corresponding pixel in P is thought to be a part of the inspection area that is glue, or 3) gray level value 0 if the corresponding pixel in P is thought to be part of the background. Based on the discussion given in Section 2.4, this processing step is divided into the following five substeps: 1) connected region extraction, 2) vertical

and horizontal edge detection, 3) threshold selection, 4) fiber grouping, and 5) border grouping.

5.1 Connected Region Extraction

The input of this substep is the labeled image W_s. The output is the labeled image CR that makes explicit the various connected regions that are thought to be part of the inspection area but are not thought to be solid wood. A pixel $cr(x,y)$ in the labeled image CR has 1) gray level value 255 if the corresponding pixel in W_s is thought to be a part of the inspection area that is solid wood, 2) gray level values 1 through 254 if the corresponding pixel in W_s is thought to be a part of the inspection area that is not solid wood, or 3) gray level value 0 if the corresponding pixel in W_s is thought to be part of the background. Two pixels $cr(x_1,y_1)$ and $cr(x_2,y_2)$ in CR that belong to the same 8-connected region are such that $cr(x_1,y_1) = cr(x_2,y_2)$. Two pixels $cr(x_1,y_1)$ and $cr(x_2,y_2)$ that do not belong to the same 8-connected region are such that $cr(x_1,y_1) \neq cr(x_2,y_2)$. A total of 254 8-connected regions can be identified.

As discussed in Section 2.4, each fiber strand in a connected region of glue will almost always have the same orientation as the other fiber strands in this glue region. Fiber strands can have only two basic orientations, horizontal and vertical. This follows from the fact that plywood is made from alternating layers of vertically- and horizontally-grained wood. Glue regions that contain two different fiber strand orientations are usually separated by at least one layer of solid wood. This again follows from the way plywood is made. Since

regions of solid wood were extracted in the last processing step, locating 8-connected regions that are not solid wood provides a way of identifying the areas that have all their fiber strands aligned in the same direction.

The procedure used to identify the various 8-connected regions [Ng, 1990] involves a number of steps. First, a pixel-by-pixel search of W_s is conducted. If $w_s(x,y) = 127$, i.e., if $w_s(x,y)$ is part of the inspection area that is not solid wood, then $cr(x,y) = -1$. If $w_s(x,y) \neq 127$ then $cr(x,y) = 0$. Let i denote the number to be assigned to the 8-connected region to be formed next. Initially $i = 1$. A pixel-by-pixel scan of CR is performed until an element $cr(x,y) = -1$ is found. If no such element is found, this procedure is terminated. Once an element $cr(x,y) = -1$ is found, $cr(x,y)$ is set equal to i. For each element $cr(x',y')$ that equals -1 and is 8-connected to $cr(x,y)$, $cr(x',y')$ is set equal to i. After no more such $cr(x',y')$ are found, i is incremented and the search for another 8-connected region is begun.

To reduce the number of 8-connected regions that have to be processed in subsequent steps, the smallest 8-connected regions are labeled as being solid wood. The motivation for changing the label of these regions comes from extensive experimentation. Very small connected regions that are labeled as not being solid wood are usually small cracks or glue stained wood. Small cracks and glue stained wood are considered to be solid wood by the APA.

The procedure used to remove these small 8-connected regions first involves ordering the 8-connected regions on the basis of area with the smallest 8-connected region at the top of the list and the largest 8-connected region at the bottom of the list. The identification, say i, of the smallest region is removed from the list and its area is checked to make sure it is less than one percent of the total inspection area surface. If i's area is less than one percent

of the total inspection area surface then for each pixel $cr(x,y) = i$, the value of $cr(x,y)$ is changed to 255, indicating it is solid wood. After all pixels in CR with identification number i have been found, the identification number, say j, of the next smallest region is removed from the list. A check is made to assure that the sum of the area of this new region plus the area of the smallest region is less than one percent of the total inspection area surface. If this sum is less than one percent of the total inspection area surface, all pixels $cr(x,y) = j$ have their value changed to 255, etc. CR for the specimen of Figure 3–1 is shown in Figure 5–1.

5.2 Vertical and Horizontal Edge Detection

The inputs of this substep are P and CR. The outputs are two images denoted by E_V and E_H. These images contain two types of information, pixel labels and gradient information. A pixel in either E_V or E_H has 1) a gray level value of 255 if the corresponding pixel in CR is labeled as a solid wood pixel, 2) a gray level value of 170 if the corresponding pixel in CR is labeled as belonging to an 8-connected region but is found to be a border pixel, 3) a gray level value of 85 if the corresponding pixel in CR is labeled as a background pixel, or 4) a gray level value equal to the absolute value of the vertical (E_V) or horizontal (E_H) edge detector, values ranging from 0 to 84, if the corresponding pixel in CR is labeled as belonging to an 8-connected region and is found not to be a border pixel. The definition of a border pixel is given below. The purpose of this substep is to apply a vertical and a horizontal edge detector to the pixels in P whose corresponding pixels in CR belong to one of the 8-connected regions determined in the previous substep.

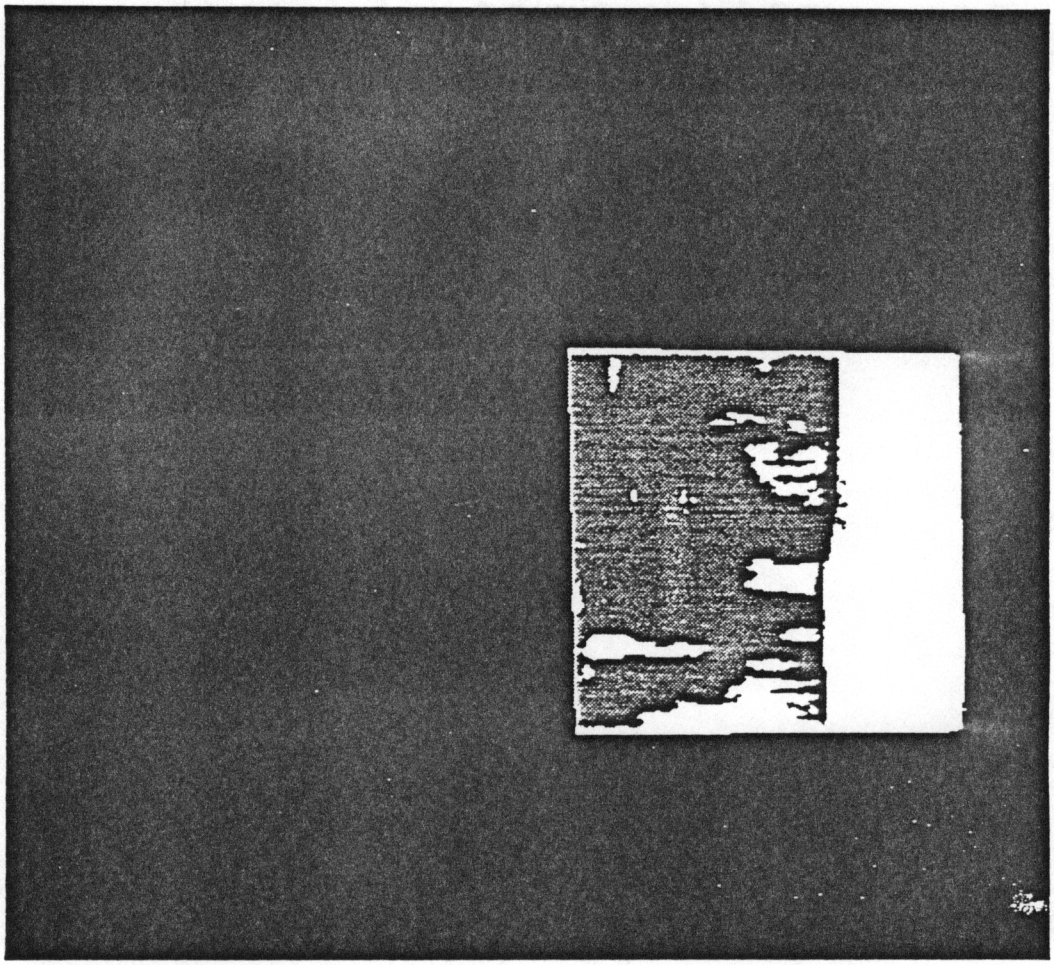

Figure 5–1 *CR* for the specimen of Figure 3–1.

As discussed in Section 2.4, a region of fiber is distinguished from a region of glue based on the difference in texture that exists between the two regions. Since a region of fiber is composed of vertically or horizontally oriented edges whereas a region of glue contains few edges, a vertically and a horizontally oriented edge detector are employed to distinguish between fiber and glue. The edge detectors utilized are discrete approximations of the gray level intensity partial derivatives with respect to the vertical and horizontal directions [Yu, 1983]. By definition, the gray level intensity partial derivatives of a pixel $p(x,y)$ with respect to the vertical and horizontal directions are given by $p(x,y) - p(x,y+1)$ and $p(x,y) - p(x+1,y)$, respectively. If the difference $p(x,y) - p(x,y+1)$ is high, a vertical edge exists between $p(x,y)$ and $p(x,y+1)$. If the difference $p(x,y) - p(x+1,y)$ is high, a horizontal edge exists between $p(x,y)$ and $p(x+1,y)$. Since the length of an individual fiber strand usually extends beyond one pixel in length, the partial derivatives are averaged over distance in the vertical and horizontal directions as follows:

$$e_V(x,y) = \left| \frac{\sum_{i=-n_f}^{n_f} [p(x+i,y) - p(x+i,y+1)]}{2n_f + 1} \right| \qquad (5-1)$$

and

$$e_H(x,y) = \left| \frac{\sum_{i=-n_f}^{n_f} [p(x,y+i) - p(x+1,y+i)]}{2n_f + 1} \right|, \qquad (5-2)$$

where n_f is a nonnegative integer.

Equation (5–1) is performed on all $p(x,y)$ in P such that 1) $cr(x,y)$ has a gray level value between 1 and 254, inclusive, and 2) $cr(x-n_f,y),\ldots,cr(x+n_f,y)$ and $cr(x-n_f,y+1),\ldots,cr(x+n_f,y+1)$ have gray level values between 1 and 254, inclusive. If the first condition is true but the second condition is false,

$e_V(x,y)$ is deemed a border pixel, and the gray level value of $e_V(x,y)$ is set to 170. Equation (5–2) is performed on all $p(x,y)$ in P such that 1) $cr(x,y)$ has a gray level value between 1 and 254, inclusive, and 2) $cr(x,y-n_f),\ldots,cr(x,y+n_f)$ and $cr(x+1,y-n_f),\ldots,cr(x+1,y+n_f)$ have gray level values between 1 and 254, inclusive. If the first condition is true but the second condition is false, $e_H(x,y)$ is deemed a border pixel, and the gray level value of $e_H(x,y)$ is set to 170. The gray level values of $e_V(x,y)$ and $e_H(x,y)$ obtained from equations (5–1) and (5–2) have always been observed to fall significantly below the maximum allowable value of 84 given at the beginning of this section. The analysis of border pixels is deferred until the last substep of this processing step. Finally, $e_V(x,y)$ and $e_H(x,y)$ are set to 255 for all $cr(x,y) = 255$ in CR while $e_V(x,y)$ and $e_H(x,y)$ are set to 85 for all $cr(x,y) = 0$ in CR.

The variable n_f in equations (5–1) and (5–2) is the fiber length parameter, i.e., the operators given in equations (5–1) and (5–2) detect fiber of pixel length $2n_f + 1$. The shorter a given fiber strand is than $2n_f + 1$, the lower the gray level value will be for the fiber strand in the appropriate output image. Hence some fiber strands may not be detected if n_f is set too high. For the processing of the specimens used in the experiment set, the best value of n_f was experimentally determined to be 1. E_V and E_H for the specimen of Figure 3–1 are shown in Figures 5–2 and 5–3, respectively. In these figures, border pixels are shown in white, the region comprising the solid wood is shown in gray, the region comprising the background is shown in black, and the results of the edge detection operations applied to the regions of the inspection area that are not solid wood are shown as they appear in E_V and E_H, respectively.

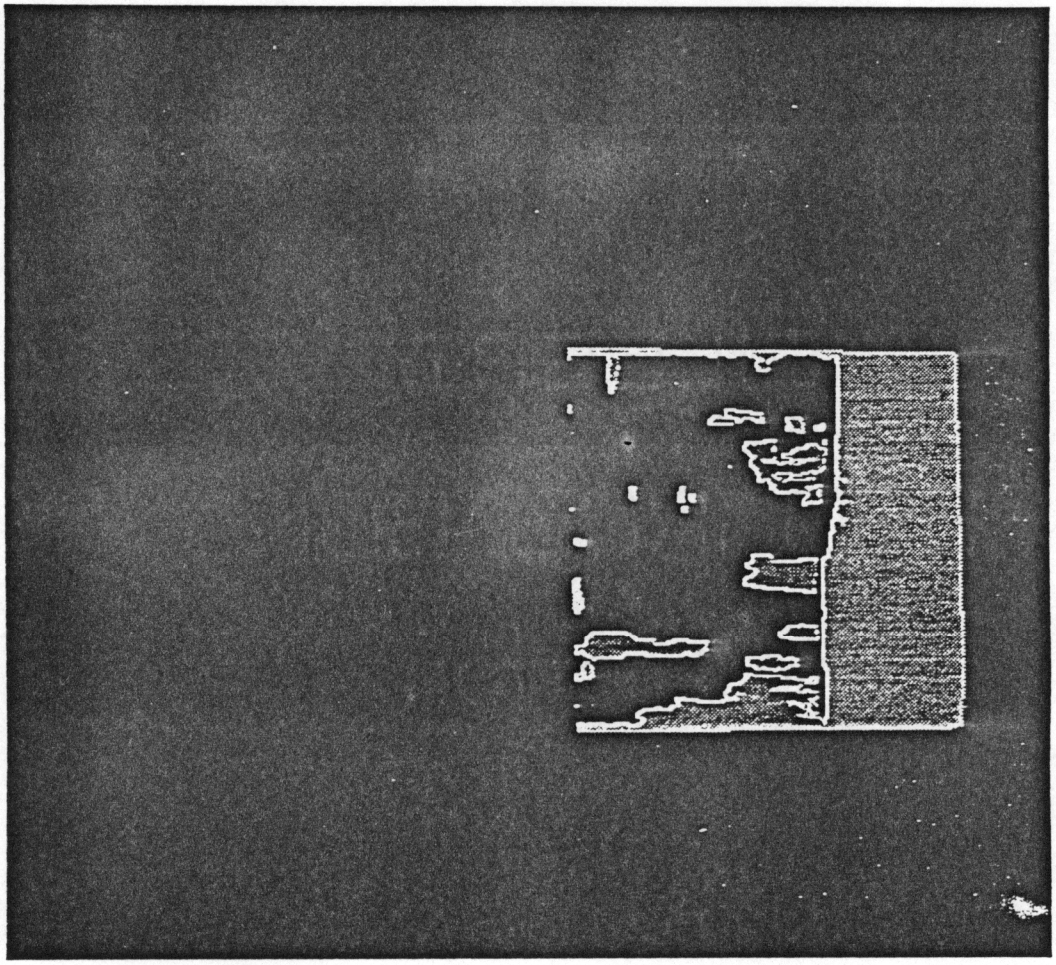

Figure 5–2 E_V for the specimen of Figure 3–1.

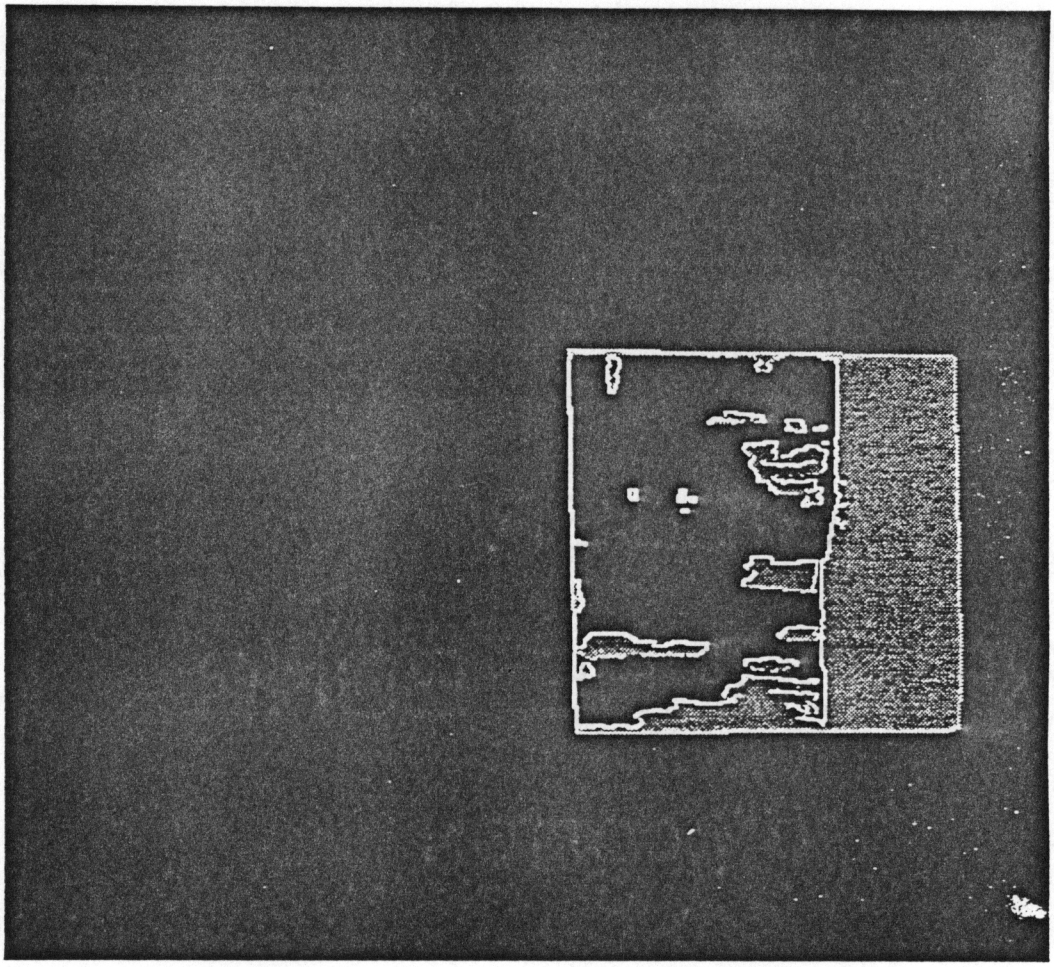

Figure 5–3 E_H for the specimen of Figure 3–1.

5.3 Threshold Selection

The inputs of this substep are CR, E_V, and E_H. The output is a labeled image, F_{ib}, where a pixel $f_{ib}(x,y)$ in F_{ib} has 1) gray level value 255 if the corresponding pixel in CR is labeled as solid wood, 2) gray level value 191 if the corresponding pixel in E_V or in E_H is labeled as a border pixel, 3) gray level value 127 if the corresponding pixel in E_V or in E_H is thought to be fiber, 4) gray level value 63 if the corresponding pixel in E_V or in E_H is thought to be glue, and 5) gray level value 0 if the corresponding pixel in CR is labeled as background. The determination of whether to use E_V or E_H in defining F_{ib} is given below.

If the corresponding region in P of an 8-connected region in CR consists of vertically oriented fiber, pixels in the corresponding region in E_V (excluding border pixels) will primarily have high gray level values while pixels in the corresponding region in E_H will primarily have low gray level values. This is illustrated in Figures 5–4 and 5–5. Figure 5–4 shows a normalized histogram of a region in E_V whose corresponding region in P has vertical fiber. Figure 5–5 shows a normalized histogram of a region in E_H that corresponds to the same region in P. The shapes of the histograms shown in Figures 5–4 and 5–5 are reversed when the fiber in the corresponding region in P is horizontally oriented. In general, the average gray level value of the histogram of an 8-connected region in E_V is higher (lower) than the average gray level value of the histogram of the corresponding 8-connected region in E_H if the fiber in the corresponding region in P is vertically (horizontally) oriented. If a pair of gray level histograms possessing shapes similar to the ones shown in Figures 5–4 and 5–5 are superimposed, Bayesian decision theory [Duda, 1973] indicates that the best threshold is the gray level value corresponding to the intersection of the two graphs as shown in Figure 5–6.

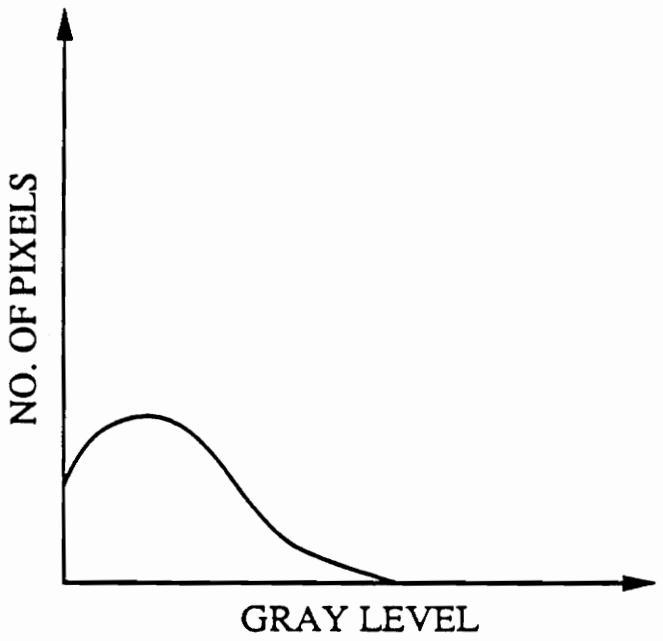

Figure 5–4 Normalized histogram of a region in E_V.

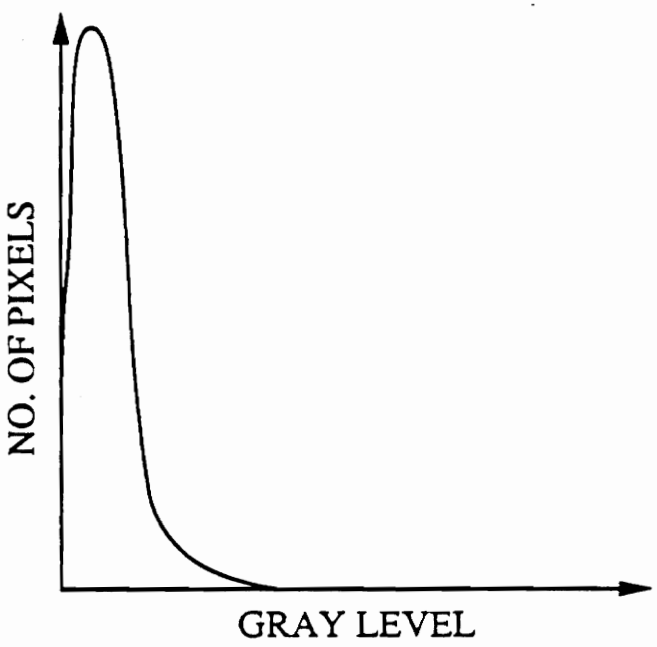

Figure 5–5 Normalized histogram of a region in E_H.

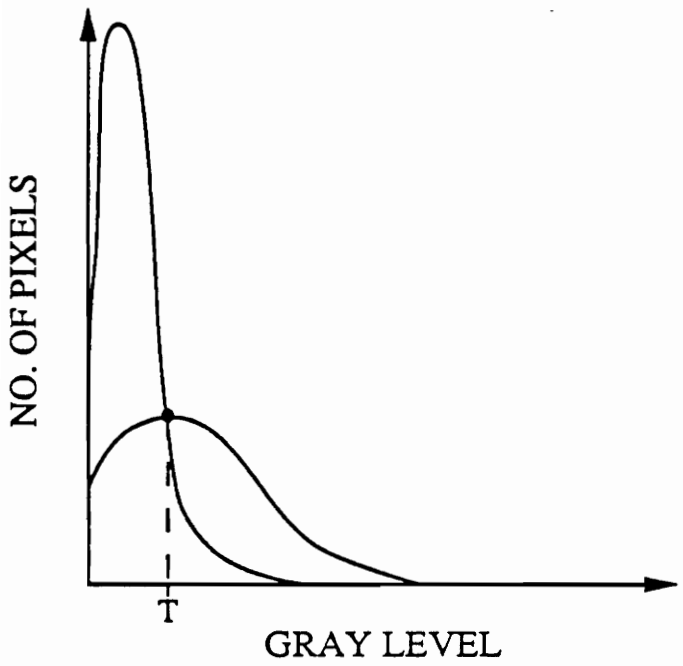

Figure 5–6 Ideal threshold.

Let R denote an 8-connected region in CR as defined in Section 5.1. The thresholding of R for all R in CR is performed as follows. The threshold value is determined from the gray level histograms of the regions in E_V and E_H that correspond to R as explained above. Let T denote this threshold value. If the average gray level value of the region in E_V corresponding to R is higher than the average gray level value of the region in E_H corresponding to R, E_V is used to define T; otherwise, E_H is used to define T. For the sake of example, let E_V define T. If $cr(x,y)$ belongs to R and $e_V(x,y) \geq T$, $f_{ib}(x,y)$ is set to 127 (fiber). If $cr(x,y)$ belongs to R and $e_V(x,y) < T$, $f_{ib}(x,y)$ is set to 63 (glue). If $cr(x,y)$ belongs to R and $e_V(x,y) = 170$ (border), $f_{ib}(x,y)$ is set to 191 (border). After all 8-connected regions in CR have been evaluated, $f_{ib}(x,y)$ is set to 255 (solid wood) if $cr(x,y) = 255$ (solid wood) while $f_{ib}(x,y)$ is set to 0 (background) if $cr(x,y) = 0$ (background) for all $cr(x,y)$ in CR. F_{ib} for the specimen of Figure 3–1 is shown in Figure 5–7 where the regions comprising the clear wood and border areas are shown in gray, the region comprising the fiber is shown in white, the regions comprising the glue and background are shown in black.

5.4 Fiber Grouping

The input of this substep is F_{ib}. The output is a labeled image, G_rF_{ib}, where a pixel $g_rf_{ib}(x,y)$ in G_rF_{ib} has 1) gray level value 255 if the corresponding pixel in F_{ib} is labeled as solid wood, 2) gray level value 191 if the corresponding pixel in F_{ib} is labeled as a border pixel, 3) gray level value 127 if the corresponding pixel in F_{ib} is thought to be part of a "grouping of fiber," 4) gray level value 63 if the corresponding pixel in F_{ib} is thought to be glue, and 5) gray level value 0 if the corresponding pixel in F_{ib} is labeled as background. The purpose of this substep is to extract as fiber all regions of glue appearing

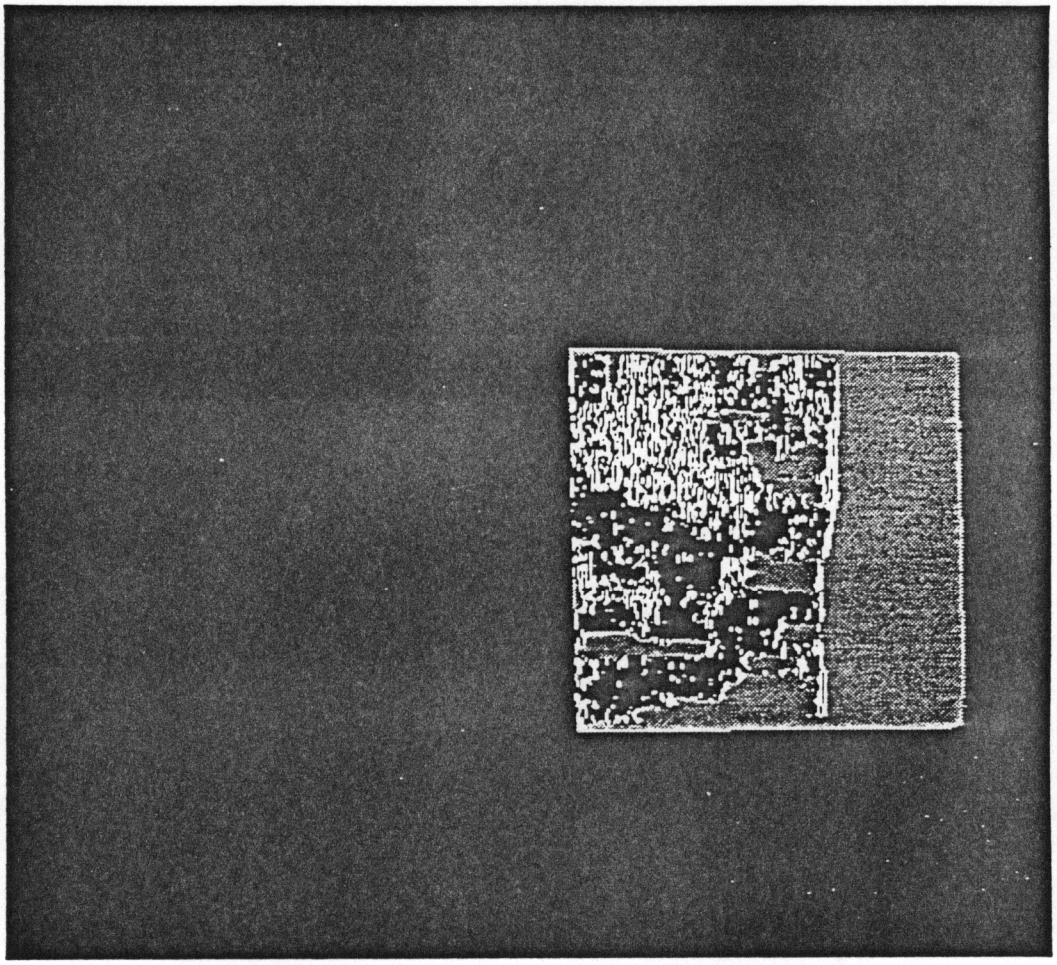

Figure 5–7 F_{ib} for the specimen of Figure 3–1.

between closely spaced regions of fiber, i.e., a grouping of fiber, as required by the APA.

Since the orientation of fiber is either vertical or horizontal, the regions comprising the fiber in F_{ib} are grouped vertically and horizontally. The vertical and horizontal fiber grouping operators are shown in Figure 5–8, where k is a nonnegative integer. Experimentation showed that grouping operations performed on one region of F_{ib} could affect changes on another region of F_{ib} previously operated upon so that more than one iteration of the application of the grouping operators is required. Thus, after setting $g_r f_{ib}(x,y) = f_{ib}(x,y)$ for all $f_{ib}(x,y)$ in F_{ib}, the grouping operators are applied to $G_r F_{ib}$ from $k = 0$ to $k = n'_f$, where n'_f is a nonnegative integer. The parameter n'_f is experimentally determined and specifies the maximum pixel spacing allowed between fiber strands in order for grouping to take place. For the specimens used in the experiment set, n'_f was set to 1.

After the application of the fiber grouping operators, regions corresponding to glue in $G_r F_{ib}$ usually contain isolated pixels corresponding to fiber. To eradicate this noise, vertical and horizontal glue grouping operators are applied to $g_r f_{ib}(x,y)$ for all $g_r f_{ib}(x,y)$ in $G_r F_{ib}$. These operators are shown in Figure 5–9, where k is a nonnegative integer. As in the case of fiber grouping, repeated iterations of the application of the glue grouping operators are performed from $k = 0$ to $k = n''_f$, where n''_f is a nonnegative integer. The parameter n''_f is experimentally determined and specifies the maximum pixel spacing allowed between pixels corresponding to glue in order for grouping to take place. For the specimens used in the experiment set, n''_f was set to to 0. $G_r F_{ib}$ for the specimen of Figure 3–1 is shown in Figure 5–10 where the regions comprising the solid wood and border areas are shown in gray, the region comprising the

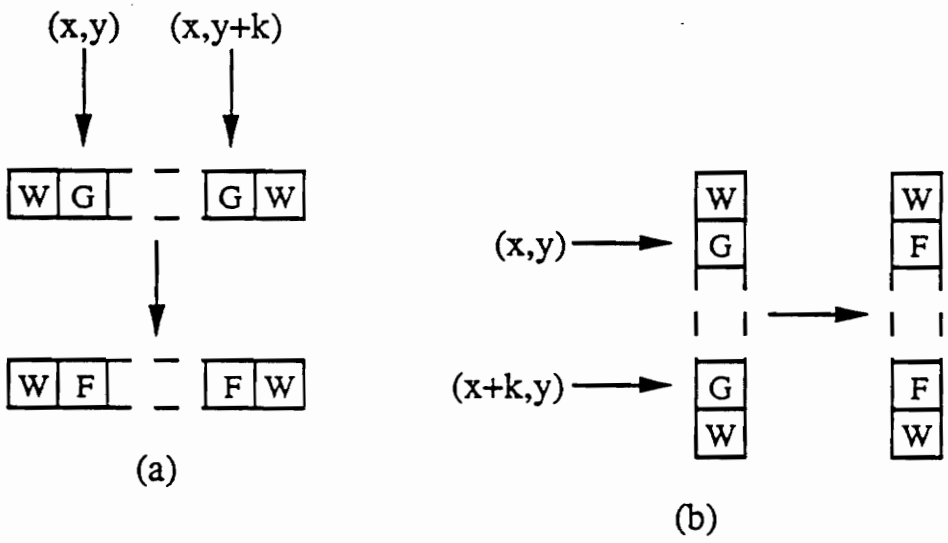

W = wood (solid wood or fiber), F = fiber, G = glue

Figure 5–8 Vertical and horizontal fiber grouping operators.

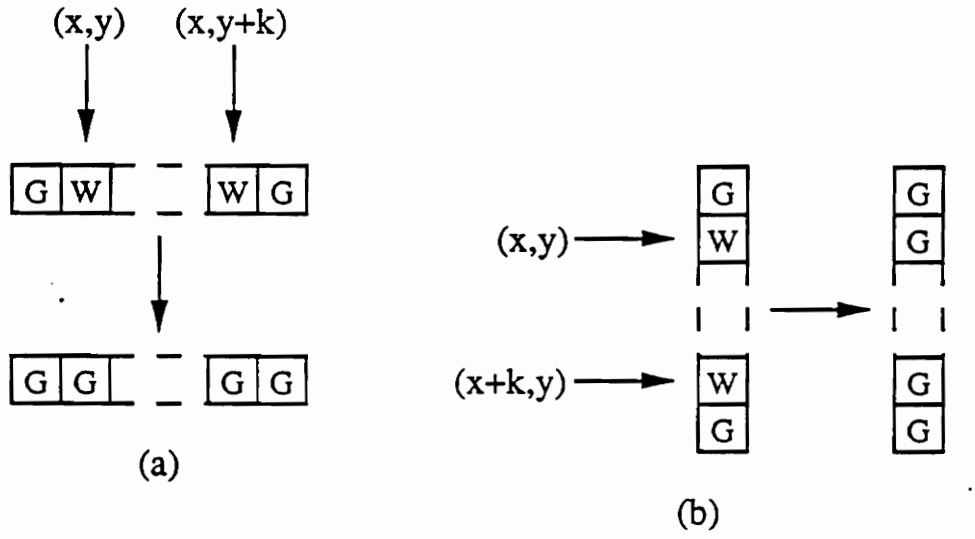

W = wood (solid wood or fiber), G = glue

Figure 5–9 Vertical and horizontal glue grouping operators.

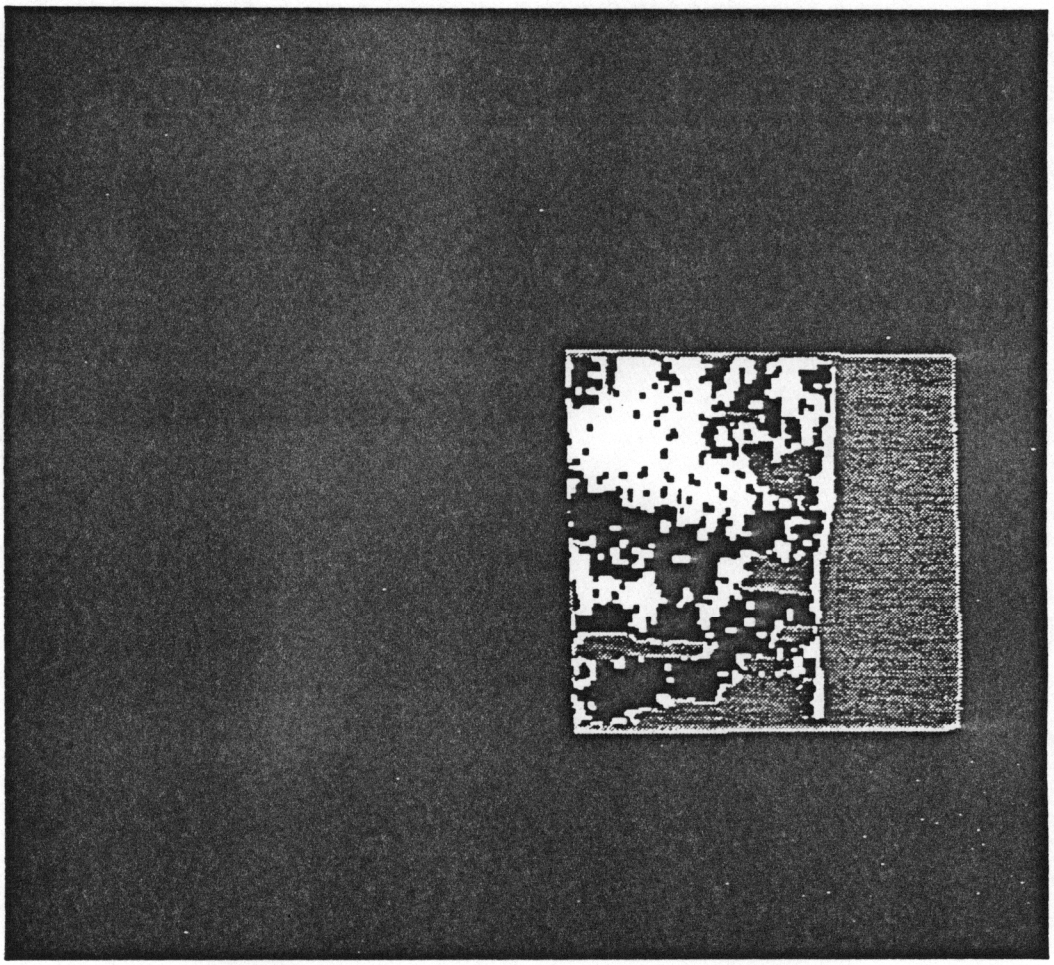

Figure 5–10 $G_r F_{ib}$ for the specimen of Figure 3–1.

fiber is shown in white, and the regions comprising the glue and background are shown in black.

5.5 Border Grouping

The input of this substep is $G_r F_{ib}$. The output is a labeled image, $B_r G_r$, where a pixel $b_r g_r(x, y)$ in $B_r G_r$ has 1) gray level value 255 if the corresponding pixel in $G_r F_{ib}$ is labeled as solid wood, 2) gray level value 127 if the corresponding pixel in $G_r F_{ib}$ is labeled as fiber, 3) gray level value 63 if the corresponding pixel in $G_r F_{ib}$ is labeled as glue, and 4) gray level value 0 if the corresponding pixel in $G_r F_{ib}$ is labeled as background. The purpose of this substep is to classify pixels labeled as border pixels in $G_r F_{ib}$ as either being part of a grouping of fiber or as being glue.

Initially, $b_r g_r(x, y) = g_r f_{ib}(x, y)$ for all $g_r f_{ib}(x, y)$ in $G_r F_{ib}$. The vertical border grouping operator is shown in Figure 5–11 while the horizontal border grouping operator is shown in Figure 5–12. These operators are applied to $B_r G_r$ for $k = 0$ to $k = n_f'''$, where n_f''' is a nonnegative integer. The parameter n_f''' is experimentally determined and specifies the maximum pixel spacing allowed between border pixels in order for grouping to take place. For the specimens used in the experiment set, n_f''' was set to to 1. $B_r G_r$ for the specimen of Figure 3–1 is shown in Figure 5–13 where the region comprising the solid wood is shown in gray, the region comprising the fiber is shown in white, and the regions comprising the glue and background are shown in black.

LI, the output image of the overall processing step is determined as follows. If either $b_r g_r(x, y) = 255$ (solid wood) or $b_r g_r(x, y) = 127$ (fiber) then $li(x, y) = 255$ (wood). If $b_r g_r(x, y) = 63$ (glue) then $li(x, y) = 127$ (glue). If $b_r g_r(x, y) = 0$

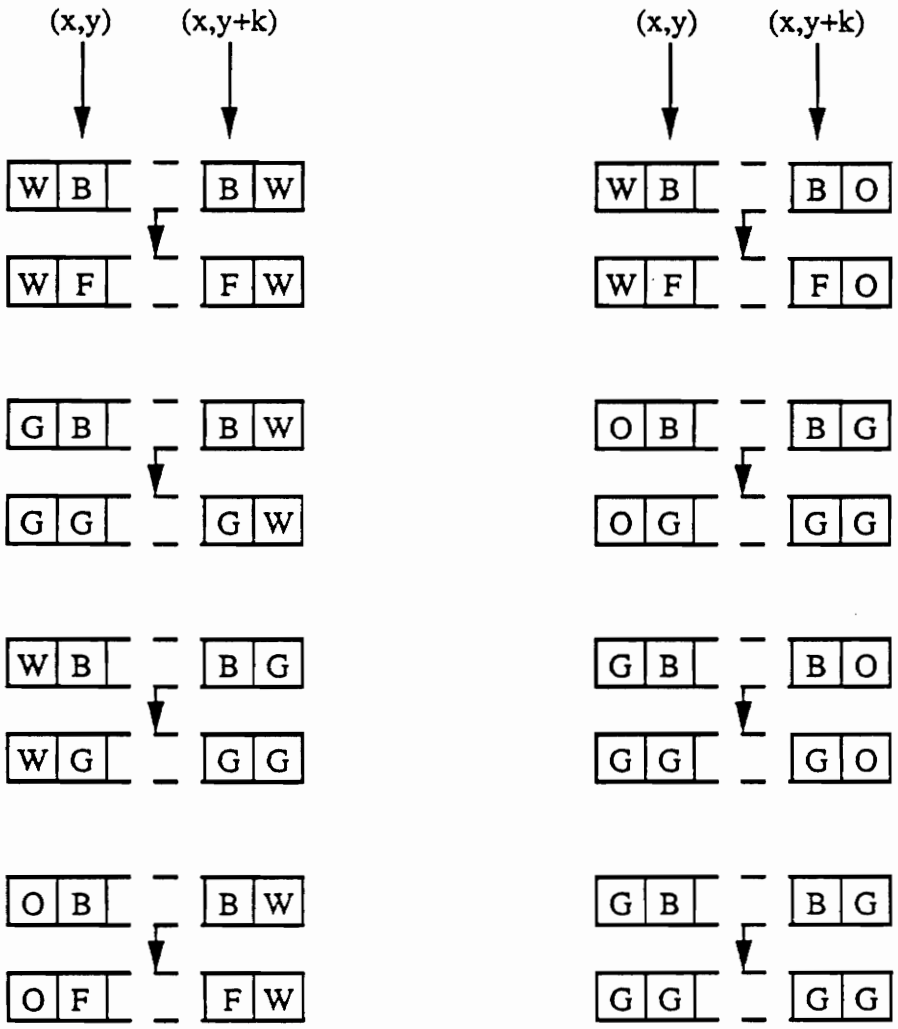

W = wood (solid wood or fiber), F = fiber, G = glue, B = border, O = background

Figure 5–11 Vertical border grouping operator.

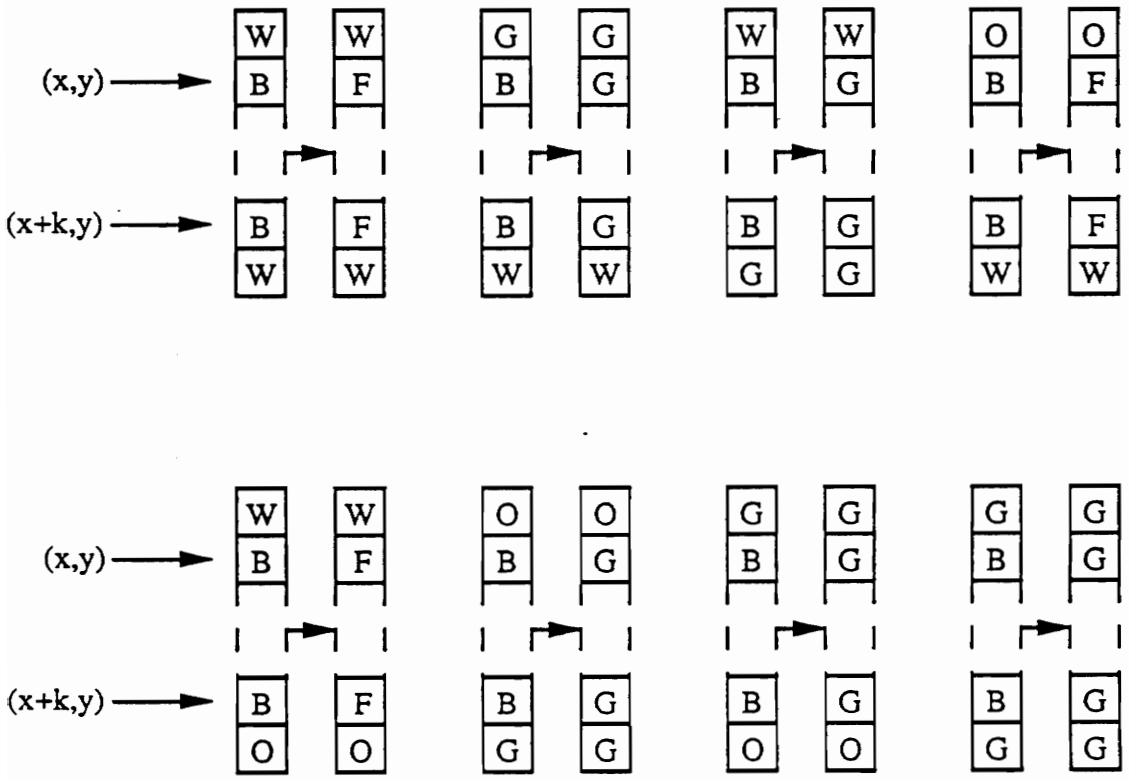

W = wood (solid wood or fiber), F = fiber, G = glue, B = border, O = background

Figure 5–12 Horizontal border grouping operator.

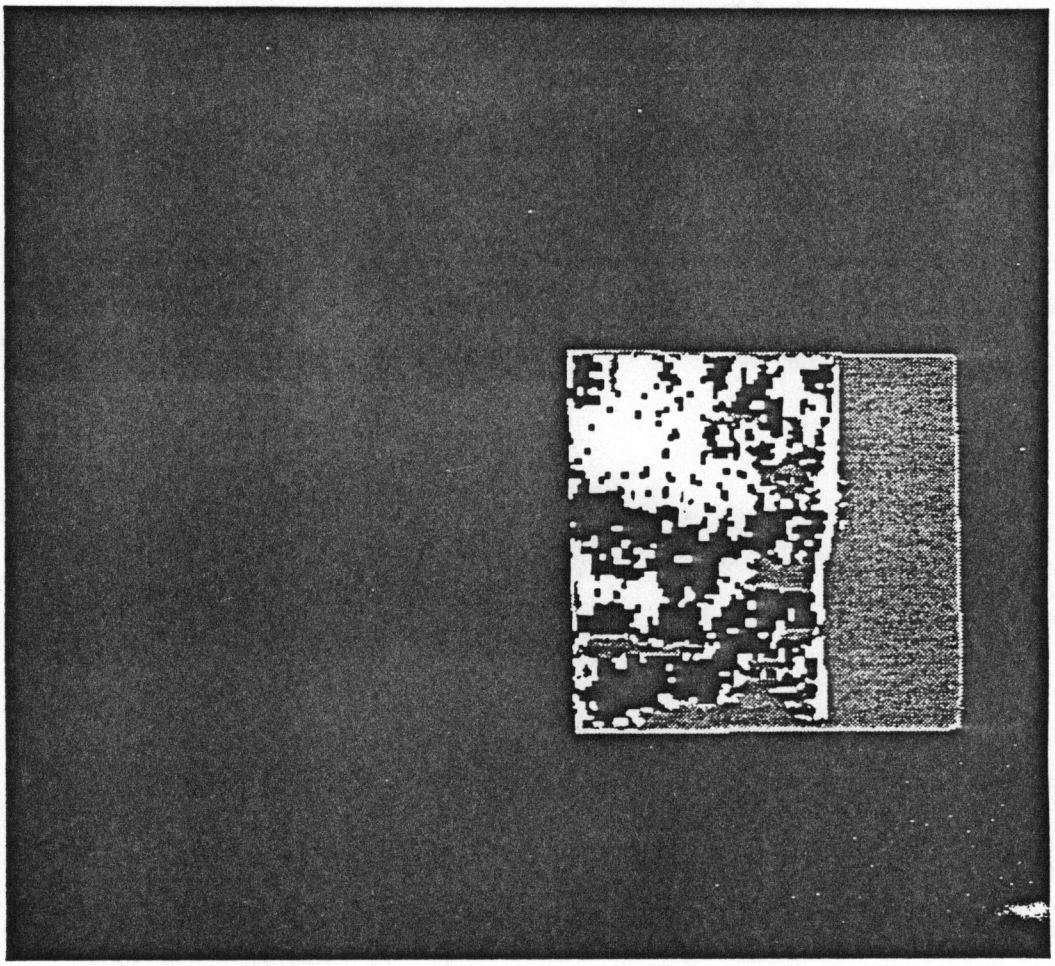

Figure 5–13 $B_r G_r$ for the specimen of Figure 3–1.

(background) then $li(x, y) = 0$ (background). Figure 5–14 shows LI for the specimen of Figure 3–1.

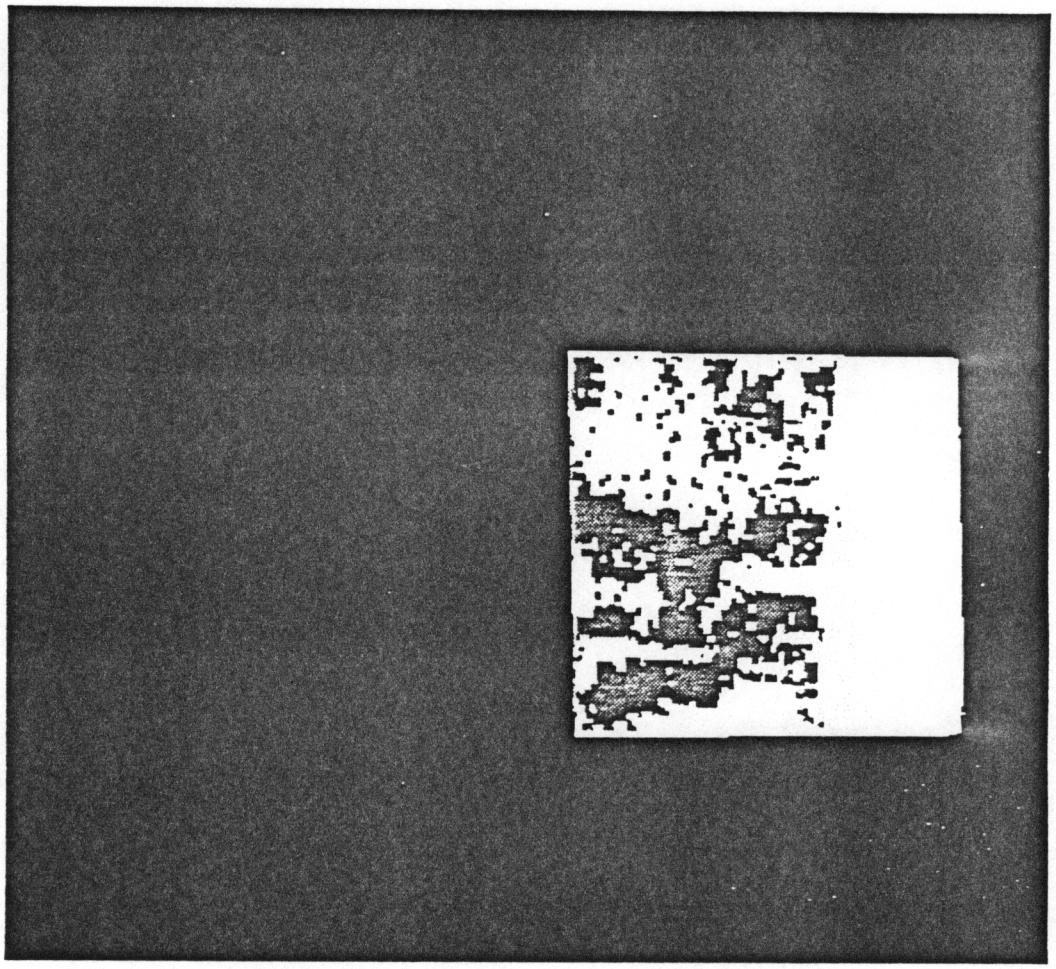

Figure 5–14 *LI* for the specimen of Figure 3–1.

6. INSPECTION AREA MAPPING

The final processing step of the automated vision system is to compare each pixel in the region comprising the inspection area of one specimen to the corresponding pixel in the region comprising the inspection area of the other specimen to determine the percent wood failure of the sample comprised of the two specimens. Thus the results of the previous processing step obtained from each of the images of the two specimens comprising a sample are combined in this processing step. Specifically, the input of this processing step consists of the output image of the previous processing step associated with each of the two specimens comprising a sample. Let LI_1 and LI_2 denote these two input images (the order is unimportant). LI_1 and LI_2 are labeled images such that a pixel in either LI_1 or LI_2 has 1) gray level value 255 if it is thought to be a part of the region that corresponds to wood in the inspection area of the associated specimen, 2) gray level value 127 if it is thought to be a part of the region that corresponds to glue in the inspection area of the associated specimen, or 3) gray level value 0 if it is thought to be a part of the region that corresponds to the background. The output is the percent wood failure of the sample comprised of the two specimens. Let f denote this output.

6.1 Mapping Function

Let R_1 and R_2 denote the regions within LI_1 and LI_2, respectively, bounded by the line equations calculated in the first processing step as shown in Figure 6–1. R_1 and R_2 are the regions comprising the theoretical inspection areas of the two specimens and may differ slightly from the actual inspection areas specified within LI_1 and LI_2. Based on the orientation of a specimen within

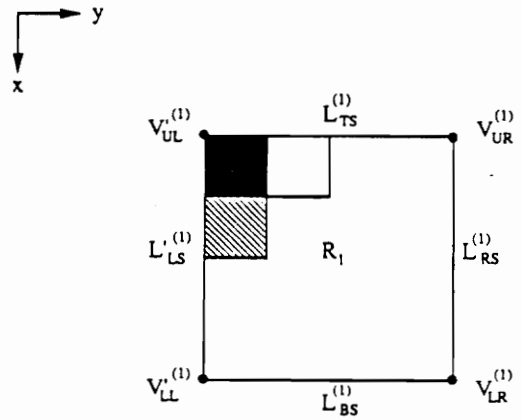

(a)

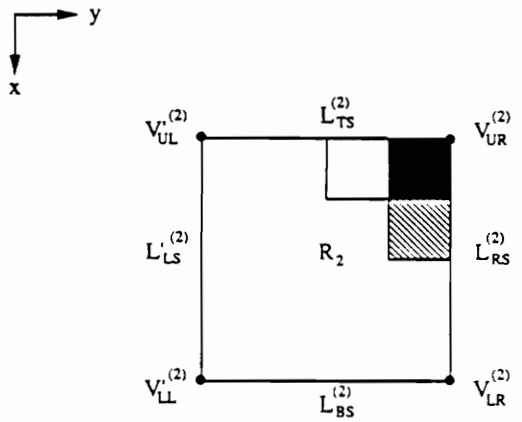

(b)

Figure 6–1 The regions R_1 and R_2.

an image (Figure 2–3) and the manner in which the specimens were shorn apart (Figure 2–4), corresponding areas within R_1 and R_2 are as shown in Figure 6–1. Hence the lines bounding R_2 correspond to the lines bounding R_1 as follows:

$$\begin{aligned} L_{TS}^{(1)} &\rightarrow L_{TS}^{(2)}, \\ L_{BS}^{(1)} &\rightarrow L_{BS}^{(2)}, \\ L_{RS}^{(1)} &\rightarrow L_{LS}^{'(2)}, \\ L_{LS}^{'(1)} &\rightarrow L_{RS}^{(2)}. \end{aligned} \qquad (6-1)$$

Figure 6–1 specifies the notation used in specifying the correspondences. The corners of the region comprising R_2 correspond to the corners of the region comprising R_1 in a similar manner:

$$\begin{aligned} V_{UL}^{'(1)} &\rightarrow V_{UR}^{(2)}, \\ V_{UR}^{(1)} &\rightarrow V_{UL}^{'(2)}, \\ V_{LL}^{'(1)} &\rightarrow V_{LR}^{(2)}, \\ V_{LR}^{(1)} &\rightarrow V_{LL}^{'(2)}. \end{aligned} \qquad (6-2)$$

Assuming that adjacent lines bounding R_1 and R_2 are perpendicular, a mathematical expression for these correspondences is derived by defining inspection area rectangular coordinate planes for R_1 and R_2 as shown in Figures 6–2 and 6–3, respectively. Let RC denote the x-y rectangular coordinates that have been used throughout this thesis. Let RC_1 denote the rectangular coordinates shown in Figure 6–1 used to establish a coordinate system on region R_1 and let RC_2 denote the rectangular coordinates shown in Figure 6–2 used to establish a coordinate system on region R_2. The origin and coordinate axes of RC_1 could have been defined at any of the side-corner-side combinations bounding R_1. The side-corner-side combination defining the origin and coordinate axes of RC_2 was chosen so that RC_1 would map onto RC_2 as dictated by equations (6–1) and (6–2).

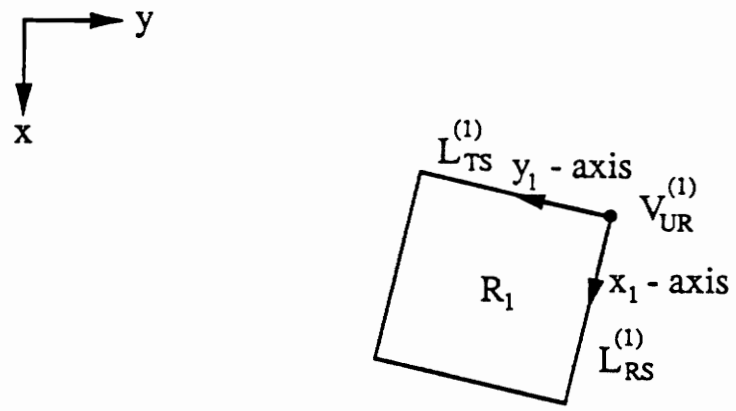

Figure 6–2 Inspection area rectangular coordinate plane for R_1.

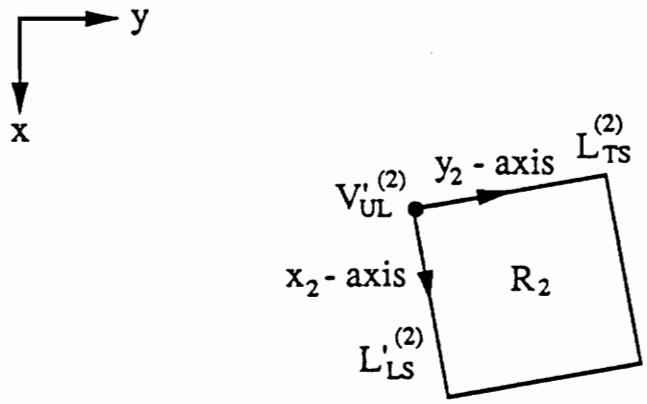

Figure 6–3 Inspection area rectangular coordinate plane for R_2.

Since the coordinates of the pixels comprising R_1 and R_2 are known with respect to RC rather than with respect to RC_1 and RC_2, respectively, one method of mapping a pixel in R_1 to its corresponding pixel in R_2 is derived by finding the equations that define the mappings of RC_1 onto RC and RC onto RC_2. From geometry, the mapping of RC_1 onto RC is accomplished by 1) translating the origin of RC_1 to the origin of RC, 2) rotating the positive x-axis of RC_1 until it is aligned with the positive x-axis of RC, and 3) negating the y-axis of RC_1 so that it is aligned with the y-axis of RC. Let k denote a pixel in R_1 at coordinates (x_1, y_1) with respect to RC. The coordinates of k after translation are given by

$$(x_{1_t}, y_{1_t}) = (x_1 - x_{UR}^{(1)}, y_1 - y_{UR}^{(1)}), \tag{6-3}$$

where $V_{UR}^{(1)} = (x_{UR}^{(1)}, y_{UR}^{(1)})$. The coordinates of k after rotation are given by

$$(r_{1_t}, \theta_{1_t}) = \left(\sqrt{x_{1_t}^2 + y_{1_t}^2}, \arctan(y_{1_t}/x_{1_t})\right), \tag{6-4}$$

$$(r_{1_r}, \theta_{1_r}) = (r_{1_t}, \theta_{1_t} - \arctan m_{RS}^{(1)}), \tag{6-5}$$

$$(x_{1_r}, y_{1_r}) = (r_{1_r} \cos\theta_{1_r}, r_{1_r} \sin\theta_{1_r}), \tag{6-6}$$

where $m_{RS}^{(1)}$ is the slope of $L_{RS}^{(1)}$. The coordinates of k after negation of the y-axis are given by

$$(x_2, y_2) = (x_{1_r}, -y_{1_r}). \tag{6-7}$$

The mapping of RC onto RC_2 is accomplished by 1) rotating the positive x-axis of RC until it is aligned with the positive x-axis of RC_2, and 2) translating the origin of RC to the origin of RC_2. Continuing from equation (6–7), the coordinates of k after rotation are given by

$$(r_2, \theta_2) = \left(\sqrt{x_2^2 + y_2^2}, \arctan(y_2/x_2)\right), \tag{6-8}$$

$$(r_{2_r}, \theta_{2_r}) = (r_2, \theta_2 + \arctan m_{LS}^{\prime(2)}), \tag{6-9}$$

$$(x_{2_r}, y_{2_r}) = (r_{2_r} \cos\theta_{2_r}, r_{2_r} \sin\theta_{2_r}), \tag{6-10}$$

where $m_{LS}^{'(2)}$ is the slope of $L_{LS}^{'(2)}$. The coordinates of k after translation are given by

$$(x_{2_t}, y_{2_t}) = (x_{2_r} + x_{UL}^{'(2)}, y_{2_r} + y_{UL}^{'(2)}), \qquad (6-11)$$

where $V_{UL}^{'(2)} = (x_{UL}^{'(2)}, y_{UL}^{'(2)})$. Since the coordinates (x_{2_t}, y_{2_t}) may not be integers (pixels have integer coordinates), the coordinates with respect to RC of the pixel in R_2 that corresponds to k are given by

$$(x_3, y_3) = (r(x_{2_t}), r(y_{2_t})), \qquad (6-12)$$

where r is a function that rounds a given real number to the nearest integer.

6.2 Percent Wood Failure Determination

Let N_T denote the total number of pixel pairs evaluated and let N_W denote the number of pixel pairs evaluated as wood failure. The percent wood failure of the sample comprised of the two specimens associated with LI_1 and LI_2 is determined as follows. Initially, N_T and N_W are set to zero. A line-by-line, pixel-by-pixel scan of LI_1 is performed. Let the coordinates (x_1, y_1) denote the coordinates of a pixel in LI_1 that constitute the input of the mapping function defined by equations (6–3) through (6–12) and let the coordinates (x_3, y_3) denote the coordinates of a pixel in LI_2 that constitute the output corresponding to this input. If $li_1(x_1, y_1) = 255$ (wood) and $li_2(x_3, y_3) = 255$ (wood), the pixel pair constitutes wood failure and both N_T and N_W are incremented. If $li_1(x_1, y_1) = 255$ (wood) and $li_2(x_3, y_3) = 127$ (glue) or if $li_1(x_1, y_1) = 127$ (glue) and $li_2(x_3, y_3) = 255$ (wood) or if $li_1(x_1, y_1) = 127$ (glue) and $li_2(x_3, y_3) = 127$ (glue), the pixel pair constitutes glue failure and only N_T is incremented. If $li_1(x_1, y_1) = 255$ (wood) and $li_2(x_3, y_3) = 0$ (background) or if $li_1(x_1, y_1) = 127$ (glue) and $li_2(x_3, y_3) = 0$ (background), the pixel in LI_2 that corresponds to the pixel in LI_1 is not a

part of the region comprising the inspection area in LI_2. In this case, neither N_T nor N_W is incremented. This case sometimes occurs because the regions comprising the inspection areas in LI_1 and LI_2 seldom have the exact same dimensions due to error incurred during inspection area extraction. Finally, if $li_1(x_1, y_1) = 0$ (background), the mapping function is not performed. The percent wood failure, f, of the sample comprised of the specimens associated with LI_1 and LI_2 is given by

$$f = \frac{N_W}{N_T} \times 100. \qquad (6-13)$$

7. EXPERIMENTAL RESULTS

7.1 Plywood Shear Sample Data Set

The experiment set consisted of 35 samples that had been tested and evaluated by a human inspector at the APA Quality Testing Laboratory in Dothan, Alabama. The species of wood used in the panels from which the samples had been milled was southern pine; samples milled from panels made from other species were unavailable.

7.2 Scanning and Preprocessing

Each pair of specimens comprising a sample in the experiment set was scanned using a CCD image sensing camera. Intensities were stored as integer bytes in the matrices described in Section 2.5. Only the red, green, and blue (RGB) level intensities of a specimen were scanned; the gray level intensities were obtained by averaging the RGB level intensities. Thus, if C is a color image and P is the black and white image to extract from C,

$$p(x,y) = [p_r(x,y) + p_g(x,y) + p_b(x,y)]/3. \qquad (7-1)$$

To compensate for lighting nonuniformity, color images underwent a shading correction analysis [Sawchuk, 1977] before the gray level intensities were extracted. In the analysis, the RGB level intensities of a solid white and solid black scene were scanned. Ideally, the RGB level intensities of each element in the image matrices of the solid white and solid black scenes scanned should be 255 and 0, respectively. Differences between the actual and ideal

intensity levels of the solid white and solid black scenes scanned were appropriately added to or subtracted from the intensity levels of each specimen scanned. New adjustment factors were calculated for every ten specimens scanned. All images were processed by a VAX 11/785 computer.

7.3 Results of Processing

The percent wood failure of the samples in the experiment set estimated by the vision system presented in this thesis versus the percent wood failure of the samples estimated by a human inspector are shown in Table 7–1. Estimations from multiple human inspectors were unavailable. As seen in Table 7–1, 1) individual sample percent wood failures estimated by the system differed by no more than 30% from those estimated by the human inspector, and 2) the average percent wood failure of the estimations issued by the system fell within 5% of the average percent wood failure of the estimations issued by the human inspector. This latter result is a requirement of the APA when multiple inspections are performed on a set of samples.

Table 7–1

SAMPLE	HUMAN	COMPUTER
A1	100%	100%
A3	100%	96%
A4	100%	85%
B4	95%	81%
B6	95%	94%
C5	90%	87%
C13	90%	86%
D7	85%	81%
D14	85%	77%
D18	85%	84%
E15	80%	75%
E18	80%	100%
E20	80%	75%
F6	75%	77%
F10	75%	84%
G14	70%	75%
G15	70%	84%
G21	70%	100%
H3	65%	56%
H5	65%	75%
H17	65%	74%
H18	65%	61%
H26	65%	63%
H29	65%	62%
I3	60%	70%
I4	60%	55%
I8	60%	67%
I10	60%	72%
J1	55%	83%
K4	50%	62%
K7	50%	55%
L2	45%	58%
M3	40%	59%
Q4	25%	54%
S3	15%	34%
AVG.	70%	74%

8. CONCLUSIONS AND RECOMMENDATIONS FOR FUTURE RESEARCH

An extensive study of output images produced by each stage of the program indicated that most discrepancies between the human- and computer-generated evaluations performed on the experiment set were caused by faulty segmentations in the fiber extraction stage of the program. As discussed in Chapter 5, fiber tends to be under-extracted in samples showing high wood failure whereas fiber tends to be over-extracted in samples showing low wood failure. This is substantiated by the results shown in Table 7–1, where only samples showing moderate wood failure received evaluations from the computer consistent with those given by the human inspector.

Several methods of improving the accuracy of estimations generated by the computer are proposed. One alternative is to increase the resolution of the scanning system utilized. Experimentation showed that the computer-generated estimations of samples scanned at high resolution were more accurate, i.e., closer to the human-generated estimations, than the computer-generated estimations of samples scanned at low resolution.

A second alternative is to automatically increase the percent wood failure of samples evaluated by the program as showing high wood failure. The percent wood failure of samples evaluated as showing low wood failure would be automatically decreased. The percent wood failure of samples evaluated as showing moderate wood failure would not be altered. The adjustment factors could be constant or a function of the percent wood failure originally assigned, depending on the results of experimentation.

Since, in practice, most samples tend to show moderate to high wood failure, a third alternative is to experimentally increase the n_f parameters of Chapter 5 until evaluations generated by the computer are consistent with those given by human inspectors. As discussed in Section 5.5, the amount of fiber extracted is increased as the values of these parameters are increased. A disadvantage of this approach is that the error incurred in the evaluations would increase as the amount of wood failure shown is decreased, i.e., the estimated wood failure of samples showing extremely low wood failure would be grossly exaggerated. If this occurs, severely defective panels could be overlooked, and the appropriate warnings will not be issued by the APA. Due to this possibility, it is felt that the first and second alternatives proposed offer a more viable solution to the accuracy problem.

REFERENCES

American Plywood Association (1970), "Proposed Standard Method for Estimating Percentage Wood Failure on Plywood Shear Specimens," Form No. TLX 32 7430.

American Plywood Association (1983), "Voice of the Structural Wood Panel Industry," Form. No. H800.

American Plywood Association (1984), "Adhesive Policy," Form No. E810.

Duda, R.O., and P.E. Hart (1973), *Pattern Classification and Scene Analysis*, John Wiley & Sons, New York.

James, M.L., G.M. Smith and J.C. Wolford (1977), *Applied Numerical Methods for Digital Computation*, 2nd ed., Harper & Row, New York.

Kreyszig, E. (1972), *Advanced Engineering Mathematics*, 3rd ed., John Wiley & Sons, New York.

McMillin, C.W. (1984), "Evaluating Wood Failure in Plywood Shear by Optical Image Analysis," *Forest Products Journal*, Vol. 34, No. 718, pp. 67–69.

Ng, C. (1990), Ph.D. Dissertation, Virginia Polytechnic Institute and State University.

Sawchuk, A.A. (1977), "Real-time Correction of Intensity Nonlinearities in Imaging System," *IEEE Trans. Comput.*, Vol. 26, No. 1, pp. 34–39.

Scheid, F. (1968), *Numerical Analysis*, McGraw-Hill, New York.

Shirai, Y. (1987), *Three-Dimensional Computer Vision*, Springer-Verlag, Berlin.

Yu, F.T.S. (1983), *Optical Information Processing*, John Wiley & Sons, New York.

VITA

Raymond Richard Avent, III, was born on September 6, 1962, in Newport News, Virginia. He graduated from Starkville High School, Starkville, Mississippi, in May, 1980. He received a Bachelor of Science degree in Electrical Engineering from Louisiana State University in May, 1987. He received a Master of Science degree in Electrical Engineering from the Virginia Polytechnic Institute in December, 1990.